

THE MECHANISM OF THE SCALLOP MYOSIN ATPase

by

ANDREW PAUL JACKSON

A thesis submitted in fulfilment of the requirements for the  
degree of Doctor of Philosophy at the University of  
Leicester.

Department of Biochemistry  
University of Leicester  
Leicester LE1 7RH.

April 1988

UMI Number: U008322

All rights reserved

INFORMATION TO ALL USERS

The quality of this reproduction is dependent upon the quality of the copy submitted.

In the unlikely event that the author did not send a complete manuscript and there are missing pages, these will be noted. Also, if material had to be removed, a note will indicate the deletion.



UMI U008322

Published by ProQuest LLC 2015. Copyright in the Dissertation held by the Author.  
Microform Edition © ProQuest LLC.

All rights reserved. This work is protected against  
unauthorized copying under Title 17, United States Code.



ProQuest LLC  
789 East Eisenhower Parkway  
P.O. Box 1346  
Ann Arbor, MI 48106-1346

X751458820

## PREFACE

The work presented in this thesis was carried out in the laboratory of Dr C.R. Bagshaw in the Department of Biochemistry, University of Leicester.

I would like to thank my supervisor, Dr C.R. Bagshaw, for the invaluable help which he has given me during my time in Leicester. I would also like to thank Dr C. Wells and Miss K.E. Warriner for their advice, especially during the early part of my work.

I acknowledge the financial assistance given to me by the S.E.R.C for the studentship which I received.

ABBREVIATIONS AND CONVENTIONS

A	F-actin
ADP	Adenosine 5'-diphosphate
ATP	Adenosine 5'-triphosphate
ATPase	Adenosine 5'-triphosphatase
AMPPNP	Adenosine 5'- $\beta$ - $\gamma$ -imidotriphosphate
Ap5A	P <sup>1</sup> ,P <sup>5</sup> -Di(adenosine-5')pentaphosphate
Ca	Divalent calcium ion
D	Nucleotide diphosphate
DTT	Dithiothreitol
EDC	1-ethyl-3-(3-(diethylamino)propyl carbodiimide
EPR	Electron paramagnetic resonance
FPLC	Fast protein liquid chromatography
FDP	Formycin A 5'-diphosphate
FTP	Formycin A 5'-triphosphate
FTPase	Formycin A 5'-triphosphatase
FMPPNP	Formycin A 5'- $\beta$ - $\gamma$ -imidotriphosphate
IASL	4-(2-iodoacetamido)2,2,6,6, tetramethyl piperdinoxyl
HMM	Heavy meromyosin
M	Myosin head
Mg	Divalent magnesium ion
N	Nucleotide
PNP	Imidodiphosphate
P, Pi	Inorganic phosphate
PPi	Inorganic pyrophosphate
RLC	Regulatory light chain
RD	Regulatory domain

S1	Myosin subfragment 1
SDS	Sodium dodecyl sulphate
T	Nucleotide triphosphate
TEAB	Triethylamine bicarbonate
TES	N-tris(hydroxymethyl)methyl-2-aminoethane sulphonic acid
TLC	Thin layer chromatography

For the  $i$ th step of a reaction  $k_i$  is the forward rate constant,  $k_{-i}$  the reverse rate constant and  $K_i$  the equilibrium constant ( $k_i/k_{-i}$ ). Superscripts '\*' and '+' indicate conformationally different species. The letters 'u' and 'c' specify a rate or species belonging to unregulated molecules or molecules in the presence of Ca. M represents the myosin head whether it be myosin, HMM or S1. For example  $M_u^C$ .D.P represents an unregulated myosin head with Ca, diphosphate and inorganic phosphate bound.

## SUMMARY

Molluscan adductor muscles display thick filament regulation. A calcium binding site (regulatory domain) near the neck of the myosin molecule is responsible for controlling the ATPase activity, hence the rate of contraction. In the absence of calcium, the ATPase activity is highly suppressed. When calcium binds to the regulatory domain the inhibition is relieved allowing contraction to occur.

Steady-state measurements are insufficient to characterise the ATPase activity in detail because of the dominant contribution from unregulated myosin molecules. Therefore spectroscopic techniques, allied to transient kinetic analysis were used to determine the effect of calcium on the various steps of the HMM ATPase mechanism.

ATP, ADP and calcium binding to HMM caused small, but measurable, enhancements (upto 8%) in the proteins tryptophan fluorescence. Stopped-flow fluorescence spectroscopy allowed the kinetics of binding and dissociation to be elucidated. Calcium bound to, and dissociated from, HMM rapidly ( $10^8 \text{ M}^{-1}\text{s}^{-1}$  and  $25 \text{ s}^{-1}$  respectively). When calcium was bound to the regulatory domain the affinity of the active site for nucleotide was reduced, an effect seen as an increase in the rate constant for nucleotide dissociation.

Fluorescent ATP analogues, based on formycin were synthesised. These nucleotides displayed large fluorescence

enhancements on binding to HMM (upto 500%). Turnover of FTP by HMM was suppressed 100-fold by the removal of calcium, as determined by transient kinetic measurements. The large fluorescence enhancements seen on binding of various formycin nucleotides allowed the effect of calcium on the association and dissociation processes to be examined in great detail. Binding was found to be a complex, multistep process in which the presence of calcium increased the rate of interconversion of the various HMM/nucleotide complexes by several orders of magnitude.

## CONTENTS

PREFACE

ABBREVIATIONS AND CONVENTIONS

SUMMARY

CONTENTS

### CHAPTER 1

INTRODUCTION	1
Muscle structure	3
Mechanism of contraction	10
Myosin ATPase	12
Acto-myosin ATPase	13
Scallop myosin ATPase	19
Transient kinetics	25
Displacement kinetics	27

### CHAPTER 2

MATERIALS AND METHODS	30
Protein preparations	30
Acto-HMM cross-linking	37
Nucleotide preparations	38
General analytical techniques	41
Spectroscopic techniques	46
Stopped-flow fluorimeter	47
ATPase assays	51
Data capture and analysis	56

### CHAPTER 3

#### ACTO-HMM CROSS-LINKING

Introduction	58
Results	
Acto-HMM cross-linking	60
Discussion	61

### CHAPTER 4

#### ADENOSINE TRIPHOSPHATASE REACTION

Introduction	63
Results	
ATP turnover rates	65
ATP binding	68
ATP hydrolysis	72
Phosphate release	74
ADP binding and release	74
Ca binding and release	79
Ca/ADP exchange	81
Discussion	82

### CHAPTER 5

#### FORMYCIN TRIPHOSPHATASE REACTION

Introduction	87
Results	
FTP turnovers	89
FTP binding	91
FTP hydrolysis	92
Phosphate release	94
FDP release	94

ATP chase of FTP turnovers	95
Pyrophosphate release	97
Spin labelled HMM	97
Discussion	98

## CHAPTER 6

TRAPPING OF REACTION INTERMEDIATES	
Introduction	101
Results	
FDP binding	101
FMPPNP binding	103
FMPPNP dissociation	104
Salt effect on FTP turnovers	106
Timed ATP chases during FTP turnovers and FMPPNP binding	109
Discussion	110
Non-hydrolysable nucleotide binding - FMPPNP	111
- FDP	113
Branched FTPase pathway	114
FDP activation of FTPase	122

## CHAPTER 7

### MYOSIN FTPase

Introduction	125
Fluorescence measurements on suspensions	125
Myosin FTP turnovers	128
Smooth muscle myosin FTP turnovers	130
Discussion	131

## CHAPTER 8

CONCLUSIONS	133
Origin of unregulated molecules	134
Role of thin filaments in molluscan regulation	136
Regulatory mechanism	138

## APPENDIX 1

Summary of computer programs	143
------------------------------	-----

## APPENDIX 2

Publications	149
--------------	-----

## REFERENCES

150

CHAPTER 1

INTRODUCTION

The ability to move is a feature common to all living organisms but which has been developed most extensively by the animal kingdom. There are many ways in which motility can occur, ranging from the movement of flagella in prokaryotes, chromosomal movement during cell division, to the highly specialized system found in muscles. The acto-myosin system is the most highly developed and is found, in various degrees of organisation, in all eukaryotic species. The ultimate degree of organisation is located in striated muscle, where a whole tissue has evolved especially for the process of movement. A single muscle can only contract, hence methods to stretch muscles (usually by the contraction of opposing muscles) are required to ensure that the organism can undergo useful movement. Acto-myosin systems are found in a variety of organisational states ranging from the highly ordered striated muscle to the relatively disordered non-muscle structures.

The classification of muscle types, out of necessity, is very broad. It is usually based on the appearance of muscles under the light microscope. Vertebrate skeletal and heart muscles show distinct stripes running at  $90^{\circ}$  to the fibres long axis. Skeletal muscles are usually under voluntary control, whereas heart muscle is under involuntary control leading the striated and cardiac muscles to be considered as two distinct types. There is a third class of vertebrate muscle, smooth muscle, which has no apparent structure at the resolution of the light microscope, and which is also under involuntary control.

Muscles have evolved to fulfill a variety of roles ranging from cardiac muscle, which may have to function continuously for > 100 years, to insect flight muscle which can contract at speeds up to 1000 times per second. Clearly some variation in gross organisation and molecular mechanism is necessary to accommodate the different functions. It is this variation which has helped scientists to probe the mechanism of contraction in great detail.

The contractile apparatus is a highly complex arrangement of proteins. The examination of particular aspects of a highly specialised muscle tissue may give an insight into how other muscle tissues function. Insect flight muscle provides a highly ordered arrangement for structural studies, but is of limited availability for biochemical work, whereas vertebrate striated muscle (especially rabbit) provides a ready source of material for biochemical studies.

There are two major problems regarding the biochemistry of muscle contraction. Firstly, how is chemical energy transformed into mechanical work? Secondly, how is this process regulated? ATP hydrolysis is the source of chemical energy, although the mechanism by which hydrolysis is coupled to contraction is not yet clear. Hydrolysis of ATP needs to be tightly controlled to prevent wastage of energy during periods of muscular inactivity. Regulatory systems vary between muscle types, but they all perform essentially the same role. Molluscan muscles provide a tissue type which has a relatively simple control system in a species

where sufficient material is available for biochemical analysis. This thesis is concerned with the regulation of ATP hydrolysis by myosin in molluscan muscle.

### Muscle structure

Striated muscles are composed of a series of muscle fibres, which themselves are composed of bundles of myofibrils. It is the myofibrils that contain the active unit of contraction, the sarcomere, which can be seen under the light microscope to consist of a series of light and dark bands. The bands are due to a variation in the refractive index within the myofibril and are referred to as the A (anisotropic) band and the I (isotropic) band. These bands, when observed in greater detail are seen to consist of a series of interdigitating filaments (figure 1-1a and 1-1b). The A band consists largely of the region of overlap between the two sets of filaments (the thick and thin filaments). In the centre of the A band there is a lighter region consisting only of thick filaments, the H zone. Down the centre of the H zone runs the darker M line, a network of proteins which hold the thick filaments in the appropriate 3 dimensional array. The I band, composed chiefly of the thin filaments, has the dense Z line running down its centre. It is to the Z line that the thin filaments are attached and it is the region between two Z lines that is referred to as a sarcomere. In resting vertebrate skeletal muscle it is typically 2-3  $\mu\text{m}$  long.

Cross-sections of the sarcomere in the positions shown in

figure 1-1b reveal the arrangement of the thick and thin filaments. In vertebrate striated muscle (as shown here), the two sets of filaments are arranged in a double hexagonal array in the area of overlap. Each thick filament is surrounded by six thin filaments. The arrangement is slightly different in the scallop adductor muscle, where twelve thin filaments surround each thick filament. The exact geometrical arrangement of these filaments is not certain but is based on the form of an elaborate hexagon (Millman and Bennett, 1976).

It was this structure of muscle which led to the sliding filament theory of muscle contraction. Huxley and Niedergerke, (1954) showed that the A band remained at constant length during contraction. Huxley and Hanson, (1954) showed that the H band and the I zone shortened in unison. This led to the proposal, from both groups, that contraction occurred when the two sets of filaments slid over one another.

A mechanism by which the sliding motion was driven was now required. Huxley, (1957) proposed that projections from one of the filament types, attached to an 'elastic element', could undergo a cyclical interaction with the other filament type, thus leading to a net motion of the filaments relative to each other. Subsequently the projection was found to be the S1 portion of the myosin molecule. This also was the portion of the myosin molecule which contained the ATPase site. The location of the elastic element has not yet been identified although the myosin head is now strongly

implicated.

### Thick filament structure

Thick filaments are composed mainly of the protein myosin, although in some invertebrates there is a large amount of paramyosin which forms the core of the filament. The filaments are bipolar, with the myosin tails pointing towards the centre of the filament (figure 1-1c). Myosin is a large, hexameric protein with a molecular weight of about 480 000 da, consisting of two heavy chains (~200 000 da) and two pairs of light chains (~20 000 da each). Myosin is a highly asymmetric molecule, consisting of a long rod (156 x 2 nm) on the end of which there are two, roughly pear shaped heads (18.6 x 6.3 nm) (Elliott and Offer, 1978) (figure 1-1d). The actin, ATP and light chain binding sites are all located on the head portion of the molecule (Margossian and Lowey, 1973, Szent-Gyorgyi et al, 1973).

The tail consists of a coiled-coil structure which is maintained by the arrangement of the charged and hydrophobic amino acid residues (McLachlan and Karn, 1982). Hydrophobic residues are placed on the internal face and charged residues on the external face of the coiled-coil. The charged residues also alternate between positive and negatively charge regions along the length of the tail which aids packing and holds the tails together allowing the filaments to form. The S2 region is held less tightly onto the filament, allowing it to project from the filament.

Proteolysis can be used to subdivide the rod into two portions, the terminal 2/3 (LMM) being responsible for filament formation with the remaining 1/3 (S2) allowing the heads to project from the filaments. Elliott and Offer (1978) showed, by electron microscopy, that there is some degree of flexibility in specific regions of the tail, corresponding to a proteolytically sensitive region. They also saw a great deal of flexibility about the junction of the rod and heads. These observations correlate well with proteolytic digestions of myosin, which could either produce isolated heads (S1) plus rods, or the two heads joined by a short length of rod (HMM) (figure 1-1d). Their work also suggested that the head of myosin was pear-shaped, forming a neck region at the junction with the tail. S1 appeared to be more globular, possibly due to removal of material from the neck region during the proteolytic digestion of myosin.

S1 and HMM subfragments of myosin have proved to be invaluable in the biochemical study of the myosin ATPase. At low ionic strength (< 200mM NaCl) myosin self assembles into filaments and precipitates out of solution making biochemical assays, particularly optical ones, very difficult. Both HMM and S1 are soluble at low ionic strength, due to the loss of the filament forming part of the molecule, yet they retain their actin binding and ATPase activities. These are the subfragments of myosin on which most biochemical studies have been carried out.

Rayment and Winkelmann, (1984), produced an S1 from avian skeletal muscle which was suitable for X-ray

crystallography. The crystals produced allowed analysis of the packing of the S1 within the crystal, giving the total dimensions of S1 as being at least 16 nm long and with a maximum thickness of 6 nm. The S1 appeared to be 'tadpole' shaped (Winkelmann et al, 1985). The data have not yet been sufficiently well analysed to provide a full 3 dimensional structure of S1. Such information would be invaluable in further studies into the S1 domain structure and the mechanism by which S1 is involved in energy transduction.

Although a high resolution structure of S1 is not yet available, other uses have been made of X-ray diffraction methods. Sufficient order exists in muscle fibres to produce interpretable X-ray diffraction patterns. From the work of Huxley and Brown, (1967) it was seen that the myosin heads projected from the filament in a helical manner with repeat distances at 14.3 nm and 42.9 nm. Squire, (1974) showed that the data were consistent with 3 pairs of heads per helical repeat for vertebrate striated muscle, a conclusion that is supported by the observation that thick filaments from rat psoas muscle can fray into three strands (Maw and Rowe, 1980). The situation is less clear for the molluscan thick filaments, with either 6 (Millman and Bennett, 1976) or 7 (Vibert and Craig, 1983) myosins per helical repeat.

Myosin light chains have been classified into two functional types: the regulatory and the essential light chains. Originally these names reflected the presumed roles of the light chains, but the exact role of each type is now far

less clear. The light chains are elongated molecules which bind along the length of the myosin head (Vibert et al, 1986). One of each type of light chain binds to each head.

The light chains are tightly coupled to the function of the heads, and a full complement is required for control of the ATPase and actin interactions in thick-filament based regulatory systems. Their structure and location provide a means by which information about the state of, say the ATP binding site, can be transmitted to the actin binding site. Recently Okomoto et al, (1986) demonstrated, by photochemical labelling, that, in smooth muscle myosin, the essential light chain is in contact with the ATPase site. Ca binding to molluscan myosin induces conformational changes in the regulatory light chain (Hardwicke et al, 1983). A central role for both light chains in the regulation of myosin ATPase is clearly possible.

It has become apparent, through the use of limited proteolytic digestion, that the myosin head is composed of three distinct domains, linked by more flexible (and protease sensitive) sections. The size of the fragments produced by limited proteolysis of S1 varies depending on the protease and origin of the S1. Limited tryptic digestion of scallop S1 located the Ca binding and RLC binding domains in the C-terminal end of S1, in a position corresponding to the neck region of the intact myosin (Szentkiralyi, 1984).

### Thin filament structure

Thin filaments are composed chiefly of the 42 000 da protein actin, which can exist either as the free monomer (g-actin) or as a polymer (f-actin). In vitro the monomer/polymer transition is affected by salt and monomer concentration, with the polymer being favoured at high salt and high protein concentration. Polymerisation occurs with the binding of 1 mole of ATP per mole of monomer, with subsequent ATP hydrolysis, although hydrolysis is not obligatory for polymerisation. Actin has a bilobal domain structure with overall dimensions of 6.7 x 4 x 3.7 nm (Such et al, 1981). The filament which forms is polar with the polymerisation and depolymerisation occurring at different rates at either end of the filament leading to the phenomena of 'treadmilling', which is important in some forms of non-muscle motility. A helical filament forms with about 13 monomers per turn giving a helical repeat of 36-38 nm.

Vertebrate striated muscle thin filaments contain the regulatory system consisting of tropomyosin, a long  $\alpha$ -helical protein to which is attached the troponin complex, comprising troponin T (tropomyosin binding), troponin C (Ca binding) and troponin I (inhibitory). The troponin complex occurs every 7th actin monomer and somehow regulates the interaction of the thin with the thick filament, thus controlling the ability of the muscle to contract.

Despite having myosin-linked regulation, molluscan thin

filaments do have a full complement of tropomyosin. It was originally thought that there was no troponin at all. Troponin I and C have been found (Lehman, 1981) but it is controversial as to whether any functional thin filament regulatory systems are present. Tropomyosin may have some other role to play, possibly being a structural rather than regulatory role. This reflects the major difference between vertebrate and molluscan striated muscle. As will be described in greater detail, the molluscan regulatory system is associated with the thick filaments.

#### Mechanism of contraction

The identity of the 'side pieces' of Huxley (1957), has been firmly established as being myosin heads. The identification of the 'elastic' element has been more elusive. Harrington (1979), proposed that the hinge joining the LMM and the S2 fulfilled this role. He suggested that a local melting of the coiled coil structure in the region of the LMM/S2 junction caused the S2 section to shorten thus moving the myosin head relative to the thin filament. Recent evidence (described below) has shown that this is probably not the case.

Two assay systems have been developed which allow the direct visualisation and quantitation of acto-myosin movement. The algae, *Nitella*, has very large cells with bundles of actin filaments running along their length. Myosin has been attached to inert particles and the movement of these particles along these actin filaments monitored (Sheetz and

Spudich, 1983). Alternatively, an assay has been developed where the movement of fluorescently labelled actin over myosin, adhered to a glass slide, can be followed (Kron and Spudich, 1986).

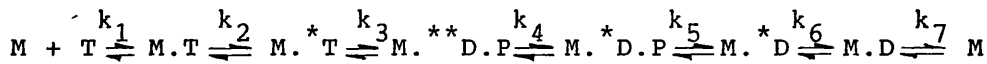
These two assays have allowed the dissection of myosin into smaller and smaller fragments to determine just how much of the molecule is needed for movement. Harada et al, (1987), demonstrated that a single-headed myosin was capable of generating movement in the glass slide assay. Albanisi et al, (1985), showed that the naturally occurring single headed myosin from the protozoa, *Acanthamoeba*, could generate movement in the *Nitella* assay. Hence it appears that only one head is required for movement. Hynes et al, (1987) produced a 'short' HMM, by tryptic digestion of standard HMM, lacking the hinge region deemed essential for movement by Harrington (1979). Short HMM did support movement in the *Nitella* assay. Toyoshima et al, (1987) modified the assay of Kron and Spudich (1986) and attached myosin and its subfragments to a nitrocellulose filter rather than a glass slide. They saw that S1 was able to move fluorescently-labelled actin over the surface of the filter.

These experiments have allowed the site of motion generation to be firmly localised in the myosin head. It also demonstrates that only one head is necessary for movement, leaving the reason as to why myosin is double headed wide open.

Myosin ATPase

Lymn and Taylor (1970) measured the ATPase activity of myosin by acid quench methods, giving a steady-state rate of  $0.1\text{s}^{-1}$ , but when the rate of  $\text{P}_i$  production was extrapolated back to zero time a rapid burst of  $\text{P}_i$  production was seen. This indicated that the rate limiting step occurred after hydrolysis and that the major steady-state intermediate was an enzyme/product complex. Lymn and Taylor (1970) also measured the maximum rate of the hydrolysis step of ATP by HMM, using a quench-flow machine, at  $50\text{-}100\text{s}^{-1}$ . Much work has gone into determining the size of the phosphate burst (as moles of phosphate released per active site). Typically 0.6-0.8 moles of phosphate are released per S1 head, (Lymn and Taylor, 1970, Kodama et al, 1986), the value is, however, variable. The phosphate burst of  $< 1$  can be explained by several theories. The most likely is that the hydrolytic step is reversible and that an equilibrium between ATP and ADP. $\text{P}_i$  is rapidly set up. Additionally the presence of inactive protein would also lead to a burst of less than 1.

The ATPase mechanism was studied by a variety of kinetic techniques, (chiefly quenched-flow and stopped-flow) leading to a seven step ATPase mechanism (Bagshaw et al, 1972, 1974, Trentham et al, 1972, Bagshaw and Trentham, 1973, 1974).

Equation 1

Values for the rate and equilibrium constants have been taken from Trentham et al, (1976) and are  $K_1 = 4.5 \times 10^3 M$ ,  $k_2 = 400s^{-1}$ ,  $k_{-2} = <0.02s^{-1}$ ,  $k_3 = >160s^{-1}$ ,  $K_3 = 160$ ,  $k_4 = 0.06s^{-1}$ ,  $k_{-4} = >3 \times 10^{-6}s^{-1}$ ,  $K_5 > 7.3mM$ ,  $k_6 = 1.4s^{-1}$ ,  $k_{-6} = 400s^{-1}$ ,  $K_7 = 2.7 \times 10^{-4}M$ .

The main features of the scheme are the sequential release of products and the reversibility of the hydrolytic step. The rate limiting step occurs after hydrolysis hence a myosin/product complex is the major steady-state intermediate. Re-evaluation of many of the rates of steps in the scheme have been carried out (Johnson and Taylor, 1978) but it remains the basis from which most work on the ATPase mechanism is carried out.

Acto-myosin ATPase

The sliding filament theory requires a mechanism by which the filaments can be driven over one another to produce movement. The tension developed by a muscle depends upon the extent of overlap of the thick and thin filaments in the sarcomere (Gordon et al, 1966) implying that there are a whole series of independent force-generating units present. The obvious candidate for this unit is the S1 head.

Huxley (1969) suggested that a cyclical interaction between myosin heads and actin could lead to filament sliding. Lymn and Taylor (1971) proposed a scheme for ATP hydrolysis-contraction coupling which depended upon the existence of two acto-S1 attached states. In the absence of ATP, a  $45^{\circ}$  state forms (rigor). When ATP binds, acto-S1 dissociation occurs allowing ATP hydrolysis. Actin and S1 now rebind in the  $90^{\circ}$  conformation and the products (ADP and Pi) are then released. To regain the  $45^{\circ}$  conformation the head needs to swivel, thus performing work (figure 1-2).

The Lymn-Taylor scheme implied compulsory dissociation before hydrolysis, and predicts that, at high actin concentrations, the ATPase rate should be reduced. In myofibrils, the effective protein concentration is about 100 mg/ml. Stein et al (1981), showed that the A.S1.ATP to A.S1.ADP.Pi transition was possible, thus the essential feature of the Lymn-Taylor scheme was not necessary. Stein et al, (1981) proposed that actin bound to the S1 with varying affinities depending upon the state of the nucleotide binding site. The lack of compulsory detachment could lead to the power stroke being reversed, thus leading to no contraction. Eisenberg and Greene (1980) showed that the mechanical state of the muscle could prevent any negative work being done if the strained attached state could rapidly detach from the actin. Geeves et al, (1984) have shown that acto-S1 binding is a two step process forming tight and weak binding states. All S1/nucleotide complexes can bind to actin in both tight and weak states

and it is the transformation from weak to tight binding which constitutes the power stroke. The binding state favoured depends on the nature of the bound nucleotide. This scheme has been termed the indirect coupling model.

The study of actin/S1 interactions has progressed from the irreversible and compulsory dissociation linked Lymn-Taylor scheme to the indirect coupling scheme of Geeves et al, (1984), where a series of equilibria are poised to favour net contraction of the muscle. All these studies have been performed in solution where no mechanical work can be done. Studies on intact myofibrils have been carried out to correlate the solution studies on acto-S1 with a more intact system. Tryptophan fluorescence studies on myofibrils during ATP turnover, in general, have confirmed the solution studies (White, 1985). 'Caged' ATP, which is an inert precursor of ATP that can be diffused into muscle at high concentrations and then rapidly converted to ATP by U.V irradiation, has allowed transient kinetic studies on the intact fibres to be performed (Goldman et al, 1982).

#### Regulation of contraction

Contraction has an absolute requirement for ATP hydrolysis, hence any regulatory mechanism which can inhibit the ATPase activity can prevent contraction. The activity of the acto-myosin ATPase is regulated by Ca ions by several different mechanisms. There are broadly two regulatory systems present, working via the thick or the thin filaments. Thick filament regulatory mechanisms can be

further subdivided into the phosphorylation-dependent and direct-Ca-binding systems.

#### Thin filament regulation

Thin filament regulation, as the name suggests, originates on the actin filament. The regulatory proteins of this system are the troponins and tropomyosin. It is the binding of Ca to troponin C that initiates a series of protein-protein interactions, culminating in an increased ATPase activity. According to the steric blocking mechanism (Huxley, 1973, Taylor and Amos, 1981), in the absence of Ca tropomyosin lies in the groove of the actin filament and prevents it binding to the myosin heads. The binding of Ca to troponin C causes the tropomyosin to move out of the actin/myosin binding site allowing actin and myosin to interact and the subsequent activation of the ATPase. Rabbit S1 binding to regulated actin (actin filaments plus the regulatory proteins) is cooperative in the presence and absence of Ca (Greene and Eisenberg, 1980). Even with Ca bound to troponin C, tropomyosin still blocks S1 binding, until the concentration of S1 added is raised above a critical level allowing binding to occur.

Chalovich and Eisenberg (1982) showed that Ca did not affect the affinity of regulated thin filaments for myosin, so proposed a kinetic activation of the product release step. Regardless of the precise mechanism of activation, a series of proteins are involved in the transmission of information about the status of the Ca binding site to the ATPase site

on the myosin head. The number of proteins involved makes this a complicated process.

#### Thick filament regulation

Thick filament regulation can occur by two different mechanisms, the phosphorylation based method of smooth and non-muscle myosins and the direct Ca binding system found in molluscs. Where contraction is regulated via phosphorylation a rise in intracellular Ca concentration leads to Ca binding to calmodulin. This activates myosin light chain kinase which, in turn, phosphorylates a serine residue on the regulatory light chain of myosin thus activating the ATPase. The process is reversed by a Ca insensitive phosphatase. Activation is a relatively slow process, taking several seconds to activate fully, but a small rise in intracellular Ca concentration can lead to a large increase in the activity of the muscle. A more complex picture of Ca regulation of smooth muscle myosin will be discussed in chapter 7.

#### Molluscan thick filament regulation

Kendrick-Jones et al (1970) discovered a thick filament regulatory system in molluscs. The complex formed between scallop myosin and pure rabbit actin had a Ca sensitive ATPase. Additionally it was found that molluscan thin filaments did not restore Ca sensitivity to rabbit myosin. Szent Gyorgyi et al, (1973) showed that it was the regulatory light chain of myosin that was vital for Ca

sensitivity. If the regulatory light chain (RLC) was removed, the ATPase became insensitive to Ca and exhibited a permanently activated rate. Rebinding of RLCs to myosin restored Ca sensitivity. RLCs could also be replaced by light chains from other species, allowing the role of the RLC in the ATPase mechanism to be studied. The ATPase and the ability of myosin to interact with actin were controlled by Ca binding to myosin. The site of Ca binding was subsequently located as being in the neck region involving the heavy chain and essential light chain (Collins et al, 1986). Vale et al, (1984), using the Nitella movement assay, demonstrated the vital role which the regulatory light chain has in regulating movement. When the light chain was present, movement was highly Ca sensitive but once the regulatory light chain had been removed, movement became Ca insensitive.

How could myosin linked regulation function? Three possible mechanisms are presented below.

(i) Steric blocking. Light chain movement induced by Ca binding could prevent actin binding and subsequent actin-activation.

(ii) Restricted flexibility. In the absence of Ca, myosin heads are unable to reach the thin filaments preventing activation.

(iii) Conformational changes. Ca alters the conformation of myosin heads and consequently the ATPase activity directly.

Figure 8-1 describes these three mechanisms for regulation. The mechanism of regulation is discussed in the light of

results presented in this thesis, in chapter 8.

### Scallop myosin ATPase

As mentioned above, molluscan myosin exhibits thick filament regulation. That is, Ca exerts its effect on the ATPase and actin binding properties of myosin directly. Regulation occurs via Ca binding to myosin not via a phosphorylation mechanism. Although the exact location of the Ca binding site has yet to be located, it is known that it binds in the neck region of the molecule, possibly involving both the essential light chain and the heavy chain (Collins et al, 1986). The ATPase site is remote from the Ca binding domain, being located towards the middle of the head (Munson et al, 1986).

There are two types of divalent metal binding sites on the myosin head which play a role in ATPase regulation. There is a non-specific site which can bind Mg or Ca ions, and is involved in the binding of the regulatory light chain to the heavy chain. It cannot be involved directly in regulation since under physiological conditions the majority of the sites would have Mg bound to them, and Mg dissociation is too slow to account for the speed of activation necessary (Bennett and Bagshaw, 1986). The specific Ca binding site is the one responsible for regulation of the ATPase activity and has a binding constant for Ca of about  $10^{-7}$  M (Chantler et al, 1981). Thus under relaxing conditions in the cell, when the Ca concentration is below 100 nM, the site is essentially free of Ca but on stimulation, when the Ca level

rises to about  $10 \mu\text{M}$ , the majority of the sites have Ca bound.

Scallop striated muscle is activated by direct Ca binding to the myosin which is both fast (c.f. the slow thick filament regulation in smooth muscle) and relatively simple in organisation (c.f. vertebrate striated thin filament regulation). Ashiba et al (1980), demonstrated that the myosin ATPase was intrinsically Ca sensitive. A 3-fold Ca-activation of the steady-state HMM ATPase was measured by Wells et al (1985). Actin appears to further enhance the degree of Ca activation of the ATPase. Direct activation of the ATPase introduces a second dimension to a study of the enzymic activity since now myosin can hydrolyse ATP in the presence or absence of Ca (see equation 4-2).

Measurements of oxygen consumption in relaxed and activated frog striated muscle allow estimates of the ATPase rates under the respective conditions to be made. They suggest that an activation of about 3000-fold of the ATPase is possible (Kushmerick and Davis, 1969, Kushmerick and Paul, 1976). Steady-state assays using purified proteins reveal that Ca induces only a four-fold activation of the acto-HMM ATPase (Wells and Bagshaw, 1984a). A discrepancy between the in vivo and in vitro levels of Ca activation exists. Acto-HMM may only exhibit a four-fold activation of its ATPase and in vivo, another regulatory system may be important. Alternatively some of the HMM molecules may be insensitive to Ca and exhibit a permanently activated rate thus artificially increasing the measured value for the

relaxed rate and masking the true activation of the regulated molecules.

Wells and Bagshaw, (1984a), distinguished between these two possibilities using a turbidity assay. This assay used the light scattering changes accompanying the dissociation of acto-HMM caused by the addition of ATP and the subsequent reassociation when the ATP was consumed. In the presence of Ca,  $4\mu\text{M}$  acto-HMM turned over ATP at a rate of  $1.4 \text{ s}^{-1}$ , in agreement with steady-state assays. In the absence of Ca, the steady-state rate was reduced about 4 fold, but the rapid recovery in the turbidity assay, which occurs when the ATP is exhausted, accounted for only 25% of the total amplitude. The remaining 75% of the amplitude recovered with a rate of  $0.0018 \text{ s}^{-1}$ . This was interpreted as 75% of the HMM molecules being highly regulated (650-fold activation) and 25% being unregulated and permanently activated. The relaxed turnover rate of the regulated molecules in steady-state assays is masked by the rapid turnover rate of the unregulated molecules.

The contribution made by the regulated and unregulated molecules to the steady-state turnover of ATP depends on the turnover rate of each population and the proportion of each population. If  $R$  is the fraction of regulated molecules in a sample, and  $k_r$  and  $k_u$  are the turnover rates of the regulated and unregulated populations respectively and  $k^c$

indicates the presence of Ca, the observed steady-state rate is described by:

$$k_{ss} = R \cdot k_r + (1 - R) \cdot k_u$$

$$k_{ss}^C = R \cdot k_u^C + (1 - R) \cdot k_u^C$$

The degree of Ca activation from steady-state measurements is defined as  $k_{ss}^C/k_{ss}$ . In the presence of Ca, both populations can be assumed to turnover ATP at the same rate ( $k_u^C = k^C$ ). Hence steady-state measurements provide a value for the activated HMM-ATPase. In the absence of Ca the unregulated HMM molecules turnover ATP at the same, rapid rate ( $k_u^C = k_u$ ), while the regulated molecules have had their ATPase activity suppressed. Steady-state assay do not measure the relaxed ATPase activity due to the presence of the permanently activated molecules. Wells and Bagshaw, (1984) showed that suitable values for the above expression are  $R = 0.75$ ,  $k_u = k_u^C = k_r^C = 0.3s^{-1}$  and  $k_r = 0.002s^{-1}$ .

The conclusion of Wells and Bagshaw, (1984) was confirmed by Jackson et al, (1986) when the two populations of HMM molecules were separated by ultracentrifugation. A sample consisting of > 95% regulated molecules was produced but the separation procedure was only suitable on an analytical scale. In order to see the true Ca sensitivity of scallop HMM in a steady-state assay a sample with > 99.9% regulated molecules would be needed. Even if such a sample could be produced, Bennett and Bagshaw, (1986) showed that spontaneous dissociation of RLCs from a solution of  $4\mu M$  HMM in  $1mM$   $MgCl_2$  could lead to about 17% desensitised molecules

after several hours. Steady-state assays are therefore of limited use in probing the relaxed ATPase mechanism of scallop myosin.

Ca and ATP binding cause an increase in the tryptophan fluorescence of myosin. Wells et al, (1985) demonstrated that each ligand affected different groups of tryptophan residues. Ca perturbs residues in the neck region whereas ATP affects residues in the central region of the head. Depending upon the digestion conditions, an S1 fragment can be produced with or without the Ca binding domain ( $S1^{+RD}$  and  $S1^{-RD}$ ). The region responsible for Ca binding, the regulatory domain (RD), can be isolated by digestion of  $S1^{+RD}$ . Although Ca binds to  $S1^{+RD}$  and enhances the tryptophan fluorescence, no effect on the turnover of ATP is seen. Only HMM shows both Ca binding and a Ca sensitive ATPase which indicates that an intact neck region is important for regulation. Whether this is due to a specific role for the neck region, or whether it is because two heads are needed to act together, is not known. The properties of a single headed HMM or myosin would answer this point.

Tryptophan fluorescence provides a method by which the intrinsic Ca sensitivity of the ATPase can be examined in the absence of actin. However, the binding of ATP to HMM causes a relatively small enhancement in the protein fluorescence which limits its use. Furthermore, the rate limiting step in the hydrolysis cycle ( $P_i$  release) cannot be seen by this technique. The binding of Ca itself causes an enhancement in the tryptophan fluorescence (Wells et al,

1985) which is reversed by the addition of EGTA, providing a potential method by which the maximum rates of activation and relaxation could be measured. Many of these changes occur instantaneously when observed using manual addition techniques, necessitating the use of rapid reaction methods.

Before this work was initiated, the characteristics and properties of the scallop myosin ATPase that had already been elucidated were:

- (i) The rate limiting step of the HMM ATPase, in the absence of Ca, was Pi release.
- (ii) Ca activated the HMM ATPase by 100-fold.
- (iii) Ca could activate the acto-HMM ATPase by at least 650-fold.
- (iv) HMM existed as two populations, typically 75% regulated which responded to Ca and 25% which were Ca insensitive and permanently activated.
- (v) Ca and adenosine nucleotides perturbed tryptophan residues in the myosin head and gave small, but measurable, fluorescence changes.
- (vi) Wells and Bagshaw (1985) had suggested that ADP release was Ca sensitive.

The aims of my work were to examine the mechanism and control of the ATPase in greater detail, involving:

- (i) Measurements of the rates of nucleotide binding and dissociation by tryptophan fluorescence, both in the presence and absence of Ca.
- (ii) Determination of the kinetics of Ca binding and release.

(iii) Synthesis and use of ATP analogues, based on formycin to analyse both the ATPase and FTPase mechanisms.

(iv) Probing the product release step under a variety of conditions to determine the mechanism of regulation.

When the signals provided by natural substrates prove too small for accurate measurement of the processes involved, it is common to try to find substrate analogues which provide larger signals. These can either enhance the original signal e.g. perturb the proteins own fluorescence in a more extreme manner, or they can provide a fluorescence signal of their own. The ATP analogue, formycin triphosphate provided the required signal. It is intrinsically fluorescent, and its fluorescence is enhanced 500% upon binding to HMM. Product release is accompanied by a reversal of the enhancement.

#### Transient kinetics

Steady-state kinetics cannot be used to probe the mechanism of the relaxed HMM ATPase since the activity of the regulated molecules is masked by that of the unregulated molecules. It is the extremely low activity of the regulated molecules in the absence of Ca which is of interest, thus methods by which it can be examined are needed. Physical separation of the two populations has proved to be impossible on the preparative scale. A kinetic separation of the two populations has been possible allowing the regulated molecules to be examined in the presence of unregulated molecules.

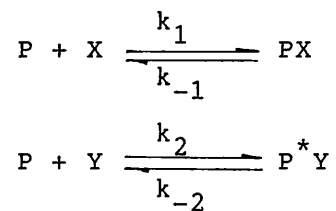
It is the use of transient kinetics techniques which allows the kinetic separation of two populations. Steady-state assays monitor the production of product (or disappearance of substrate) from an enzyme saturated with substrate. If the appearance and disappearance of enzyme/substrate intermediates can be monitored, more details of the enzyme mechanism can be obtained. If the enzyme is given a limited amount of substrate (i.e. equimolar) any molecules with a high activity (unregulated) will rapidly turn over and release products. These molecules now become effectively silent. The molecules with the lower activity (regulated) are now the only ones contributing to the observed signal, and the rate of turnover of these molecules can now be measured. Providing that the substrate binds to both populations at an equivalent and rapid rate, the rapidly turning over species can be silenced. For effective kinetic separation of populations the turnover rate must differ by  $> 5$ -fold otherwise the two phases will tend to merge making analysis difficult.

The scallop myosin ATPase is an ideal system in which to use transient kinetic techniques to determine the enzymic mechanism for the following reasons. The turnover rate is low, even in the presence of Ca, hence the concentration of enzyme bound intermediates is relatively high. Fluorescence (tryptophan or formycin) can be used to monitor the enzyme/substrate intermediates. The turnover rates of the regulated molecules is  $\sim 100$  fold slower than of the unregulated molecules.

Displacement kinetics

Non-hydrolysable substrate analogues can be used to examine particular aspects of a reaction mechanism. Binding of these analogues can often readily be monitored but measurement of the dissociation steps can be more difficult. There will be no net dissociation of such a ligand from an equilibrium mixture of protein and ligand unless the conditions are changed. A common method of achieving this is the introduction of a second ligand to compete for the same binding site. The addition of sufficient competing ligand effectively makes the concentration of free primary ligand zero, ensuring dissociation. The competing ligand can either be chromophoric, so that its binding is followed, or it can be silent, in which case the dissociation of the original ligand is monitored. Care must be taken to ensure that the process being monitored does accurately reflect the dissociation of the ligand of interest.

Displacement reactions can be summarised by the equation 1-2 (Jackson et al, 1987).

Equation 1-2

X and Y are two ligands competing for the same site on P and

only  $P^*Y$  exhibits an observable signal. Under conditions where the affinity of P for X and Y is high, the observed rate of formation of  $P^*Y$  is represented by equation 1-3 (Jackson et al, 1987).

Equation 1-3

$$k_{\text{obs}} = \frac{k_{-1}}{1 + (k_1X/k_2Y)} + \frac{k_{-2}}{1 + (k_2Y/k_1X)}$$

To ensure that  $k_{\text{obs}}$  does reflect an accurate measurement of  $k_{-1}$ , the concentration of the displacing agent must be increased several fold with little change in the value of  $k_{\text{obs}}$ .

Since the affinity of P for X is high,  $k_1 > k_{-1}$ . Consequently under conditions of effective competition  $k_2Y > k_1X > k_{-1}$ . In practice if  $k_2Y$  is 10-fold greater than the observed rate, then effective kinetic competition is assumed.

During the course of this work, two types of displacing compounds were used, non-hydrolysable substrate analogues (i.e. AMPPNP or ADP) and hydrolysable substrates (ATP and FTP). The use of hydrolysable displacing agents introduces a further complication into displacement reactions. Sufficient competing ligand must be added to ensure that it is not consumed before the reaction being monitored is complete. There must be effective kinetic competition both at the start and finish of the displacement curve. An example where this was a prime consideration was in the displacement

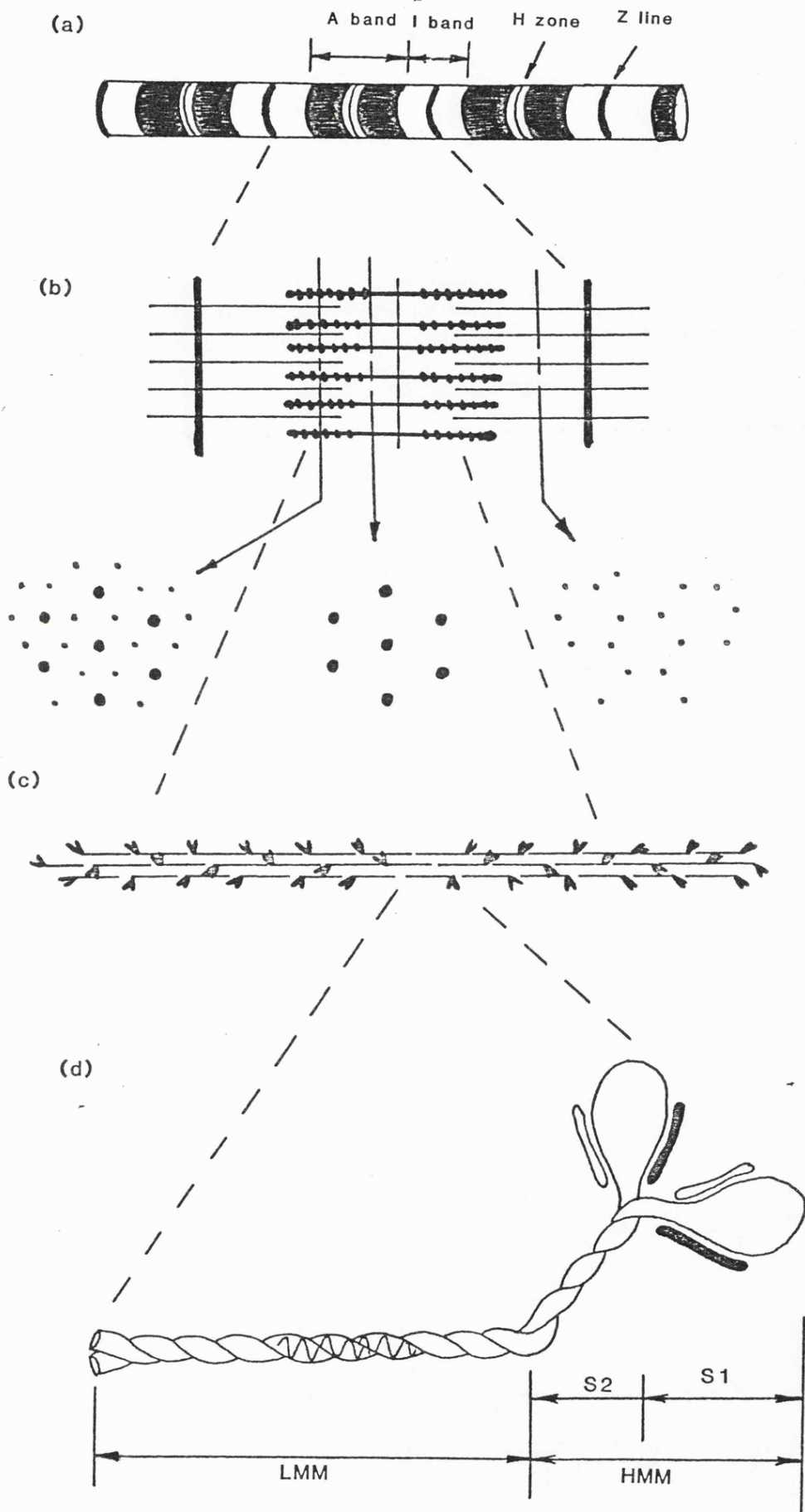
of ADP from HMM in the absence of Ca with FTP (figure 4-7a).

In this thesis I present results obtained from a study of both the ATPase and FTPase activities of scallop HMM, S1 and myosin. The use of both adenosine and formycin nucleotides has provided complementary and confirmatory evidence about the mode of regulation. No one nucleotide has been able to provide sufficient information to describe the regulatory mechanism, but the combination of several nucleotides has allowed a generalised scheme for regulation to be proposed.

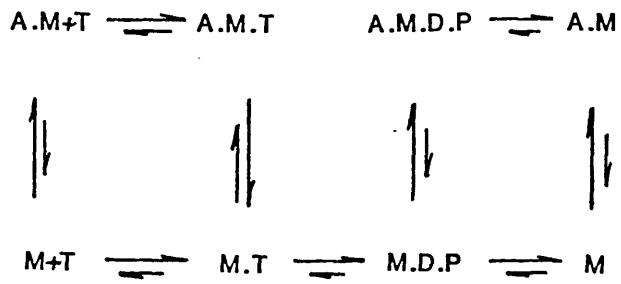
Figure 1-1

Diagram of the substructure of:

- (a) myofibril
- (b) sarcomere (transverse and longitudinal section)
- (c) thick filament
- (d) myosin



(a)



(b)

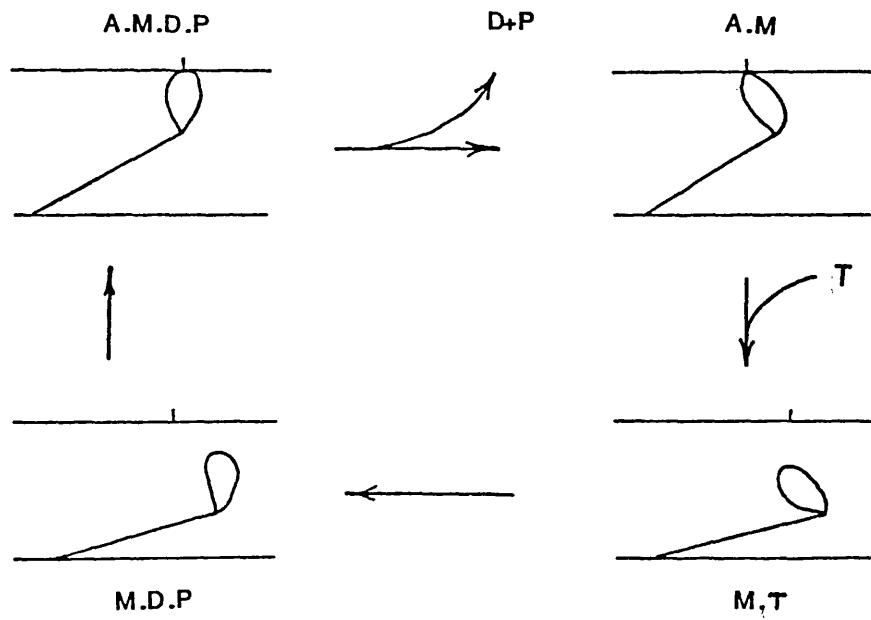


Figure 1-2

Cross-bridge cycle based on the Lymn-Taylor scheme (Lymn and Taylor, 1971).

(a) Kinetic scheme of Lymn and Taylor.

(b) Correlation of kinetic scheme with structural states of the cross-bridge cycle.

CHAPTER 2

MATERIALS AND METHODS

## General

Unless otherwise stated all protein preparations were carried out at 0-4°C. All the solutions were made up using water which had been distilled and passed through a Millipore SuperQ filtration system.

Biochemicals and proteolytic enzymes were purchased from Sigma (Poole, England). General laboratory reagents were purchased from BDH (Poole, England), Sigma (Poole, England) or Fisons (Loughborough, England). Analytical grade reagents were used where possible, but even so contaminant  $\text{Ca}^{2+}$  may reach  $10\mu\text{M}$  in the buffers used (Bagshaw and Kendrick-Jones, 1979).

## Protein Preparation

### Scallop Muscle Storage

Live scallops (Pecten maximus), obtained from the Marine Biology Station, Millport, Scotland or the Marine Biology Association, Plymouth, were dissected to leave only the striated adductor muscle in the shell. The muscle was stored at extended length overnight in glycerination solution (40mM NaCl, 5mM NaPi pH 7.0, 1mM  $\text{MgCl}_2$ , 1mM EGTA, 50% glycerol, 3mM sodium azide). The muscle was then cut out of the shell and teased into approximately 50 strips and placed in fresh glycerination solution for a further 48 hours with two changes of solution. The muscle was then stored in glycerination solution at -20°C.

### Scallop Myofibril Preparation

Myofibrils were prepared by a method based on Lehman and Szent-Gyorgyi (1975). Approximately 50ml of glycerinated scallop muscle (equivalent to about 1.5 muscles) were blended in 1 litre of EGTA wash buffer (40mM NaCl, 5mM NaPi pH 7.0, 1mM MgCl<sub>2</sub>, 0.1mM EGTA) for 4 x 10 seconds. Any unblended material was removed by filtering through a fine nylon mesh before centrifuging at 17000g for 10 minutes (Sorvall RC5B, GSA rotor) to sediment the myofibrils. The myofibrils were resuspended in 1 litre of EGTA wash buffer and recentrifuged. The washing procedure was repeated twice. The resulting myofibrils, typically 3g of protein, were then usually used to make myosin.

### Scallop Myosin Preparation

Scallop myosin was prepared by an ammonium sulphate fractionation procedure based on Chantler and Szent-Gyorgyi (1978). The myofibril pellet was resuspended in 40mM NaCl, 5mM NaPi pH 7.0, 1mM EGTA and then NaCl added to 0.6M. The suspension was gently homogenised, ATP added to a final concentration of 5mM and left to stand for 10 minutes before centrifugation at 17000g (Sorvall RC5B, GSA rotor) for 10 minute leaving acto-myosin in the supernatant. A further 5mM ATP and 20mM MgCl<sub>2</sub> was added to the supernatant and saturated ammonium sulphate added to 40%. The actin precipitate was removed by centrifugation at 17000g (as above) for 10 minutes. The supernatant was then made 70%

ammonium sulphate and the myosin precipitate collected by centrifugation (as above). The pellet was then taken up in Ca wash buffer (40mM NaCl, 5mM NaPi pH 7.0, 1mM MgCl<sub>2</sub>, 0.1mM CaCl<sub>2</sub>) and dialysed against this buffer overnight. The myosin suspension was pelleted by centrifugation at 30000g for 10 minutes (Sorvall RC5B, SS34 rotor). The myosin was washed twice by resuspension in Ca wash buffer and centrifugation. Typically 500mg of myosin could be obtained from 3g of myofibrillar protein.

#### Scallop Heavy Meromyosin (HMM) preparation

Scallop HMM was prepared by a method based on Wells and Bagshaw (1983). Myosin was dissolved in 0.6M NaCl Ca wash buffer and any undissolved material removed by centrifugation at 30000g for 10 minutes (Sorvall RC5B, SS34 rotor). The myosin was made to 10-15mg/ml and warmed to 20°C. Digestion was carried out for 3 minutes with 1/1000 w/w (myosin/trypsin) TPCK treated trypsin. The digestion was terminated by the addition of soy bean trypsin inhibitor to a five fold weight excess and by placing on ice. The solution was then dialysed against zero NaCl Ca wash buffer for 1 hour and then Ca wash buffer for a further 3 hours. Precipitated light meromyosin (LMM) and undigested myosin were removed by centrifugation (as above). The HMM was concentrated by making the supernatant 0.1mM EGTA and adding solid ammonium sulphate to 65% and centrifuging (as above). The pellet was then taken up in 10mM TES pH 7.5, 1mM MgCl<sub>2</sub>, 20 mM NaCl and dialysed against this buffer overnight. Any precipitate which formed was

removed by centrifugation before use.

#### Scallop Subfragment 1 (S1) Preparation

Two forms of scallop S1 could be prepared, depending upon the ionic conditions under which the digestion was carried out. In the presence of Mg and Ca ions, S1 with the associated regulatory domain (S1<sup>+RD</sup>) was the product, whereas in the absence of divalent metal ions, an S1 without the regulatory domain (S1<sup>-RD</sup>) was produced (Wells and Bagshaw, 1983).

The method was based on that used to produce rabbit S1 (Bagshaw and Reed, 1976) with the two forms of S1 being prepared according to the digestion conditions (Margossian et al, 1975, Stafford et al 1979). Freshly made myosin was prepared as a fine suspension in 0.12M NaCl, 20mM NaPi pH 7.0 plus either 1mM MgCl<sub>2</sub>, 1mM CaCl<sub>2</sub> or 1mM EDTA to approximately 15mg/ml. Activated papain solution (132μl papain, 300μl 0.1M DTT, 500μl 3M KCl, and 2.06ml water) was prepared and added at 3μl of papain mix per mg of myosin. Digestion was carried out at 20°C for 7 minutes before being terminated by the addition of iodoacetate (10mg/ml in 0.5M potassium phosphate, pH 6.8) to 0.1mg/ml followed by incubation for a further 5 minutes. The undigested myosin and the myosin rods were precipitated out by diluting to 40mM NaCl with 1mM CaCl<sub>2</sub>, 1mM MgCl<sub>2</sub> and removed by centrifugation at 30000g for 10 minutes (Sorvall RC5B, SS34 rotor). The S1 in the supernatant was concentrated by making to 70% ammonium sulphate and centrifuging (as

above). The pellet was resuspended in 10mM TES pH 7.5, 20mM NaCl, 1mM MgCl<sub>2</sub> and dialysed against this buffer overnight. Any precipitate which formed was removed by centrifugation (as above) before use.

#### Rabbit Myosin Preparation

Rabbit skeletal myosin was prepared by a method based on Margossian and Lowey (1982). A white New Zealand rabbit (7-8 kg) was killed, bled and the back and white leg muscles removed and placed in iced water. The muscle was then minced and weighed before being placed in 3 volumes of Guba-Straub buffer (0.3M KCl, 0.15M potassium phosphate pH 6.5) for 30 minutes and gently stirred. The extraction was stopped by dilution with 4 volumes of water and filtering through a fine nylon mesh. The mince was retained for the acetone powder preparation. The filtrate was further diluted to 40mM KCl and left for 4 hours. The supernatant was syphoned off, and the precipitate collected by centrifugation (10 minutes at 17000g, Sorvall RC5B, GSA rotor). The pellet was dissolved in 0.6M KCl, 5mM imadazole pH 7.0 and left to stand overnight. Acto-myosin was precipitated by the addition of 1.14 volumes of water and removed by centrifugation (as above). The supernatant was diluted with a further 6 volumes of water and the precipitated myosin collected by centrifugation (as above). The pellet was redissolved in the high salt buffer and the dilution steps repeated. The final pellet was dissolved up in 1.2M KCl, 10mM NaPi pH 7.0, 2mM MgCl<sub>2</sub>, 0.2mM EGTA, 6mM sodium azide to give a final concentration of approximately

40mg/ml. An equal volume of glycerol was added, stirred in thoroughly and stored at  $-20^{\circ}\text{C}$ . Just prior to use, the myosin was diluted 15-20 fold with water and centrifuged (as above) to pellet the myosin.

#### Rabbit Acetone Powder Preparation

The minced muscle pellet obtained during the myosin preparation was stirred into 5 volumes of 0.4%  $\text{Na}_2\text{CO}_3$ , 0.1mM  $\text{CaCl}_2$  for 30 minutes. The suspension was then filtered through a fine nylon mesh and the filtrate discarded. The pellet was then resuspended in 1 volume of 10mM  $\text{NaHCO}_3$ , 10mM  $\text{Na}_2\text{CO}_3$ , 0.1mM  $\text{CaCl}_2$  for 10 minutes. The suspension was poured into 5 litres of water at room temperature and immediately filtered thorough nylon mesh at  $4^{\circ}\text{C}$  to remove as much liquid as possible. The pellet was resuspended in 1 litre of cold acetone, left to stand for 15 minutes and filtered. The pellet was washed in a further 800ml of acetone, to remove all traces of water, and filtered. This time the pellet was chopped into small strands and left overnight. When all the acetone had evaporated the acetone powder was stored at  $-20^{\circ}\text{C}$ .

#### Rabbit Actin Preparation

This method was based on Spudich and Watt (1971). Approximately 4g of acetone powder was suspended in 10mM Tris pH 8.0, 0.5mM ATP, 0.5mM DTT, 0.2mM  $\text{CaCl}_2$  at  $0^{\circ}\text{C}$  for 1 hour with occasional stirring. The suspension was filtered through a nylon mesh and the pellet discarded. The

supernatant was then centrifuged at 100 000g for 1 hour (Sorvall OTD65B Ultracentrifuge, TFT 50.38 rotor). It was then brought to 20°C and made to 50mM KCl, 1mM MgCl<sub>2</sub>, 10mM NaPi pH 7.0 and allowed to stand for 1 hour. Solid KCl was added, to give a final concentration of 0.85M and left to stand overnight. It was then centrifuged at 100 000g (as above) for 2.5 hours to pellet the F-actin. The pellet was resuspended in 2mM Tris pH 8.0, 0.1mM ATP, 0.1mM DTT and dialysed overnight followed by a further 4 hours against 2mM Tris pH 8.0, before being given a clarifying spin at 30000g for 10 minutes (Sorvall RC5B, SS34 rotor). The actin was polymerised by the addition of 2mM MgCl<sub>2</sub>, 100mM NaCl and 1mM sodium azide added to aid storage at 4°C.

#### Yeast S100 preparation

S100 is a cell free extract of yeast which contains the aminoacyl tRNA synthetases used in the synthesis of some ATP analogues. The method was based on that of Nirenberg (1963) but has been substantially simplified. Nirenberg originally used E.Coli as his source of material. Lysing these cells released large quantities of DNA into the preparation which made the solution very viscous. In this preparation fresh bakers yeast was used. The advantages are two fold: firstly, upon lysis most of the DNA remains in the nucleus and is spun out with the cell debris, secondly, large quantities of live yeast can be readily purchased.

Approximately 40g of fresh bakers yeast was suspended in

60mM KCl, 10mM Tris pH 8.0, 14mM MgCl<sub>2</sub>, 6mM 2-mercaptoethanol, and the cells lysed by passing through a French Press twice. It was then spun at 30000g (Sorvall RC3B, SS34 rotor) for 1 hour to remove the cell debris. The supernatant was then dialysed against the above buffer for 4 hours (4 x 1 litre) after which it was spun at 100 000g (Sorvall OTD65B Ultracentrifuge, TFT 50.38 rotor) for 2 hours producing the S100 supernatant. This could be used directly or rapidly frozen in dry ice/ethanol bath and stored at -70°C.

#### Acto-myosin Cross-linking

Covalent cross-linking of the myosin head to actin was carried out using the cross-linker 1-ethyl-3-(3-(diethylamino)propyl) carbodiimide (EDC), (Sigma). Acto-HMM (or S1) was incubated with EDC. EDC initially reacts with a carboxyl group on actin, which can then react with an amino group on the myosin head, forming a peptide linkage. No extra atoms are introduced into the resulting complex, thus EDC is called a 'zero length' cross-linker. The cross-linking reaction is not very specific, which caused many problems with unwanted cross-links forming.

EDC cross-linking was carried out by a method based on Sutoh (1983). The Sutoh one-step method proved to be easier to perform and gave better results than the two-step method of Rouayrenc *et al.* (1984). To a mixture of 4µM actin, 2µM HMM in 10 mM TES pH 7.5, 1mM MgCl<sub>2</sub>, 20mM NaCl,

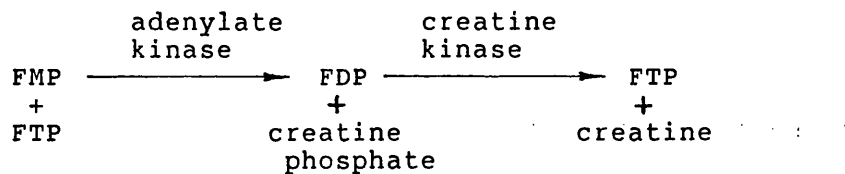
0.1mM CaCl<sub>2</sub> at 0°C, 5mM EDC was added. Aliquots were removed at various times for analysis by SDS PAGE or ATPase assays.

### Nucleotide Syntheses

#### Formycin Triphosphate (FTP)

FTP was prepared enzymically from FMP by the method of (Rossomando et al, 1981) using adenylate kinase and creatine kinase (pyruvate kinase can also be used with no change in yield). Initially a trace of FTP (or ATP) is required to react with the adenylate kinase and FMP to produce FDP, which is then converted to FTP by the creatine kinase. The reaction continues until all the FMP is consumed.

i.e.



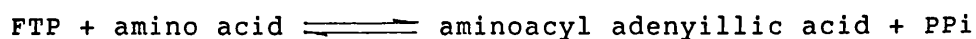
A mixture of 10mM FMP, 20μM FTP, 50mM creatine phosphate, 10mM MgCl<sub>2</sub>, 50 units/ml creatine kinase (Sigma), 40 units/ml adenylate kinase (Sigma), 100mM Tris pH 8.0 was incubated for 2 hours at room temperature. The reaction was halted by boiling for 3 minutes and the denatured protein removed by centrifugation (MSE Minor bench centrifuge, maximum speed, 10 minutes). The FTP was then

purified by column chromatography using DEAE-Sephadex A25 in a 1 x 25 cm column. Crude FTP was loaded in 0.1M triethylamine bicarbonate (TEAB) pH 7.3, which was produced from a stock prepared by bubbling CO<sub>2</sub> (from dry ice) through a 1M solution of triethylamine until the pH had fallen below pH 7.3. See figure 2-1a for details of running conditions and elution profile. The two major peaks (FDP and FTP respectively) were pooled, evaporated to dryness using a rotary evaporator and washed twice with ethanol. The FTP (or FDP) was removed from the flask with 2 x 1ml of water and stored at -20°C. Typically about 70% of the FMP was converted into FTP and 10% into FDP.

#### FMPPNP preparation

FMPPNP was prepared from FTP by a method based on that of Rodbell et al, (1971) which was scaled up to the micromolar level. The activation of amino acids prior to the production of aminoacyl tRNA is a reversible reaction, in which aminoacyl adenylic acid plus pyrophosphate is formed. The pyrophosphate analogue, imidodiphosphate (PNP), can then be incorporated irreversibly by the reverse reaction.

i.e



Theoretically the reaction should proceed until all the FTP

is converted into FMPPNP. This does not occur due to the presence of competing phosphatases in the S100 preparation which hydrolyse the FTP. FTP reacts relatively poorly with the aminoacyl tRNA synthetases thus the yield of FMPPNP is much lower than the corresponding yield of AMPPNP.

A mixture of 3mM FTP, 12mM PNP, 140mM Tris pH 8.0, 15mM MgCl<sub>2</sub> and 0.4mM of all amino acids except leucine (omitted by Rodbell et al (1971), for unstated reasons) was made to volume with yeast S100, and incubated for 1 hour at room temperature. A white precipitate formed (possibly MgPNP) but this did not appear to affect the reaction. The incubation was halted by placing in a boiling water bath for 3 minutes and the precipitate removed by centrifugation (MSE Minor bench centrifuge, maximum speed, 10 minutes) and allowed to cool to room temperature. Adenylate kinase (Sigma, 25 units/ml) and rabbit S1 (2.5 μM) was added and incubated overnight at room temperature, to convert any remaining FTP and FDP to FMP, to aid the purification. The reaction was stopped by boiling for 3 minutes and the precipitate removed by centrifugation (as above). The FMPPNP was partially purified by column chromatography as for FTP, see figure 2-1b for details of the column and a typical elution profile. The major peak produced is FMP which was discarded. FDP, FMPPNP and FTP are poorly resolved so these peaks were pooled and evaporated to dryness on the rotary evaporator. The sample was taken up in about 20ml of 0.1M TEAB pH 7.6 at room temperature, applied to the mono Q column attached to a FPLC machine (see below for full details of equipment and method) and

eluted with a 0.1M-0.7M TEAB pH 7.6 gradient at room temperature. The additional resolution provided by the mono Q column allowed the FMPPNP to be separated to a purity of >98% in one step. Useful quantities of FDP were also separated from the mixture, see figure 2-1c for details of conditions and elution profile. The FMPPNP and FDP were then concentrated to about 2mM by centrifugation under vacuum (Gyrovac, Howe). The samples were then stored at -20°C for future use. A yield of about 10% of FMPPNP and 15% FDP was produced from the FTP.

#### AMPPNP Synthesis

AMPPNP was produced in the same way as FMPPNP was prepared. ATP is a far better substrate for the synthetases so the problem of phosphatase activity was not so severe. The adenylate kinase and rabbit S1 also hydrolysed the unreacted ATP and ADP to AMP so the purification did not require the FPLC to provide the added resolution. A yield of about 60% of AMPPNP could be obtained from the ATP. The sample was stored in aqueous solution at -20°C.

#### General Analytical Techniques

##### Protein Concentration

All protein concentrations were measured using a Pye-Unicam SP8-100 UV/VIS spectrophotometer and scanned from 340nm to 220 nm to enable a correction for light scatter to be made. Insoluble proteins were solubilized by boiling for 1

minute in a 1% SDS solution. Table 2-1 gives the absorption coefficients which were used, (Chantler and Szent-Gyorgyi, 1978, Bagshaw and Kendrick-Jones 1979, Wells and Bagshaw 1983).

Table 2-1

Protein	$A_{280}$ 1mg/ml 1cm
Scallop myofibrils	0.72
myosin	0.54
HMM	0.65
S1 <sup>+RD</sup>	0.79
S1 <sup>-RD</sup>	0.75
Rabbit myosin	0.54
actin	1.10

The concentration of myosin and HMM is quoted as concentration of heads not molecules in this thesis to allow direct comparison with S1.

### Nucleotide concentrations

Concentration of adenosine and formycin nucleotides was determined using the SP8-100 UV/VIS spectrophotometer. Table 2-2 gives the absorption coefficients used.

Table 2-2

Nucleotide	$A^{1mM\ 1cm}$
Adenosine	15.4 (259nm)
Formycin	9.95 (295nm) (Ward <u>et al</u> , 1969a)

### pH measurements

All pH measurements were made at 20°C using either a Radiometer PHM82 standard pH meter with a Russell CMAWL combination electrode or on a Pe. tracourt PHM4 portable pH meter with a Russell gel filled combination electrode.

### Analysis of Nucleotides

#### Thin Layer Chromatography

TLC provided a quick, convenient assay system for nucleotides although it was relatively insensitive and only qualitative. It was used during syntheses to check the

progress of the reactions. 0.1mm cellulose MN 300 polyethyleneimine (PEI) impregnated TLC plates with a fluorescent background marker were spotted with samples and run in 0.75M potassium phosphate, pH 3.8, until the solvent front reached the top of the plate. The plate was then dried and viewed under short wavelength UV and the positions of the samples noted. Adenosine nucleotides showed as dark spots and formycin nucleotides as pale blue spots.

#### Rapid Ion Exchange Chromatography

This proved to be a highly sensitive and quantitative analytical technique. It was used to determine the purity of nucleotide samples produced, analyse the progress of the myosin ATPase in a discontinuous assay system and as a final purification step in the production of FMPPNP. A Fast Protein Liquid Chromatography (FPLC) machine consisting of a gradient programmer, GP-250, two P-500 pumps, a two channel chart recorder, REC-482, a single path monitor, UV1 and a frac-100 fraction collector together with a mono Q anion exchange column (all from Pharmacia) was used. The chart recorder output was also connected directly into an Apple II+ microcomputer via an A/D converter so data could be stored on disc for future analysis.

For analytical work, approximately 10 nmols of sample were loaded onto the column in 20mM Bis-Tris pH 6.5 and eluted on a 0 - 1.0 M NaCl gradient. The relative positions of the peaks were recorded and compared to known standards. Figure 2-2 shows the separation obtained with ATP, AMPPNP and ADP

and the corresponding separation of FTP, FMPPNP and FDP. Adenosine nucleotides were monitored at 254nm and formycin nucleotides at 280nm. When the relative quantities of mono-, di- and triphosphate were required, the area under each peak was computed using the Integrator programme.

For preparative work up to 10  $\mu$ mols of sample could be loaded onto the column. The samples were loaded onto the column in 0.1M TEAB pH 7.6 and eluted with a 0.1M-1.0M TEAB gradient. TEAB was used because it is volatile and readily removed during the subsequent concentration of the sample. Large scale purification of nucleotides requires that the eluent was monitored away from the peak absorbance, i.e. formycin nucleotides were monitored at 254nm and adenosine nucleotides at 280nm. Figure 2-1c shows a preparative run on the FPLC. The peaks were identified by comparison with known standards. In all cases the nucleotides eluted in the order monophosphate, diphosphate, imidotriphosphate and triphosphate. The absolute position of the peaks varied, but not their relative position.

### Gel Electrophoresis

SDS polyacrylamide gel electrophoresis (SDS PAGE) was carried out to analyse the composition of various protein samples. Two solutions were mixed to produce a linear gradient of 7% to 20% w/v acrylamide. The gel (15 x 11 x 0.2cm) was overlaid with butanol. Once set, the excess butanol was removed and a 4.5% (w/v acrylamide) stacking gel placed on top. A comb was inserted into the stacking gel to

produce sample wells. Gel samples were prepared by mixing with equal volumes of sample buffer (180mM Tris-HCl, 5.7% SDS, 29% v/v glycerol, 0.005% bromothymol blue) and adding 5 $\mu$ l 2-mercaptoethanol and boiling for 1 minute. Typically 20  $\mu$ g of protein were loaded per well and run at 20mA with water cooling, using a Chandos power pack, until the marker dye had reached the bottom of the gel. The running buffer was 25mM Tris base, 200mM glycine, 0.1% SDS. The gel was stained overnight in 0.2% w/v Kenacid blue, 10% v/v acetic acid, 50% v/v methanol and destained in 10% v/v acetic acid, 50% v/v methanol. Once fully destained, the gel was stored in 10% acetic acid.

#### Spectroscopic Equipment

Three different fluorimeters were used, a Baird Atomic SFR100, a custom built and a stopped-flow fluorimeter. The first two relied upon manual addition of sample, the latter two had very similar optical systems. All three machines complemented each other.

A Baird-Atomic SFR100 ratio recording spectrofluorimeter with either a 3ml (1cm pathlength) cuvette or a 0.5ml (0.5cm path length) cuvette in a thermostatted block, maintained at 20 $^{\circ}$ C with a Tempette TE8A circulator and a Techne RB5 refrigerated water bath, was used. Fluorescence was monitored at 90 $^{\circ}$  to the exciting light. Data were collected on a Tarkan 600 chart recorder or digitised directly using an Apple II+ microcomputer, as was done for the FPLC, for later analysis.

A custom built fluorimeter was also used which had the advantage that it used the same optics and detection system as the stopped-flow apparatus (see the stopped-flow section for details) thus allowing better comparison of fluorescence amplitudes. A 3ml cuvette (1cm path length) was maintained at 20°C using a Tempette TE8A circulator and a Techne RB5 refrigerated water bath. Two photomultipliers could be used to detect 90° fluorescence (at different wavelengths if necessary) or light scatter and a photodiode used to detect transmitted light. An overhead stirrer could be used to stir the sample continuously while additions were made into the cuvette through a fine needle which allowed mixing times of about 3 seconds to be achieved. The stirrer also allowed fluorescence assays on suspended aggregates, such as myosin filaments to be carried out. In these assays the photodiode was used to check that scattering artifacts were not causing artefactual fluorescence changes. Data were collected as for the stopped-flow experiments.

#### Stopped-flow Fluorimeter

When additions are made manually, the time resolution is limited to about 3 seconds. Stopped-flow spectroscopy was used to allow the measurement of processes which occur within the manual mixing time. Time resolution down to 1ms is possible. A diagram of some of the key features of a stopped-flow machine is shown in figure 2-3a. The reactants are held in different syringes (B) which can be pushed simultaneously (A). The solutions are then brought together

in the mixing block (C) before filling the observation cell (D). The solution which was in the cell from the previous push fills the stopping syringe (H) which then hits the stopping block. The detection system is triggered (E) so that the reaction can be followed. The entire system was encased in a thermostatted aluminium block for accurate temperature control.

The mixing block is designed to ensure rapid and homogeneous mixing of the two solutions, figure 2-3b. The solution from each syringe is split into two and recombined with the solution from the other syringe in a 4 way mixing jet. It is placed as close as possible to the observation cell (typically a few millimetres) to ensure a minimum time from mixing to when observations can begin.

The observation cell is a quartz flow cell with a 2 x 2 x 5 mm cavity (figure 2-3c). All four faces are polished to allow observation at  $90^{\circ}$  and  $180^{\circ}$  to the exciting light.

The light source was a 100W mercury arc lamp (Wotan) held in an Ealing Stabilarc lamphousing powered by a stabilized power supply. Mercury lamps provide a very intense light source at a few wavelengths corresponding to the mercury emission lines (figure 2-4a) which limits the wavelengths that can be used to excite the fluorophore. The appropriate wavelength light was selected using a monochromator (Applied Photophysics) and directed onto the observation cell via a 2 x 600 mm silica light guide (Oriel Scientific). The transmission characteristics of the light guide is given in

figure 2-4b. Fluorescence was detected at  $90^{\circ}$  using a 9924B photomultiplier in a QL-30 housing powered by a PM28B high voltage supply (Thorn EMI). To ensure a linear response to light, the photomultiplier voltage was set between 400 and 800V. Filters (UG11 and WG 335, Schott Filters) were placed in front of the photomultipliers to prevent scattered light from entering. When exciting at 297 or 313 nm, >99.9% of the exciting light was absorbed (figure 2-4c).

The signal from the photomultiplier was then filtered, backed off and amplified before capture on a transient recorder (Datalab DL 902). The signal from the transient recorder could then be displayed on an oscilloscope (Leader LBO 522) or transferred to an Apple II+ microcomputer for storage on disc (500 points, 10 bit resolution). A diagram of the layout is shown in figure 2-5.

The transient recorder could capture data from 2ms to 100s full scale under internal time control, or could be driven using a variable time loop program for longer times. It was usually used in the pre A/B mode in which the first 10% of the trace was recorded over a faster time-scale. This was used to record the fluorescence of the solutions just prior to the flow stopping.

Initially one photomultiplier was used, recording over one time-base. Subsequently a second photomultiplier, a photodiode (Hamamatsu, S1136) for detection of transmitted light, and a second transient recorder (Datalab DL 902) were added, which allowed the recording of several different

signals at two different time bases. An Apple II+ microcomputer could also be used to record slower reactions directly (>100s for 1 channel and >200s for 2 channel).

The equipment was very flexible in use, allowing measurement of rate constants which varied by 6 orders of magnitude. The components could be used in many different configurations which will be described later when they differ from the basic stopped-flow arrangement.

The dead time of the apparatus was measured, by following the dissociation of acto-S1 at increasing ATP concentrations (Millar and Geeves, 1983), at 1ms. The dead time of a stopped-flow apparatus refers to the time taken for the solutions to pass from the mixing jet to the observation cell. A second order reaction is followed as a function of ligand concentration until the reaction is complete before it reaches the observation cell and no signal is seen. The rate constant when half the amplitude has been lost (i.e one half time of an exponential) allows calculation of the the time taken for the solution to reach the observation cell.

The stopped-flow fluorimeter has a 2mm optical path length compared to the 1cm pathlength in the manual addition fluorimeters. Consequently the fluorescence signals are much smaller, leading to a smaller signal to noise ratio. This can be partially overcome by the use of post-data collection manipulation. Signal averaging of many individual traces helps to remove random noise while enhancing the true signal. The stopped-flow apparatus is a

single beam spectrophotometer which can therefore suffer from fluctuations in the lamp intensity during the course of a reaction. Signal averaging can also remove these artefactual changes. Systematic errors, such as photo decomposition and scattering artefacts, can be eliminated from the experimental record by the subtraction of control traces. Rapid reactions need very small electrical time constants to prevent the observed changes being limited by the instrumental response time. However this can result in excessive high frequency noise in the trace that can often be removed by judicious digital filtering and signal averaging. Any non-random noise, such as mechanical vibrations, cannot be removed by these techniques. All of these data manipulation techniques are carried out once the raw data have been saved on disc by an Apple II+ microcomputer. These techniques have allowed the characterisation of processes associated with fluorescence changes of only 3% (Ca dissociating from HMM).

#### ATPase Assays

All the ATPase assays (unless otherwise stated) were carried out at 20°C in 10mM TES, 1mM MgCl<sub>2</sub>, 20mM NaCl, pH 7.5 with a 100µM excess of either Ca or EGTA. ATP was added as the Mg complex to ensure that the free Mg concentration was maintained close to 1mM.

### Malachite Green Phosphate Assay

This is a discontinuous assay for inorganic phosphate (Itaya and Ui, 1966). 0.8ml of malachite green reagent (1 volume of 4.2% ammonium molybdate/5M HCl plus 3 volumes 0.05% malachite green solution, incubated for 30 minutes and filtered) was added to 0.17ml of sample containing up to 20 nmols phosphate. The mixture was incubated for 30 minutes at 0°C, 30µl 0.5% Tween 20 added and incubated for a further 15 minutes at room temperature. The  $A_{640}$  was measured against a water blank. If any precipitate had formed in the malachite green reagent, it was refiltered and a new calibration curve carried out.

### Ion Exchange ATPase Assay

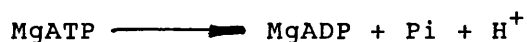
The FPLC was used to follow the course of the ATP and FTP hydrolysis reaction. At various times after mixing the nucleotide with protein, the reaction was quenched by the addition of perchloric acid. Addition of potassium hydroxide partially neutralised the sample and the precipitate was removed by centrifugation. The supernatant was carefully removed and the pH brought to 6.5. The resulting mixture, could then be analysed for mono, di and triphosphate content, using the FPLC, and the relative proportions of each determined.

These assays were carried out at 40µM HMM and 30µM nucleotide. High concentrations were required to ensure

that there was sufficient nucleotide to analyse in an appropriately small volume (<500 $\mu$ l after quenching and neutralisation) and to ensure that the nucleotide bound sufficiently rapidly.

#### pH-stat

The ATPase reaction liberates protons as a product of hydrolysis.



At pH 7.5, 0.7 protons are released per ATP hydrolysed (White, 1982). The quantity of 20 mM NaOH needed to maintain the pH at 7.5 is a measure of the steady-state ATPase activity. A pH-stat (Radiometer PHM82 pH meter coupled to a Russell CMAWL combination electrode, a TTT80 titrator, an ABU 80 autoburette and a REA-160 titigraph chart recorder) was used to follow the ATPase activity. The volume of alkali added was calibrated by the addition of a standard 0.1M HCl solution. Assays were carried out at 20°C in 1mM MgCl<sub>2</sub>, 0.1mM EGTA and the reaction started by the addition of 1mM MgATP. 0.2mM CaCl<sub>2</sub> was added during the assay to measure the activated rate.

Turbidity Assay

The amount of light scattered by a protein solution depends upon the molecular weight and shape of the molecules. The amount of light scattered can be measured either by monitoring at  $90^\circ$  to the exciting light (genuine light scatter) or by following the apparent change in absorption of the solution (turbidity). Monitoring  $90^\circ$  scatter is a very sensitive method but is prone to large artefactual changes if there are any large aggregates in the sample. The turbidity changes are less sensitive than light scattering changes but they suffer less from large artefactual changes. When two macro molecules in solution bind, the amount of light scattered increases since the light scatter of the complex is greater than the sum of the individual values. This has been exploited as an ATPase assay in the acto-myosin system (White and Taylor, 1976, Wells and Bagshaw, 1984). Here the changes in light scatter are sufficiently large so as to allow turbidity to be measured in a conventional spectrophotometer. In the absence of ATP, actin and S1 (or HMM) form a tight rigor complex. The addition of ATP causes the dissociation of the complex resulting in a drop in turbidity which rises once the ATP runs out and the rigor complex reforms.

The turbidity assays were carried out in a Pye Unicam SP8-100 UV/VIS spectrophotometer at  $20^\circ\text{C}$  in a 3ml cuvette measuring the apparent change in absorbance at 340nm. Typically  $20\mu\text{M}$  ATP was added to a mixture of  $4\mu\text{M}$  actin and  $4\mu\text{M}$  S1.

## Fluorescence Assays

The intrinsic tryptophan fluorescence of myosin and its proteolytic subfragments and the formycin nucleotide fluorescence have been exploited in the study of the ATPase mechanism.

### Tryptophan fluorescence

The amino acid tryptophan is fluorescent and the magnitude of the fluorescence signal is highly dependent on the environment in which it is situated. When adenosine nucleotides bind to the myosin head, they cause a perturbation in the environment of a group of tryptophan residues which leads to an increase in the observed fluorescence. In the scallop myosin head there is an additional and separate group of tryptophan residues which respond to Ca binding and release (Wells *et al*, 1985). The magnitude of the percentage enhancement seen also depends upon the contribution of non-perturbed tryptophan residues to the overall signal. The higher the background signal the smaller percentage enhancement seen. Hence  $S1^{-RD}$  exhibits a larger percentage enhancement in fluorescence than  $S1^{+RD}$  does upon ATP binding (16% compared to 12%) due to the loss of the tryptophan residues in the regulatory domain.

Tryptophan fluorescence was recorded using the Baird Atomic fluorimeter by exciting at 298 nm (5 nm slit width) and recording the emission at 338 nm (10 nm slit width). When

the mercury lamp was used, for the stopped-flow and custom-built fluorimeters, the excitation wavelength was 297 nm (see figure 2-4a) and the peak emission corresponded to 350 nm (fwhm 20 nm, see figure 2-4c).

Formycin is intrinsically fluorescent and the fluorescence is enhanced as it binds to the active site of myosin and its subfragments. The fluorescence is also sensitive to protein conformational changes which affect the active site. The excitation spectrum of formycin reveals a peak at 295 nm but since it is very close to the tryptophan fluorescence excitation maximum, this wavelength was not used. The excitation spectrum shows a plateau at 313 nm, which although it is only about 20% of the intensity of 295 nm, is almost clear of protein fluorescence and coincides with an emission wavelength for the mercury lamp. Hence 313 nm was the excitation wavelength of choice for all the fluorimeters used. For convenience, the same filters were used in front of the photomultipliers in the stopped-flow and custom-built fluorimeters, as was used for tryptophan fluorescence. When the Baird Atomic was used, the emission wavelength was set at 338 nm with 10nm slit widths.

#### Data Capture and Analysis

Experimental data was stored on computer (Apple II+ microcomputer) in two different forms. A binary file (500 points, 10 bit resolution) was used to store data transferred from the transient recorder and to store the data entered directly into the computer via the A/D

converter. The A/D converter allowed the computer to act as a chart recorder and could be attached to most pieces of equipment in the laboratory. The data analysis system was primarily designed for the capture and analysis of data generated by the stopped-flow apparatus. The analysis and manipulation which was carried out on these traces mainly involved signal averaging and least squares fits to exponentials (both biphasic and monophasic). The addition of the A/D converter allowed other forms of data to be collected under the same format which led to the development of other data analysis programs. These data could be manipulated by techniques such as digital filtering, baseline subtraction and expanding time bases for display purposes.

Text files, of varying length, formed the other system by which data were stored. These data were entered via the keyboard, a Cherry graphics tablet or generated by a computer simulation. A wider range of equations could be fitted to the data in this form. Data could be interconverted from one form to the other. Hard copies of the data were obtained using either a Silent Type dot matrix printer or an Epson Hi-80 plotter.

The curve fitting programs were based on those provided by Millar (1983) and extensively modified by C.R. Bagshaw. All data capture and manipulation programs were written by C.R. Bagshaw. For a further description of the programs used see appendix 1.

Figure 2-1

a Purification of FTP

Approximately 10ml of sample loaded onto 1 x 25cm DEAE Sephadex A25 column in 0.1M TEAB pH 7.3. The nucleotide was then eluted with a 0.1M - 0.7 M TEAB gradient. The FTP and FDP peaks were pooled separately and concentrated.

b Purification of FMPPNP

(1) Approximately 10 ml of sample loaded onto the column (as above).

(2) Nucleotide eluted with a 0.1M - 0.5M TEAB pH 7.3 gradient (2 x 500 ml). The nucleotide eluted as two major peaks, the first containing FMP (i), which was discarded, and the second containing a mixture of FDP, FMPPNP and FTP (ii). This was pooled and concentrated for further purification.

(3) Column washed with 1M TEAB pH 7.3.

c Purification of FMPPNP

The concentrated sample from part (b) which contained the FMPPNP was taken up in about 20ml of 0.1M TEAB, pH 7.6 and loaded onto a Mono Q column in 10 $\mu$ mol aliquots. Each aliquot was eluted with a 0.1M - 1.0M TEAB pH 7.6 gradient running the column at 2ml/min and monitoring the eluate at 254nm. The nucleotides were eluted in the order FDP (i), FMPPNP (ii), FTP (iii). The FDP and FMPPNP were concentrated for future use.

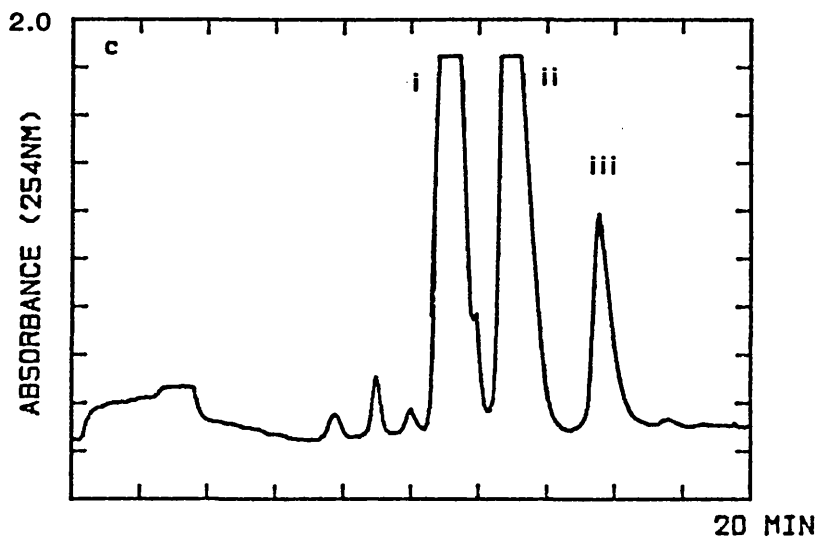
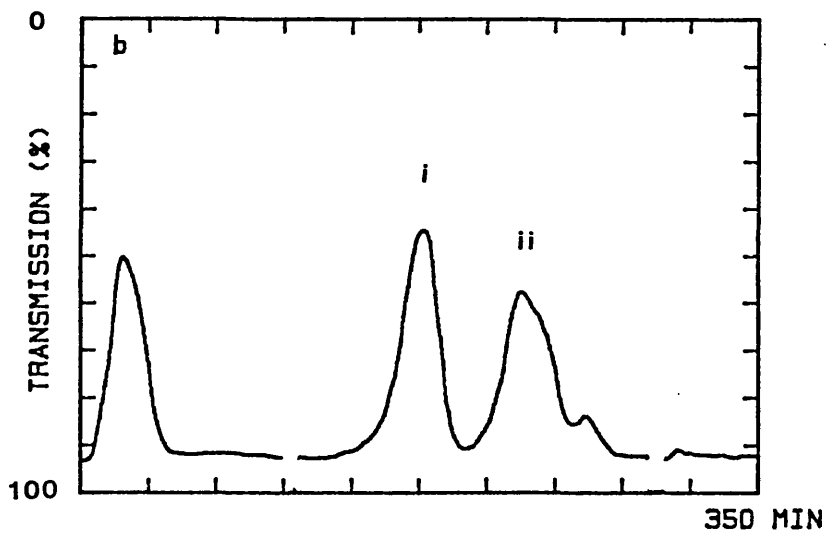
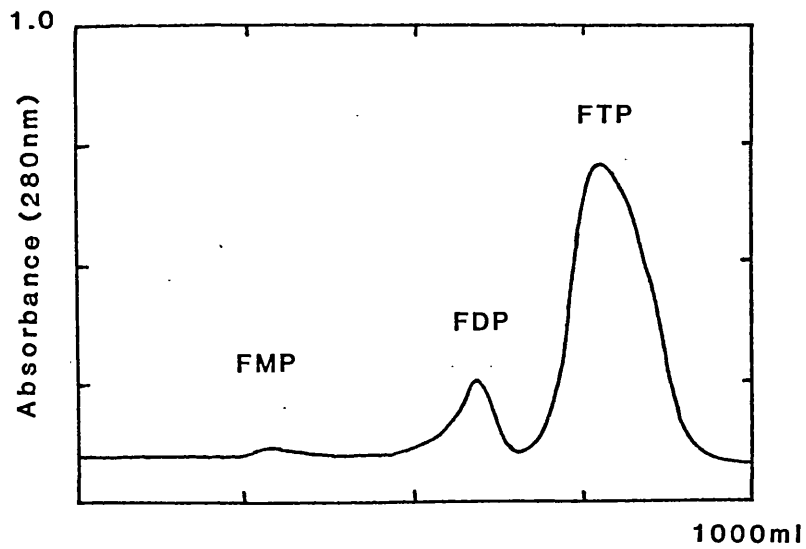
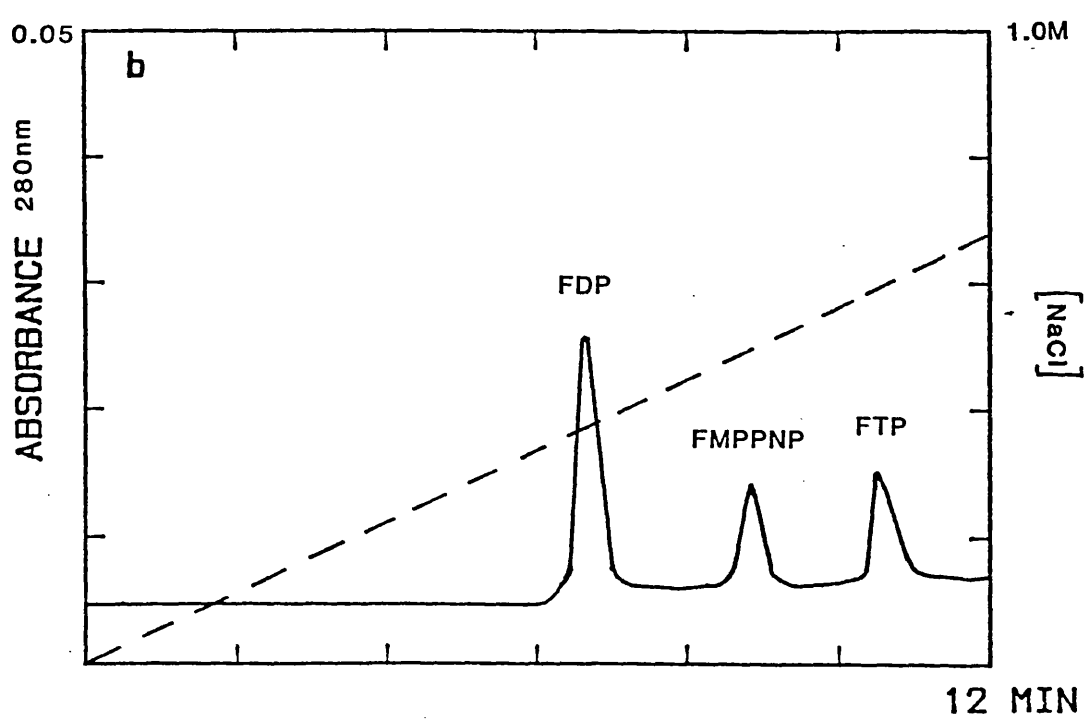
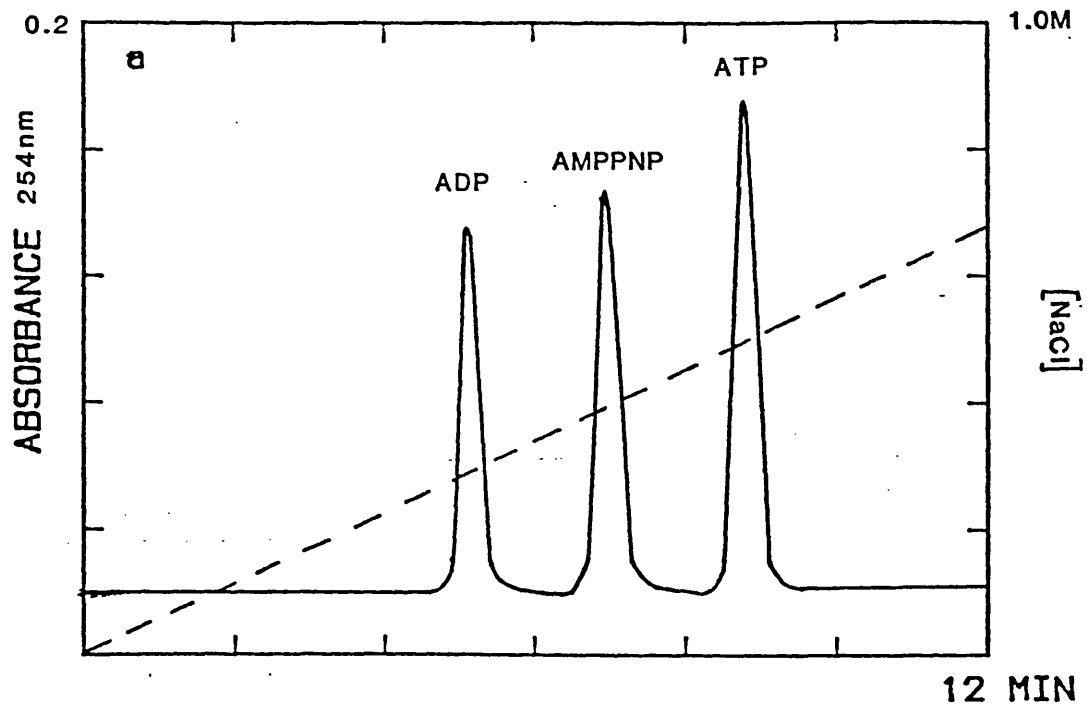


Figure 2-2

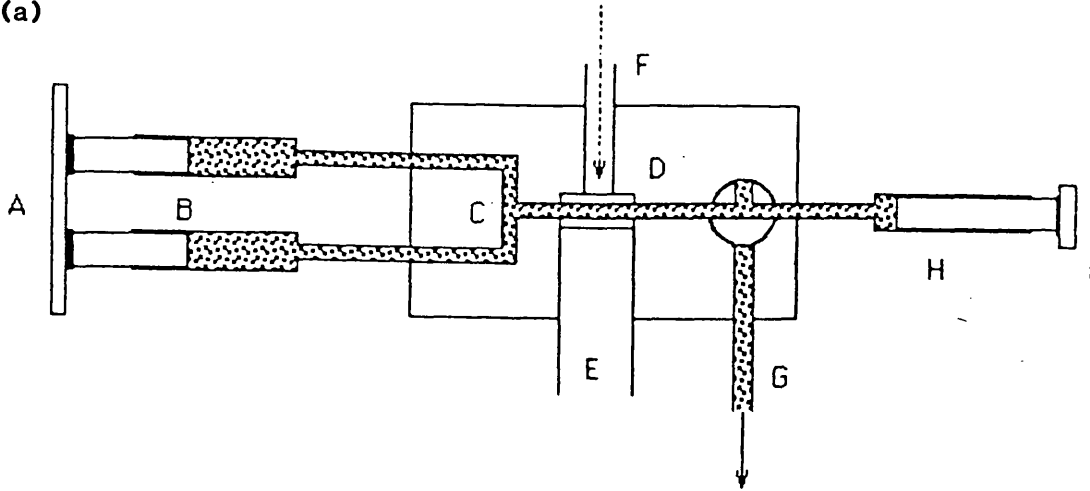
a Analysis of a mixture of ATP, AMPPNP and ADP by FPLC. Approximately 10 nmols of each nucleotide was loaded onto the Mono Q column at 2ml/min in 20 mM Bis-Tris pH 6.5 and eluted with a 0 - 1.0 M NaCl gradient (- - -) while monitoring the eluate at 254 nm. The nucleotides eluted in the order ADP, AMPPNP and ATP. When the AMPPNP, which had been produced from ATP, was analysed on its own, it was > 98% pure.

b Analysis of a mixture of FDP, FMPPNP and FTP by FPLC. The nucleotide was loaded and eluted as above with the exception that the eluate was monitored at 280 nm. The nucleotides eluted in the same order as above but the absolute position on the gradient was shifted up the gradient. All three nucleotides, when run individually, were > 98% pure.

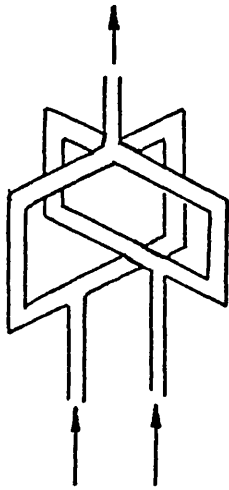




(a)



(b)



(c)

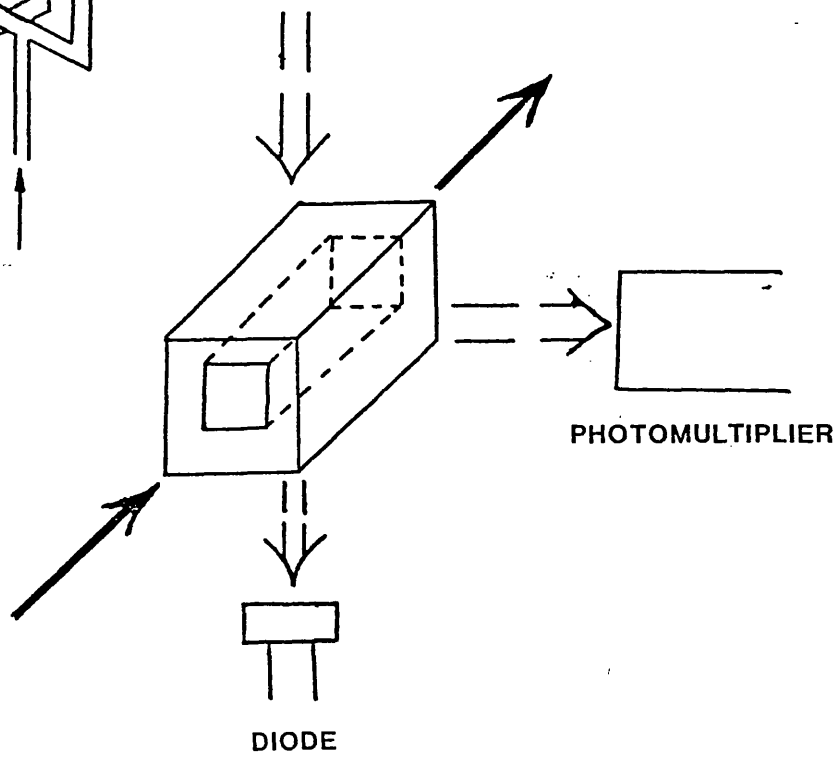


Figure 2-4

The optical characteristics of various components of the stopped-flow fluorimeter.

a Emission spectra of the mercury lamp.

b Transmission of the light guide.

c Transmission of the filter combination UG11/WG335 used for selection of formycin and tryptophan fluorescence emission.

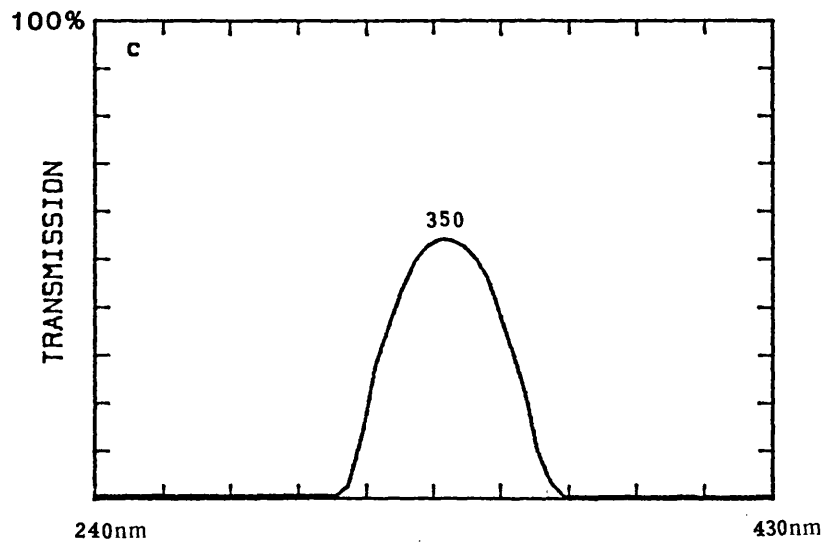
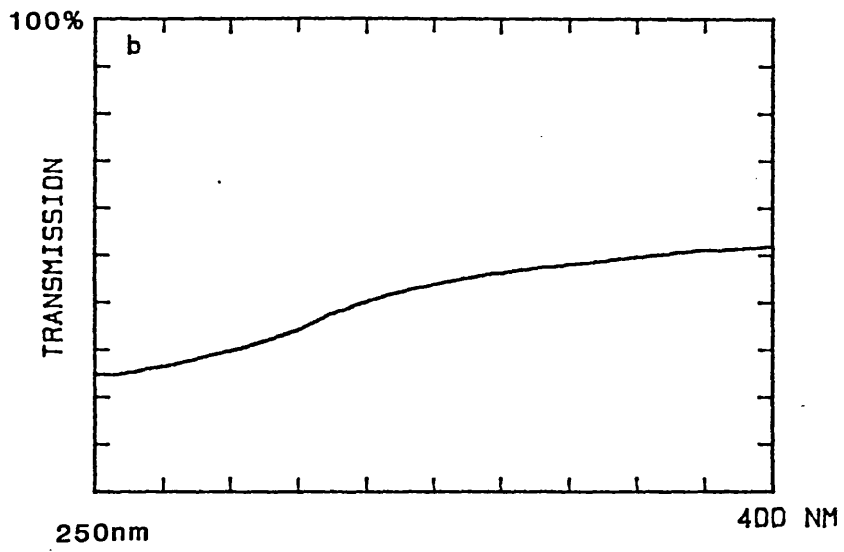
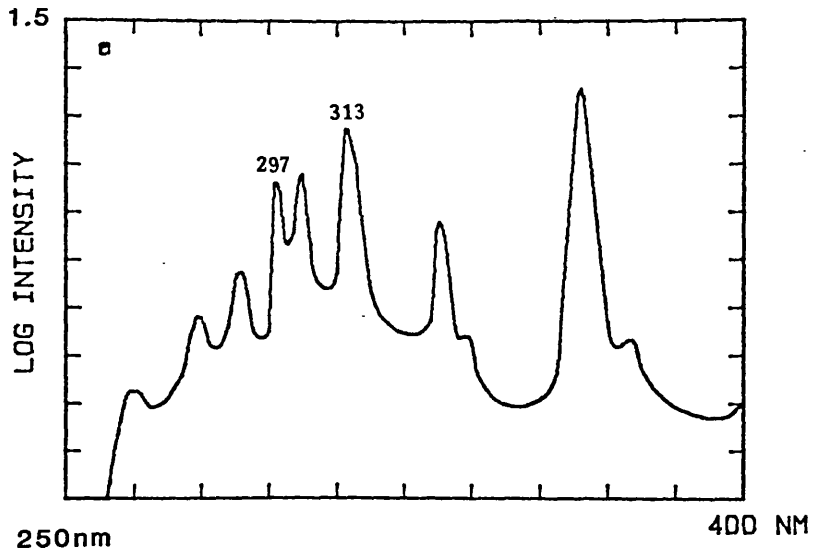
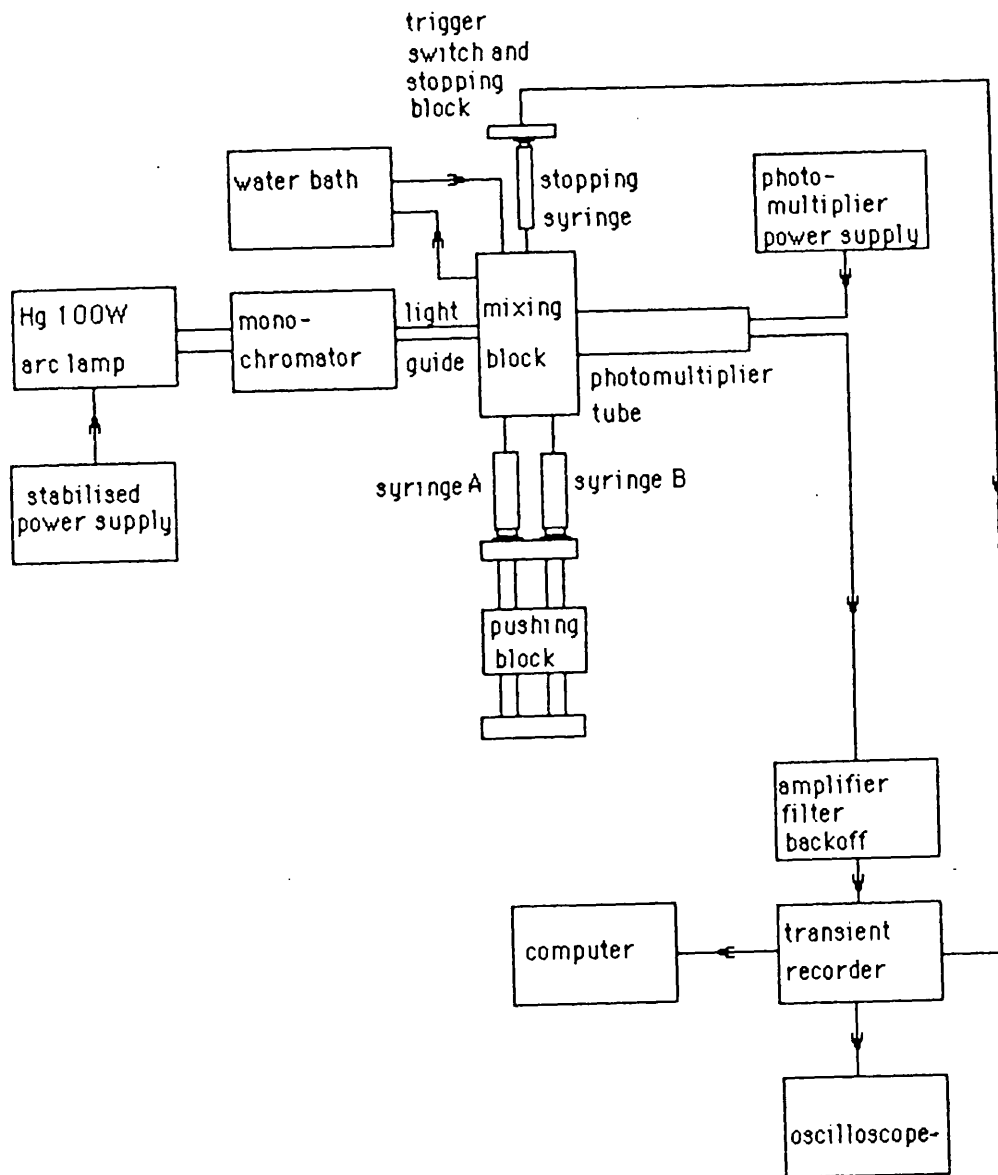


Figure 2-5

Diagrammatic representation of the components of the stopped-flow fluorimeter. Arrows represent the direction in which information flows between the various components.



CHAPTER 3

ACTO-HMM CROSS-LINKING

## Introduction

In vivo measurements have suggested that an inhibition of the acto-myosin ATPase of >2000 fold would be required to fulfill the needs of the organism in vivo (Kushmerick and Davis, 1969, Kushmerick and Paul, 1976). Measurement of the potential level of activation needs both the maximum and minimum rates of ATP turnover to be determined. Under steady-state conditions (saturating ATP) and in the presence of Ca, scallop myosin can hydrolyse ATP at a rate of  $0.3s^{-1}$ . Addition of  $4\mu M$  actin increases the turnover rate to  $1s^{-1}$ . The more actin added, the greater the degree of actin activation seen. Theoretically the maximum rate for the acto-HMM ATPase could be measured by increasing the actin concentration until no further increase in rate was observed. Several practical difficulties prevent this experiment from being performed.

Actin and HMM associate only weakly under the conditions usually used for ATPase assays (20mM NaCl, 1mM Mg, 10mM TES pH7.5) hence high actin concentrations would be required to saturate the HMM with actin. Under the conditions given above, actin becomes very viscous and thus difficult to manipulate at concentrations above  $20\mu M$ . This is below the estimated value for the  $K_m$  for actin-activation of the ATPase.

Since the affinity of actin for HMM increases with decreasing salt concentration, the  $K_m$  for actin activation

of the ATPase also decreases. Chalovich et al, (1984) reduced the ionic strength (10mM imadazole, 1.8mM Mg) in an attempt to allow sufficient actin to be added so that an accurate determination of  $V_{max}$  could be made. Using the scallop Aquiptecten, Chalovich et al, (1984) measured the  $V_{max}$  for actin activation as  $14s^{-1}$  (+Ca) and  $3s^{-1}$  (-Ca). By working at low ionic strength they were able to measure the acto-HMM ATPase activity over a large range of actin concentrations (upto  $400\mu M$ ).

Reducing the salt concentration has an additional effect on the acto-HMM system. At very low ionic strengths ( $<1mM$ ) f-actin depolymerises making the measurement of  $V_{max}$  impossible. The dual effect that ionic strength has on actin and acto-HMM interactions makes it very difficult to measure the maximum acto-HMM ATPase rate.

Solution studies are usually done at relatively low protein concentrations which is in contrast with the situation found in muscle. Not only is the protein concentration very high ( $\sim 100mg/ml$ ) in vivo but the actin is held in the ideal position for interactions with myosin heads, making the actin concentration effectively infinite. The true maximum ATPase activity will only be revealed under conditions of saturating levels of actin, as found either in vivo, or by methods which mimic the in vivo conditions.

Acto-HMM cross-linking

The problems of achieving high actin concentrations appeared to be solved when a method of chemically cross-linking actin to S1 (or HMM) was found (Mornet et al, 1981). The cross-linking reagent (EDC) forms a peptide bond between a carboxyl group from actin and an amide group from the myosin head. The resulting complex showed an elevated ATPase activity. It appeared that it would be possible to mimic the in vivo conditions where each myosin head was held in very close proximity to an actin monomer. This approach held particular promise in the scallop system where both the fully relaxed and the fully activated ATPase rates might be seen on the same sample.

Chemical cross-linking of actin to scallop HMM using EDC was performed at 0°C by the method of Sutoh (1981). As cross-linking proceeded the ATPase activity of the sample increased, as seen by pH-stat assays (figure 3-1a). Unfortunately in conjunction with the increase in the ATPase activity, the Ca sensitivity of the sample was lost, leading to Ca inhibition of the ATPase at long incubation times. Ca inhibition is a phenomenon also noticed during the turnover of ATP by S1.

Cross-linking was also followed by SDS gel electrophoresis. The appearance of a doublet at about 160 Kd represented the acto HMM cross-linked species (figure 3-1b). After several hours a gradual inactivation of the ATPase activity was

seen, probably due to the formation of very high molecular weight material which could barely enter the gel (figure 3-1b). These complexes presumably formed by additional inter- and intra-molecular cross-links. EDC is a relatively non-specific reagent, hence the formation of unwanted cross-links was always a possibility.

The loss in activity made the estimation of the maximum ATPase activity difficult. From figure 3-1, the maximum turnover rate observed was  $4.2 \text{ s}^{-1}$ , if there had been no inactivation the turnover rate may have been higher. When S1 was cross-linked to actin, a maximum observed turnover rate of  $10 \text{ s}^{-1}$  was observed. Attempts to purify the active cross-linked material proved to be unsuccessful. Despite the draw backs, cross-linking has demonstrated an additional 10 fold activation of the ATPase giving a total dynamic range of 5000 fold (regulated HMM -Ca turnover rate =  $0.002 \text{ s}^{-1}$ , maximum observed rate for cross-linked acto-S1 =  $10 \text{ s}^{-1}$ ).

### Discussion

Cross-linking has extended the observed range of the scallop myosin ATPase but unfortunately Ca sensitivity is destroyed in the process.

Of the possible reasons for the loss in Ca sensitivity the most likely are:

(i) cross-linking could lock the HMM in a conformation which overrides regulation (i.e. rigor). Cross-linking had to be carried out in the absence of nucleotide hence the acto-HMM

will be in the rigor state before cross-linking commences.

(ii) EDC can also react with thiol groups (i.e. -SH rather than -OH). If it reacted with the reactive thiol on the HMM (SH1) it could lead to desensitisation in much the same way as IASL labelling of this residue did (Jackson et al, 1987). This is at least part of the reason since the addition of EDC to HMM alone caused a gradual desensitisation of the protein (as seen by FTP turnovers, see later for details).

The maximum actin-activated ATPase activity was obtained using S1 where a rate of  $10\text{s}^{-1}$  was measured. The true value for the  $V_{\text{max}}$  for actin activation of the ATPase may well be higher than this due to problems of inactivation due to over cross-linking. These results, therefore, are in agreement with those presented by Chalovich et al, (1984).

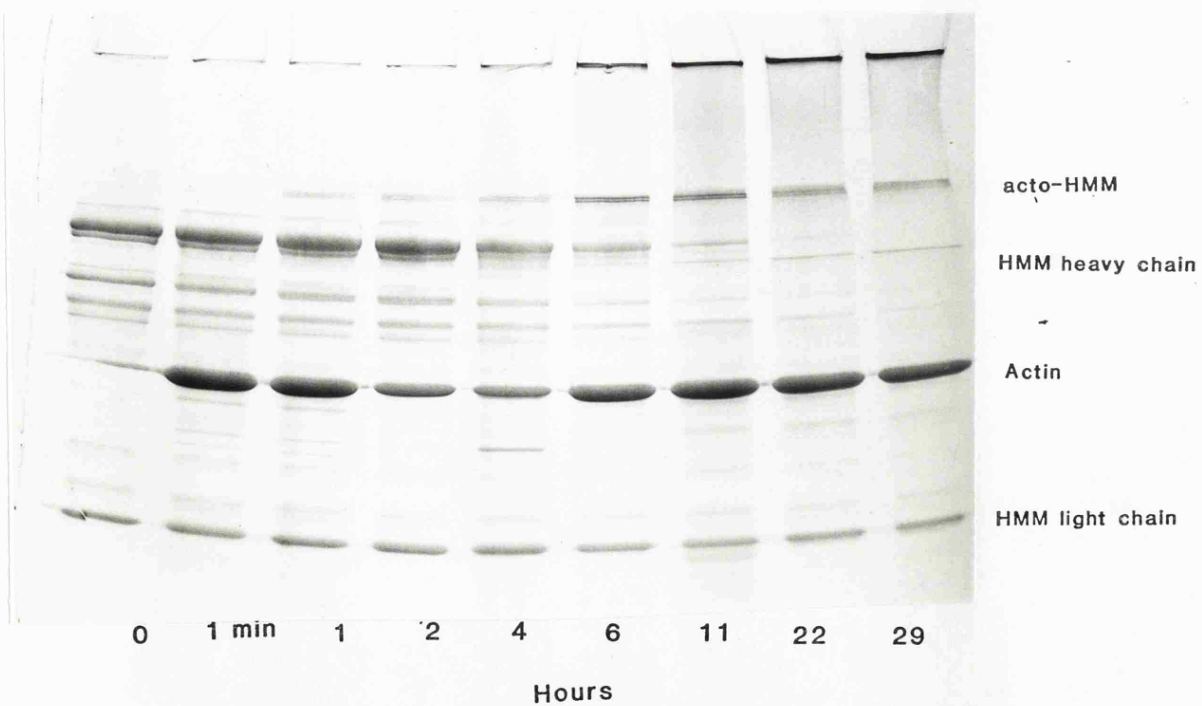
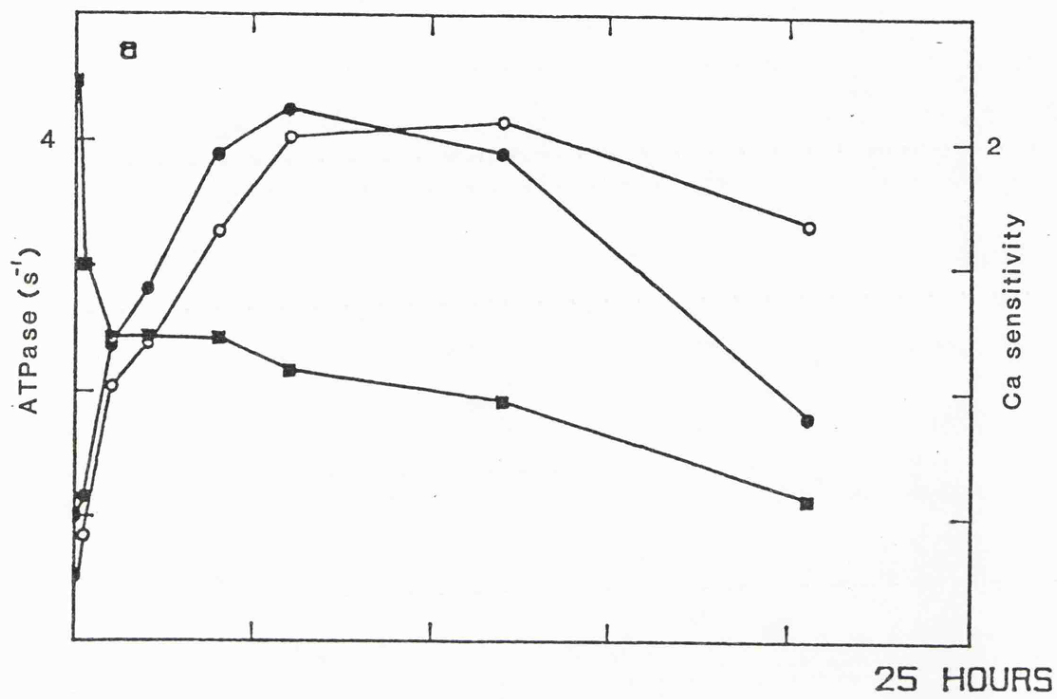
Figure 3-1

Covalent cross-linking of actin to HMM.

(a) Time course of the steady-state ATPase activity and Ca sensitivity during cross-linking, measured using a pH stat, in the presence and absence of Ca.

- - HMM ATPase +Ca.
- - HMM ATPase -Ca.
- - Ca sensitivity of HMM ATPase.

(b) Time course of cross-linking monitored by SDS gel electrophoresis.

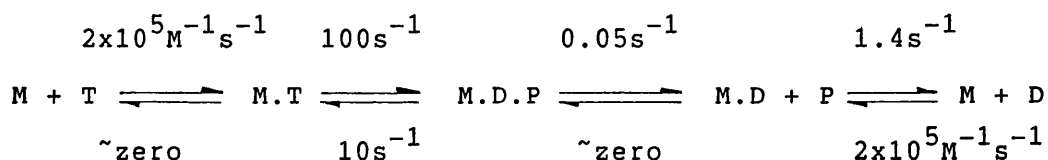


CHAPTER 4

ADENOSINE TRIPHOSPHATASE REACTION

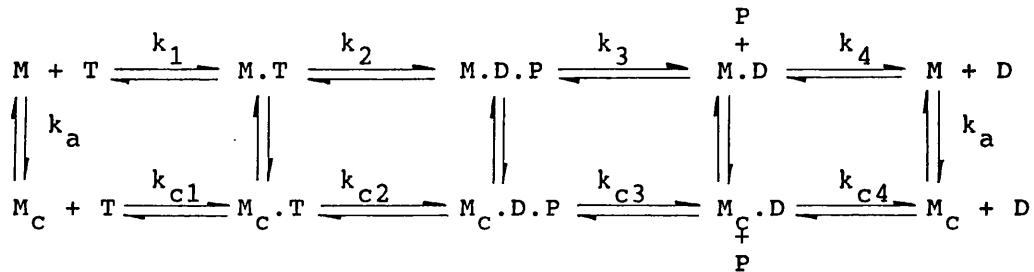
Introduction

The binding of adenosine nucleotides to rabbit HMM and S1 causes an increase in the tryptophan fluorescence of the protein (Werber et al, 1972, Bagshaw et al, 1972). Various nucleotides produced different levels of fluorescence (ATP and ADP binding to rabbit S1<sup>+RD</sup> cause a 18% and a 7% enhancement respectively, (Bagshaw et al, 1974)) providing a sensitive method for analysing the ATPase mechanism. A mechanism was proposed that entailed ATP binding, hydrolysis followed by simultaneous product release (Werber et al, 1972). Bagshaw and Trentham, (1974), extended the analysis and proposed a 7 step mechanism for the ATPase activity. ATP bound, underwent several conformational changes during which hydrolysis occurred and the products were released sequentially (Pi first), with Pi release being the rate limiting step. This scheme was subsequently modified by Johnson and Taylor (1978), who changed the assignment of some of the rate constants. The ATPase mechanism can be simplified into the equation below.

Equation 4-1

Adenosine nucleotides binding to molluscan myosin and its subfragments, also causes an increase in the intrinsic tryptophan fluorescence (Shibata-Sekiya, 1982, Wells et al, 1985). The fluorescence enhancements are smaller than those seen with rabbit subfragments (ATP binding to rabbit and scallop HMM causes a 16% and an 8% enhancement respectively (Wells et al, 1985)) but they do provide a method by which the ATPase mechanism can be analysed. Ca binding to scallop myosin subfragments also enhances the tryptophan fluorescence (Wells et al, 1985) where a 3% increase is seen. These fluorescence changes have been used to probe the mechanism of the scallop myosin ATPase. A comparison of the kinetic mechanism in the presence and absence of Ca has allowed the mode of action of Ca to be deduced.

Equation 4-2 describes the scallop myosin ATPase reaction in a similar way that the rabbit ATPase reaction was described in equation 4-1. The fundamental difference between the two schemes is that, even in the absence of actin, the scallop myosin ATPase is sensitive to the presence of Ca. Scallop myosin and HMM ATPase activities are increased in the presence of Ca over that seen in the absence of Ca whereas scallop S1 ATPase is insensitive to Ca and in this aspect resembles the rabbit myosin ATPase activity.

Equation 4-2

The rate of Ca binding and release ( $k_a$ ) has also been measured to test whether it occurs fast enough to act as a competent signal to trigger contraction.

Most of these changes in tryptophan fluorescence occur instantaneously when observed by manual addition methods. A fluorescence stopped-flow machine was used to measure many of these rates.

ATP Turnover Rates

The limited-turnover experiments of Wells et al, (1985) demonstrated that the turnover of ATP by S1 was unaffected by Ca. The turnover by HMM gave approximately a 3-fold activation of the steady-state ATPase rate by Ca. Single turnover assays demonstrated that the true degree of activation of the HMM ATPase was nearer 100-fold (Wells and Bagshaw, 1985). The rate of product (Pi) release during a single turnover of ATP by HMM was followed by rapid gel filtration. Pi which had been released from the protein was retained by the column, whereas bound Pi eluted with the protein. In the absence of Ca, Pi release occurred over

about 30 minutes but in the presence of Ca, all the Pi had been released before any measurements could be made. These results correlated well with the slow recovery in turbidity seen during the acto-HMM ATPase assays (Wells and Bagshaw, 1984).

Manual addition methods are too slow to resolve much detail about single turnovers of ATP by S1 and HMM. Both column centrifugation and assays monitoring tryptophan fluorescence, using manual addition, fail to provide much information about the turnover of ATP by unregulated HMM or HMM +Ca. In the absence of data to the contrary, it has been assumed that the unregulated molecules behave as a permanently activated population (i.e. HMM +Ca). To test this assumption single turnover experiments were carried out using the fluorescence stopped-flow apparatus.

These experiments are shown in figure 4-1. When the tryptophan fluorescence decay of HMM +Ca was fitted to a single exponential, a  $k_{\text{obs}}$  of  $0.16\text{s}^{-1}$  was obtained (figure 4-1d). A double exponential provided a better fit to the data with  $k_{\text{obs}}$  of  $0.12\text{s}^{-1}$  and  $0.49\text{s}^{-1}$  with approximately equal amplitudes. When  $\text{S1}^{-\text{RD}} + \text{Ca}$  turned over ATP the curves were nearly identical (figures 4-1a and 4-1b). The fluorescence decays were subjected to the same analysis and gave  $k_{\text{obs}}$  of  $0.17\text{s}^{-1}$  when fitted to a single exponential. When fitted to double exponentials,  $k_{\text{obs}}$  of  $0.14\text{s}^{-1}$  and  $0.4\text{s}^{-1}$  were obtained.

In the absence of Ca, the release of products from the unregulated HMM molecules alone can be seen (figure 4-1c). When fitted to an exponential, a  $k_{\text{obs}}$  of  $0.23\text{s}^{-1}$  was obtained. The regulated population binds ADP with high affinity when all the ATP has been utilised. The change in fluorescence enhancement from M.ADP.Pi to M.ADP is too small to be able to measure this rate by tryptophan fluorescence. It has been estimated using a discontinuous, column centrifugation method (Wells and Bagshaw, 1985) and a rate constant of  $0.002\text{s}^{-1}$  obtained. The release of products in the absence of Ca has been further examined using formycin nucleotides.

If, during the turnover of ATP by HMM + Ca, the tryptophan fluorescence decayed as a single term exponential, then both the regulated and unregulated molecules were behaving in the same manner (i.e the rate of the unregulated molecules is equivalent to the rate of the regulated molecules in the presence of Ca). If a double exponential was required to obtain a satisfactory fit, there must be two populations of molecules present with different rates (regulated +Ca and unregulated). Single turnovers of ATP by  $S1^{-RD}$ , with and without Ca, were also carried out to act as a control for a totally unregulated population. The turnover of ATP by HMM in the absence of Ca, allows a direct measure of the turnover rate of the unregulated population, since the release of Pi by the regulated population causes only a very small fluorescence change and thus was not measurable.

The  $S1^{-RD}$  experiments demonstrate how difficult this type of analysis is. The  $S1^{-RD}$  might be expected to exist as just one population and therefore should have fitted to a single term exponential well. Exponential fits suffer from the phenomenon of 'ill conditioning' (Cornish-Bowden, 1979) which occurs when two different equations can be fitted equally well through the same set of data. The more variables in the equation, (i.e the number of rates and amplitudes being fitted), the more this becomes a problem. Thus, almost by definition, a biphasic exponential will provide a better fit to experimental data than a monophasic fit. Any artefact would be very difficult to test for, especially if the two rates obtained differ by less than a factor of 2. Additionally, the exponential decays in these traces do not have a well defined start point which prevents the early part of the fluorescence decay curve being fitted.

There could be up to a 3-fold difference in the turnover rates between regulated HMM +Ca and unregulated HMM. Any difference which does exist between these species is small when compared to the 100-fold activation caused by Ca. When it was necessary to consider the unregulated population, it was therefore treated as HMM +Ca.

#### ATP Binding

The initial rise in tryptophan fluorescence, corresponding to ATP binding, was examined as a function of ATP concentration. If the increase in fluorescence is due solely to the formation of the initial binary complex, then,

as the ATP concentration is increased, the rate of the fluorescence change should increase linearly. Figures 4-2a and 4-2b show a plot of rate of fluorescence change against ATP concentration, and figure 4-3 shows typical traces from which this graph was obtained. By carrying out the experiments in the presence and absence of Ca, any effect of Ca on the rate constants for ATP binding will be seen.

At low ATP concentrations ( $< 20\mu\text{M}$  in the reaction chamber) the rate of increase in fluorescence was linear, and gave a second order binding constant of  $5 \times 10^6 \text{M}^{-1} \text{s}^{-1}$ . At high ATP concentrations ( $> 80\mu\text{M}$  in the reaction chamber), the rate of fluorescence increase became virtually independent of ATP concentration, with a maximum rate constant of  $200 \text{s}^{-1}$ . As can be seen from figures 4-2a and 4-2b all of these rate constants are independent of Ca. After correcting for the loss in amplitude caused by the dead time of the stopped-flow, about 60% of the signal remained at the highest ATP concentration. This implies that it is not a feature of the unregulated fraction.

A similar experiment was carried out in which the rate of tryptophan fluorescence change upon ATP binding to  $\text{S1}^{-\text{RD}}$  was monitored as a function of ATP concentration. Similar results to those obtained with HMM were achieved, with the exception that the plateau rate constant was  $400 \text{s}^{-1}$ . The cause of the higher plateau rate constant was not investigated further, but considering the errors in measuring these fast rates no special significance is given to this result.

Those traces shown in figure 4-3c and 4-3d demonstrate, that despite signal averaging, the signal to noise ratio was very poor, which must introduce errors into the values obtained for the rate constants. In general, the error for any one trace in the calculated value of  $k_{obs}$  was about  $\pm 20\%$  at the high ATP concentrations. The error between different experiments tended to be greater than this. Figure 4-2a and 4-2b demonstrate the scatter which was obtained from a range of different experiments using several protein preparations.

The fluorescence change induced by ATP binding is clearly not a simple one step process. If the fluorescence enhancement reflected only initial association (i.e only the true second order binding), its rate would increase linearly with increasing ATP until it became too fast to measure. It must therefore reflect changes occurring after the initial association. At low ATP concentrations, association is rate limiting thus the second order binding constant could be determined from the early part of the curve in figure 4-2a and 4-2b. At high ATP concentrations the fluorescence change becomes independent of ATP concentration suggesting that some first order transition is now limiting the rate of fluorescence enhancement.

If binding occurred as an optically silent association, in rapid equilibrium, followed by an isomerisation to give a fluorescent species, a hyperbolic dependence of the observed rate constant on nucleotide concentration would be seen. The curves superimposed on the data in figures 4-2a and 4-2b

are hyperbolae with  $V_{max} = 200s^{-1}$  and  $K_d = 35\mu M$ . There is considerable deviation of the data from the calculated curve indicating that binding is more complicated than the scheme described above.

ATP binding to rabbit S1 has been studied in detail by Johnson and Taylor, (1978) and Millar, (1984). Rabbit S1 exhibits larger fluorescence enhancements upon ATP binding allowing the analysis of the profile of ATP binding to be examined in greater detail than has been possible with scallop HMM. Under some conditions the increase in fluorescence could be seen to be biphasic, and at high ATP concentrations some of the amplitude of the signal was lost. The plot of rate of fluorescence enhancement against ATP concentration was not hyperbolic, with the observed rate of binding tending to drop at very high ATP concentrations. This occurs as a consequence of fitting a single exponential through data which is better described by a double exponential. Johnson and Taylor, (1978) concluded that ATP binding was a three-step process, an initial, silent rapid binding, followed by two conformational changes to fluorescently enhanced states, the second appearing coincident with the hydrolysis step.

The signals obtained during the binding of ATP to scallop HMM were only enhanced by 8% at the most, which prevented rigorous analysis of their amplitudes and completely ruled out any attempts to split the signal into two phases. The profile of the ATP binding curve does closely resemble that obtained with rabbit S1, strongly suggesting that the

binding mechanism is very similar.

### ATP Hydrolysis

By analogy with the rabbit myosin ATPase, it is thought that the M.ADP.Pi complex is the major steady-state intermediate of the ATPase pathway. For this to be so, the hydrolysis step must occur faster than product release. A quench-flow machine was not available for studies on the sub-second time-scale, but the slow product release steps characteristic of the scallop myosin ATPase system allowed manual quenching experiments to be carried out.

In the absence of Ca, the hydrolysis of a single turnover of ATP by HMM was followed by perchloric acid quench, neutralisation, followed by FPLC determination of the ATP/ADP ratio. If hydrolysis is rapid ( $\sim 100\text{s}^{-1}$  for rabbit S1) and ATP binding is also rapid ( $> 50\text{s}^{-1}$  at the concentrations used) the ATP should be converted instantaneously to ADP.Pi if measured by manual quenching methods. The ratio of ATP to ADP at equilibration gives information about the equilibrium position of the hydrolysis step. Rather than the instantaneous disappearance of ATP there was a gradual decay in the relative amount of ATP present in the assay mixture, which occurred with a rate constant of  $0.5\text{s}^{-1}$  (figure 4-4). This rate is much faster than the product release step ( $0.002\text{s}^{-1}$ ) so therefore reflects the build up of the steady-state intermediates. After  $\sim 10$  seconds 7% of the ATP remained, which decayed only very slowly over the remaining period of the assay.

In the presence of Ca, the product release step occurs at  $0.2\text{s}^{-1}$  which is of a similar magnitude to the hydrolysis rate measured above. This, coupled to the limits of time resolution from manual addition techniques, does not allow any rigorous conclusions to be drawn about the Ca sensitivity of hydrolysis of ATP. Since hydrolysis is relatively rapid, any Ca sensitivity of this step will have relatively little effect on the overall flux through the pathway.

Detailed examination of the hydrolysis of ATP by rabbit S1 (Chock et al, 1979) led to the suggestion that the plateau rate constant seen by tryptophan fluorescence during ATP binding, reflected the hydrolysis step. Other estimates of the rate of hydrolysis have also been made, all suggesting that the rate is fairly fast ( $>50\text{s}^{-1}$ ) (Lyman and Taylor, 1970, Johnson and Taylor, 1978). Hydrolysis of ATP by scallop HMM appears to consist of three phases, a very rapid phase not measurable by manual methods, an intermediate phase with a rate constant of about  $0.5\text{s}^{-1}$ , and a very slow phase. It is the appearance of the intermediate phase which is a novel feature of hydrolysis in the scallop system.

Slow changes are seen to accompany other steps in the ATPase and FTPase mechanism. Evidence presented later suggests that they may result from the formation of a series of kinetically trapped intermediates away from the linear flux of hydrolysis. The relatively slow decay in the amount of ATP could reflect the equilibration of a series of trapped

states around the hydrolytic step. Quench-flow experiments (minimum time resolution  $\sim 5\text{ms}$ ) are required to define the kinetics of hydrolysis more rigorously.

#### Phosphate release

In the absence of Ca, phosphate release from the regulated fraction is accompanied by a very small change in tryptophan fluorescence ( $<2\%$ ) which occurs with a half time of about 5 minutes. It is thus impossible to measure the Pi dissociation rate constant by this technique due to instrumental drift and protein ageing. Phosphate release was measured by rapid column centrifugation in the absence of Ca at  $0.002\text{s}^{-1}$  (Wells and Bagshaw, 1985).

Phosphate release in the presence of Ca was too fast to be measured by column centrifugation. All steps prior, and subsequent, to phosphate release occur at a faster rate, hence phosphate release must still be the rate limiting step. The single turnover experiments described earlier give a rate constant for phosphate release of  $0.16\text{s}^{-1}$ . Ca therefore causes an increase of about 100-fold in the rate constant for phosphate dissociation.

#### ADP binding and release

ADP binding to regulated HMM in the absence of Ca causes a 6% increase in the tryptophan fluorescence (the observed enhancement in a HMM preparation containing 70% regulated molecules would be about 4%). Although it is smaller than

the corresponding change observed with ATP binding, the kinetics of binding and release have been measured. The observed rate constant of the tryptophan fluorescence enhancement has been plotted as a function of the ADP concentration (figure 4-2c). Figure 4-5 shows typical traces from which the graph was drawn. These experiments were only possible in the absence of Ca since the fluorescence change observed in the presence of Ca was <1%. From the linear portion of the ADP binding curve (<20 $\mu$ M), a second order binding constant of  $8 \times 10^5 \text{M}^{-1} \text{s}^{-1}$  was calculated. Although the rate of binding could not be measured in the presence of Ca, it was possible to calculate (from the dissociation rate constant and equilibrium binding constants) that the second order binding constant for ADP in the presence of Ca was in the range  $10^5 \text{M}^{-1} \text{s}^{-1}$  to  $10^6 \text{M}^{-1} \text{s}^{-1}$  ( $k_{\text{off}} = 6 \text{s}^{-1}$ ,  $K_{\text{eq}} = 10 - 50 \mu\text{M}$ , see below). At high ADP concentrations the observed rate constant became independent of ADP concentration, levelling off at  $40 \text{s}^{-1}$ . This, unlike ATP, cannot be due to hydrolysis but must be some other conformational change which occurs after binding. At the higher ADP concentrations, >70% of the amplitude of the signal remained.

The amplitude of the signal induced by ADP binding is relatively small thus introducing some degree of error into the determination of the rate constants. Each experimental record was the average of 6-12 individual traces. In order to assess the variation between experiments each point in figure 4-2c was repeated 3-5 times. The error bars represent  $\pm$  one standard deviation from the mean.

The superimposed fit is a hyperbola with a  $V_{max}$  of  $40s^{-1}$  and a  $K_d$  of  $35\mu M$ . Significant deviation of the data from the curve can be seen indicating that binding is more complex than a 2 step-one fluorescent species mechanism.

Trybus and Taylor, (1982) examined ADP binding to rabbit S1 and found a non-hyperbolic dependence of the observed rate constant of tryptophan fluorescence enhancement on the ADP concentration. The profile of the ADP binding data closely resembled the ATP binding results of Millar, (1984) and Johnson and Taylor, (1978) which was discussed earlier. The scallop ADP binding data are very similar to those results of Trybus and Taylor (1982) (apart from the differences in the actual second order and plateau rates).

The form of the data shown in figure 4-2c suggests an ADP binding mechanism which is similar to the ATP binding scheme. Despite the smaller changes being observed, more confidence can be attached to these data than the corresponding ATP data. The processes being observed were ten times slower hence it was easier to record the full amplitude of the signal. Additionally the experiment was repeated several times using identical conditions, allowing each point in figure 4-2c to be constructed from very many individual traces.

The near zero change in the tryptophan fluorescence caused by the addition of ADP in the presence of Ca could either be due to ADP having a far weaker binding constant (i.e. not

binding under the concentrations used) or due to it binding in a non-enhanced fluorescent state. It was shown that ADP does bind in the presence of Ca since the rate of binding of ATP to HMM, which has had ADP prebound to it, is dramatically reduced. This provided a method of measuring the rate of ADP dissociation (see below). It appears therefore, that ADP binding does occur both in the presence and absence of Ca.

ADP release was measured by displacing it from HMM with a second nucleotide (ATP or FTP). Care was taken to ensure that the rate of binding of the displacing agent was >10 fold faster than the dissociation rate being measured and that the ATP (or FTP) had not been consumed by the unregulated molecules before displacement was complete. If this was not done then the observed rate constant would not reflect the true dissociation rate constant. Adenosine nucleotides do not contribute to the fluorescence signal, hence a vast excess of ATP could be added to prevent it from being consumed before the end of the reaction. Formycin nucleotides are fluorescent, hence as more FTP is added the background fluorescence level increases, decreasing the observed fluorescence enhancement. In order to maximise the observed signal a minimum amount of FTP was used. To ensure that sufficient had been added, the fluorescence signal was monitored beyond the end of the ADP displacement reaction and the drop in fluorescence when the FTP was consumed noted. This usually occurred 2 - 3 minutes later.

In the presence of Ca, there is a 6% enhancement in the

tryptophan fluorescence going from the  $M_c$ .ADP to  $M_c$ .ATP state. ATP can therefore be used as a displacing agent to measure the rate constant for ADP dissociation in the presence of Ca. In the absence of prebound ADP,  $40\mu\text{M}$  ATP (reaction chamber) bound with a rate constant of  $200\text{s}^{-1}$  (figure 4-2a) and was instantaneous over the timescale shown here (figure 4-6b). When  $50\mu\text{M}$  ADP was prebound to the HMM, the rate constant for ATP binding slowed to  $6.3\text{s}^{-1}$  (figure 4-6a) and provided an estimate of  $k_{c+4}$  (equation 4-2). The experiment also indicates that the binding constant of ADP for HMM in the presence of Ca is  $< 50\mu\text{M}$ . It is this measurement which allowed the calculation of the approximate second order binding constant of ADP for HMM in the presence of Ca as above.

FTP was also used to displace ADP from HMM +Ca. An accurate estimate of the dissociation rate constant could not be obtained since insufficient FTP, due to the increase in the background fluorescence, could be added to ensure effective kinetic competition. At the concentrations used  $90\mu\text{M}$  FTP bound to HMM with a rate constant of  $24\text{s}^{-1}$ , which was reduced to  $4.5\text{s}^{-1}$  by prebinding ADP to the HMM. Simulations of the displacement reaction showed that this underestimated the true dissociation rate by about 10%.

ATP cannot be used as a displacing agent in the absence of Ca because the fluorescence change from M.ADP to M.ATP is too small ( $<2\%$ ). It had been suggested that ADP release in the absence of Ca would be slow, with a half time of about 30 seconds (Wells and Bagshaw, 1985). If this were so, FTP

could be used as a displacing agent. Sufficient FTP had to be added to ensure that it would compete kinetically and that it would not be consumed by the unregulated molecules before the displacement was completed. The latter was the constraint on the amount of FTP which needed to be added.

In the absence of ADP,  $90\mu\text{M}$  FTP (reaction chamber) bound with a rate constant of  $24\text{s}^{-1}$  (figure 4-7b). When  $4\mu\text{M}$  ADP was prebound, the rate of FTP binding dropped to  $0.016\text{s}^{-1}$  (figure 4-7a). The trace was monitored beyond the end of the time shown and the FTP was consumed 150 seconds later. Thus, it was an accurate measurement of the ADP dissociation rate constant from HMM in the absence of Ca. Only about 40% of the amplitude of the trace shown in figure 4-7a exhibits the slow phase. Possible explanations for this are discussed later.

These experiments demonstrate that the release of ADP from HMM is highly Ca sensitive, exhibiting a 600-fold activation of the dissociation rate constant on Ca addition. These rates of dissociation are faster than the rates of phosphate dissociation, hence phosphate release is the rate limiting step both in the presence and absence of Ca.

#### Ca binding and release

Ca binding to scallop HMM causes a 3% enhancement in the intrinsic tryptophan fluorescence (Wells et al, 1985). The removal of Ca by the addition of EGTA causes this change to be reversed. By manual addition methods, these changes are

instantaneous. It is important that if Ca is the primary event in the regulation of contraction, that it can bind and dissociate rapidly. Physiological measurements show that peak tension is reached within 90ms of stimulation and that relaxation occurs with a half time of 100ms (Rall, 1981). Ca must bind and dissociate at rates faster than these if it is to be a competent trigger signal. The small nature of the fluorescence changes which occur on Ca binding, made these rate constants difficult to measure. It was found necessary to subtract blank signals to correct for artifactual apparent changes in fluorescence.

Figure 4-8a shows Ca dissociation from HMM, which occurred with a rate constant of  $26\text{s}^{-1}$ . Figure 4-8b shows the trace obtained when Ca binding was followed. No enhancement in fluorescence was seen although it was known, from manual addition measurements, that a fluorescence change of 3% does occur. The reaction must therefore have been completed before the solutions had reached the observation cell i.e. within the dead-time of the stopped-flow apparatus. Chantler et al, (1981), measured the equilibrium binding constant of Ca for HMM at  $10^{-7}\text{M}$ . From equilibrium binding constant and the measured dissociation rate constant, the second order binding constant of Ca for HMM was calculated as  $3 \times 10^8 \text{M}^{-1} \text{s}^{-1}$ . At the concentrations used in the above experiment (figure 4-8b), Ca would have bound at  $9 \times 10^5 \text{s}^{-1}$ , which is far too fast to measure by stopped-flow techniques. It had however been anticipated that Ca binding would be very rapid, but experiment 4-8b was carried out to ensure that no signal was seen.

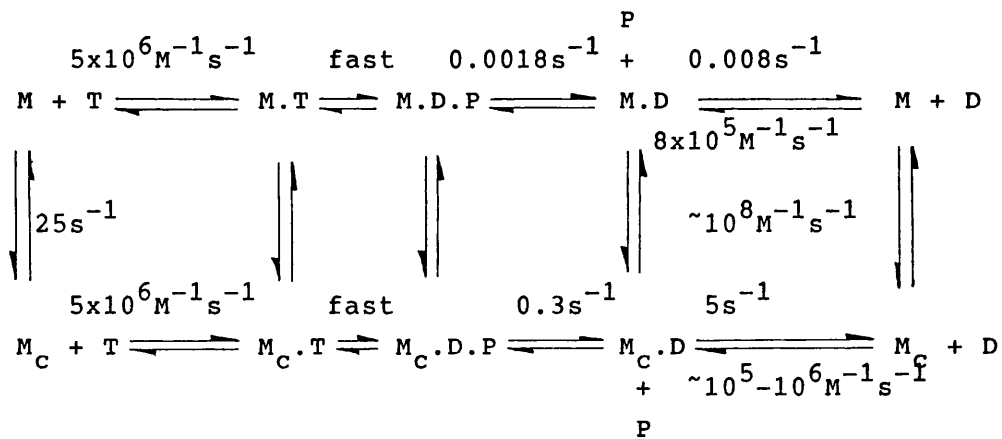
The calculated and measured rate constants fit in well with the need for rapid binding and release of Ca to HMM to control the ATPase and are well within the constraints imposed by the physiological data.

#### Ca/ADP Exchange

ADP release and Ca binding cause approximately equal, but opposite, changes in the tryptophan fluorescence enhancement. A test for the multistep nature of ADP binding which is proposed in equations 4-4 and 4-5, would be to follow the fluorescence changes induced by Ca within the HMM.ADP complex. A number of combinations are possible, each giving data regarding the rates of conversion between species within the scheme. Figure 4-9a shows the transition from  $M^*.ADP$  to  $M_C.ADP$ . Ca binds very rapidly and is not seen, since it occurs within the dead-time of the instrument, allowing the fluorescence change of  $M_C^*.ADP$  to  $M_C.ADP$  to be followed. Addition of EGTA and ADP to the  $M_C$  complex should allow the transition from  $M_C$  to  $M^*.ADP$  to be followed. A biphasic trace composed of a fluorescence decrease as Ca dissociates, followed by an increase, as ADP binds, is seen (figure 4-9b). These types of experiments proved difficult to repeat reproducibly due to the small nature of the fluorescence changes being followed and the heterogeneity of the sample being used.

Discussion

The data presented here allows a detailed description of the ATPase mechanism to be made. The minimum scheme for the turnover of ATP by HMM in the presence and absence of Ca was presented at the beginning of the chapter (equation 4-2). It is useful to rewrite the ATPase scheme from equation 4-2 to include those rates which have been measured.

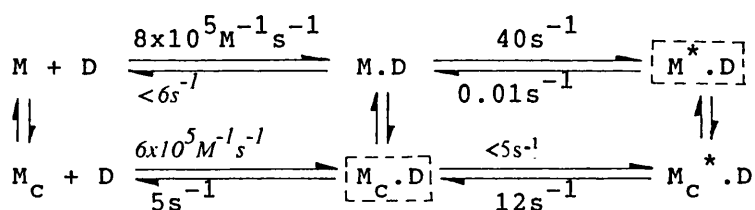
Equation 4-3

This emphasises the effect which Ca has on the flux through the hydrolytic pathway. The rate of dissociation of products is increased at least 100-fold by the addition of Ca.

However, the ATPase mechanism is not quite this simple. As mentioned previously, nucleotide binding is not the single step process depicted in equation 4-3. Figure 4-2 shows

that the fluorescence change, which accompanies nucleotide binding, exhibits a complicated dependence upon ATP and ADP concentration. That ADP can bind to HMM in the presence of Ca and not induce a fluorescence change also demonstrates the over simplification which one step binding entails. Nucleotide binding will be discussed in terms of ADP binding since these results are free from the complications introduced by the hydrolysis reaction which must be considered in the interpretation of the ATP binding data. A scheme for two step ADP binding can therefore be proposed.

Equation 4-4.



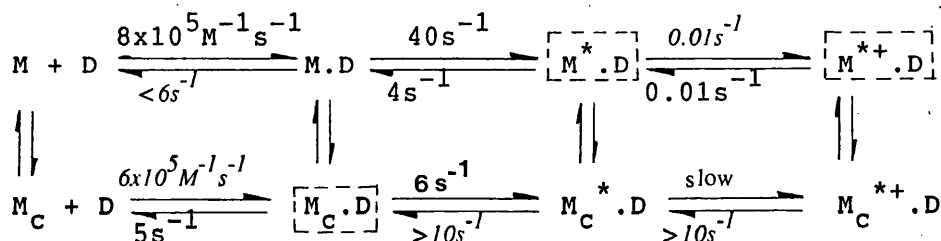
The rates in italics are those which have been inferred rather than measured. Those species which are boxed predominate in the nucleotide bound states.

ADP binds to HMM in a low fluorescence state which then isomerises to give a high fluorescence state. The equilibrium position of these isomerisations are such that in the presence of Ca the low fluorescence state predominates, whereas in the absence of Ca the high fluorescence state predominates. This type of scheme can explain some of the characteristics of ADP binding. At low ADP concentrations the rate of fluorescence enhancement is limited by the second order association rate whereas at high

ADP concentrations it is the first order isomerisation which is rate limiting. In the above scheme only  $M^*$  states are fluorescent allowing ADP to bind without inducing any changes. This predicts that the observed dependence of the fluorescence change on ADP concentration would be hyperbolic and that very large changes in Ca concentration would be required to reach the fully activated state.

Ca binds to free HMM with an equilibrium binding constant of  $10^{-7}M$  (Chantler et al, 1981). Thus at  $\mu$ molar levels of Ca, HMM exists in the activated state. The second step of equation 4 has a >4000 fold dependence of the equilibrium constant of isomerisation on Ca. This factor would also be reflected in the relative affinities of  $M^*.ADP$  and  $M_C^*.ADP$  for Ca. From these calculations, 1mM Ca would be required to achieve the fully activated state. In practice  $10\mu M$  Ca produces full activation of the ATPase. Equation 4-4 has a slow dissociation and fast association rate constants of ADP for HMM -Ca, which is incompatible with the observed binding constant. The introduction of a third step in the binding mechanism can overcome these problems.

Equation 4-5



Equation 4-5 includes a slow, optically silent isomerisation, which reduces the variation of the Ca affinity of the HMM.ADP complexes to a 10-fold difference. If the equilibrium constant for this slow transition is close to 1 and if M.D displays some fluorescence enhancement then equation 4-5 can be used to explain most of the nucleotide binding data.

The slow displacement of ADP by FTP shown in figure 4-7a is due to the isomerisation at  $0.01s^{-1}$ . It also helps to explain why only about 40% of the displacement occurs with the slow rate constant. 20% of the fast rate would be due to ADP dissociation from the unregulated molecules and the other 40% is due to the release from  $M^*.D$ , as a consequence of the equilibrium value of 1, at a rate of  $4s^{-1}$ .

It has been proposed for rabbit S1 that the initial second order binding of ATP of  $\sim 10^6 M^{-1} s^{-1}$  is really a diffusion controlled rapid association ( $\sim 10^8 M^{-1} s^{-1}$ ) followed by a first order transition (Bagshaw et al, 1974, Johnson and Taylor, 1978, Trybus and Taylor, 1982). At this stage it was considered unnecessary to invoke this complicating factor in the scallop mechanism. Further evidence for the slow conformational changes, which occur subsequent to binding, comes from the interaction of the formycin nucleotides, where these transitions can be observed (chapter 5 and 6).

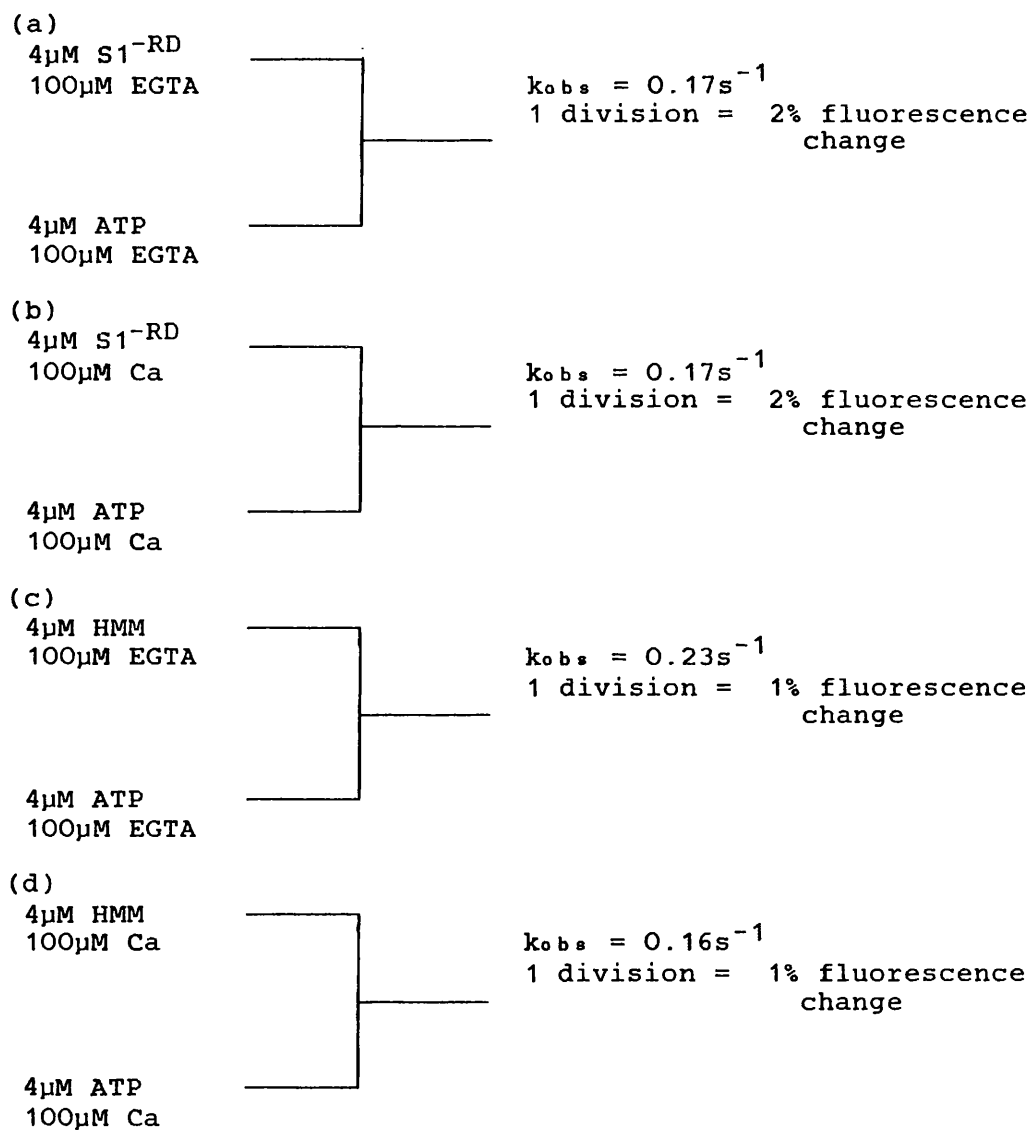
ATP binding is much harder to examine in as much detail

since hydrolysis occurs relatively rapidly after binding. The profile of figure 4-3a and 4-3b demonstrates that there must be at least one conformational change subsequent to association, with the possibility of further optically silent changes. Rapid hydrolysis hinders the measurement of ATP dissociation but ATP chase experiments allowed the rate of dissociation of ATP from rabbit S1 to be measured at  $<10^{-2}\text{s}^{-1}$  (Bagshaw and Trentham, 1973). The rate of dissociation from scallop HMM in the presence of Ca is likely to be of similar magnitude, and even slower in the absence of Ca, but this would have no effect on the turnover rate. The acid quench experiments also demonstrate that there are relatively slow changes accompanying ATP binding and hydrolysis.

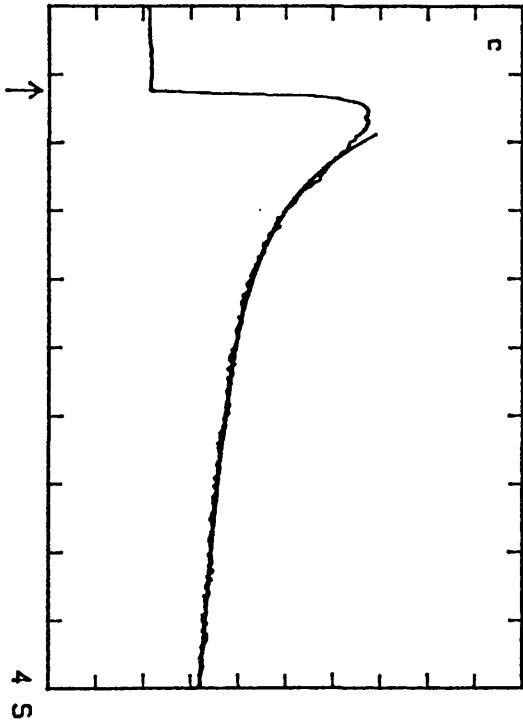
These complications to the ATPase pathway must not be allowed to obscure the basic mechanism by which Ca regulates the activity. Nucleotide binding remains unaffected by Ca, while it is the conformational changes which occur once the nucleotides have bound which are Ca sensitive. It is the conformational changes which control product release that are the most obvious expression of this Ca sensitivity.

Figure 4-1

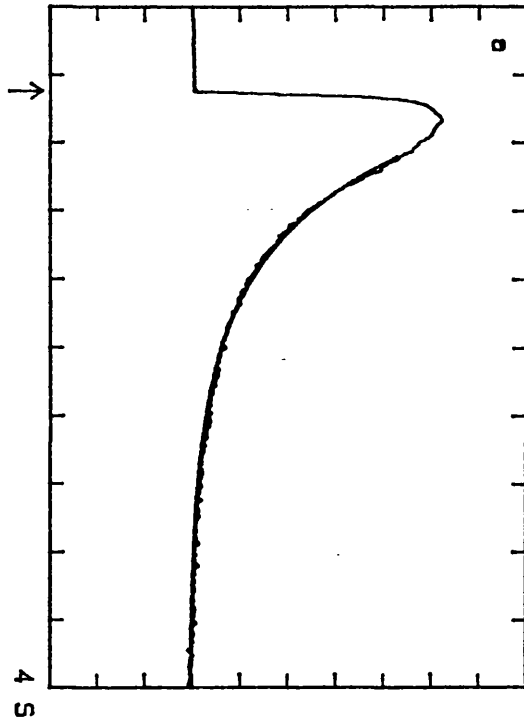
Stopped-flow records of single turnovers of ATP by HMM and S1<sup>-</sup>RD in the presence and absence of Ca, monitored by tryptophan fluorescence.



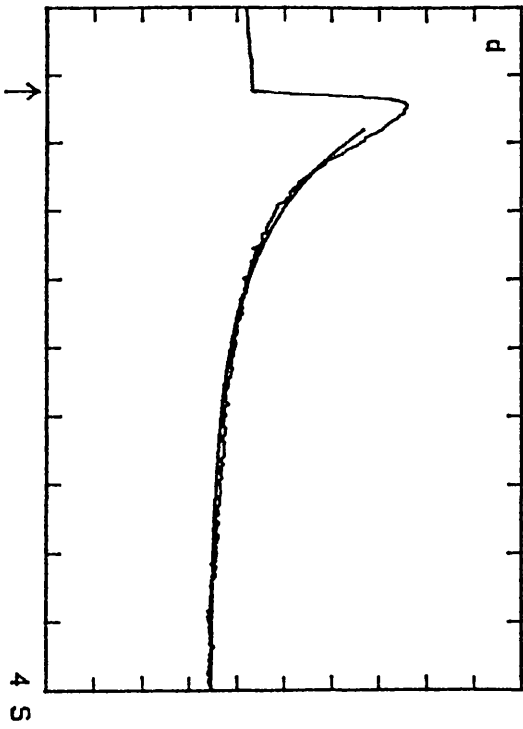
FLUORESCENCE



FLUORESCENCE



FLUORESCENCE



FLUORESCENCE

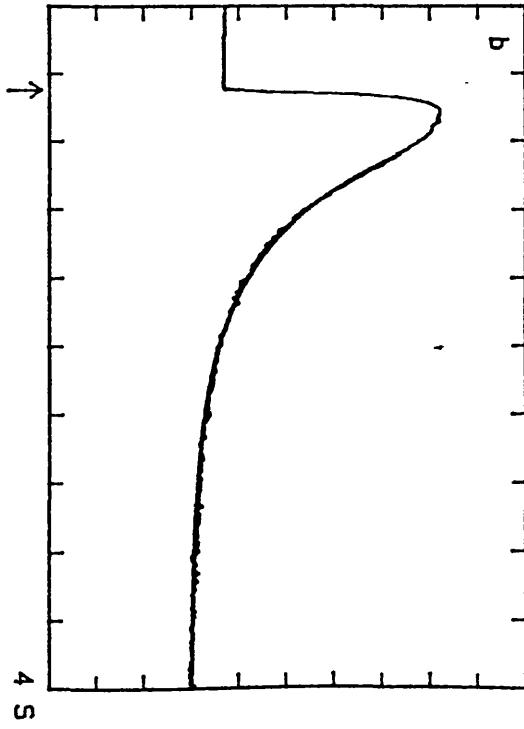


Figure 4-2

The dependence of the observed association rate constant of ATP and ADP for HMM on the nucleotide concentration. The  $k_{\text{obs}}$  of ATP and ADP binding was plotted as a function of nucleotide concentration.

(a) ATP binding to HMM in the presence of Ca.

The hyperbolic fit through the data has a  $V_{\text{max}} = 200\text{s}^{-1}$  and  $K_m = 35\mu\text{M}$ .

(b) ATP binding to HMM in the absence of Ca.

The hyperbolic fit through the data has a  $V_{\text{max}} = 200\text{s}^{-1}$  and  $K_m = 35\mu\text{M}$ .

(c) ADP binding to HMM in the absence of Ca.

The hyperbolic fit through the data has a  $V_{\text{max}} = 40\text{s}^{-1}$  and  $K_m = 35\mu\text{M}$ .

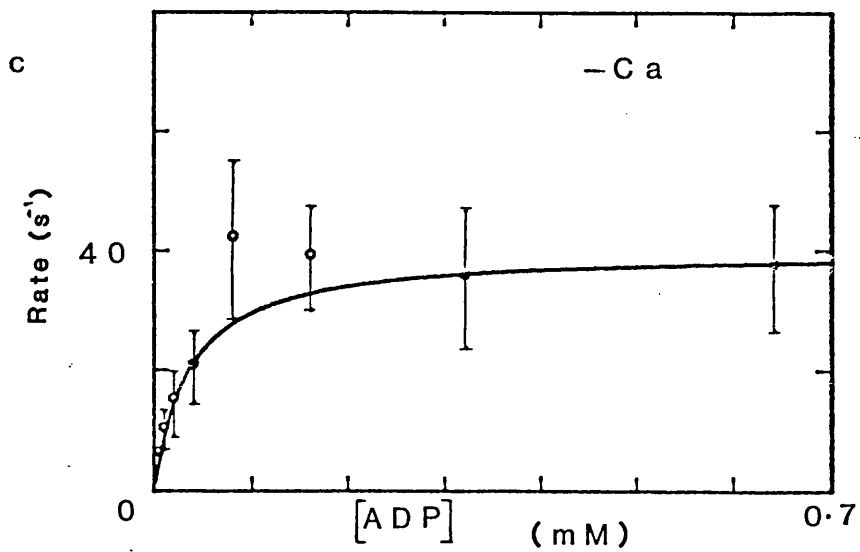
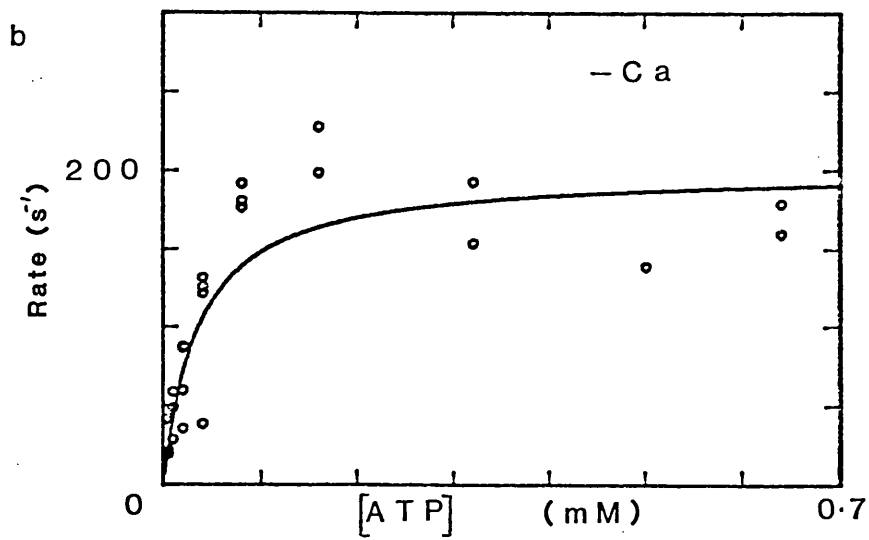
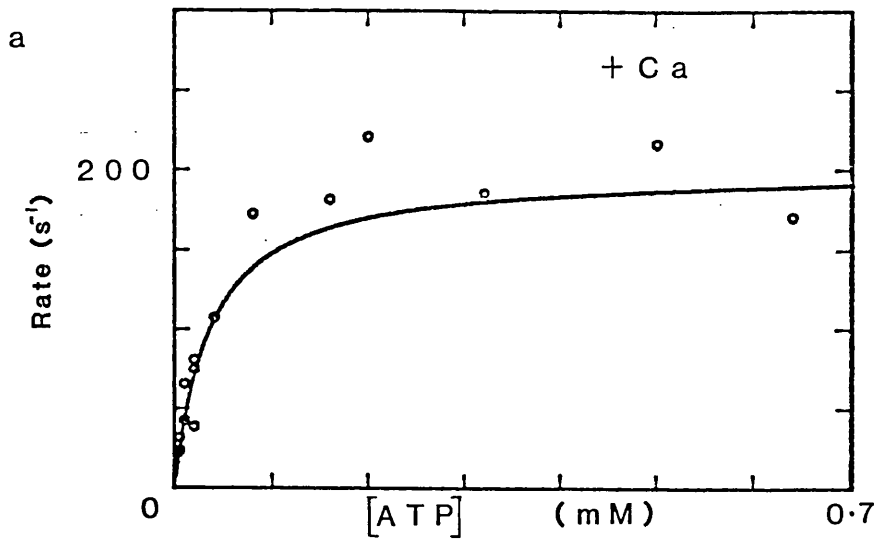
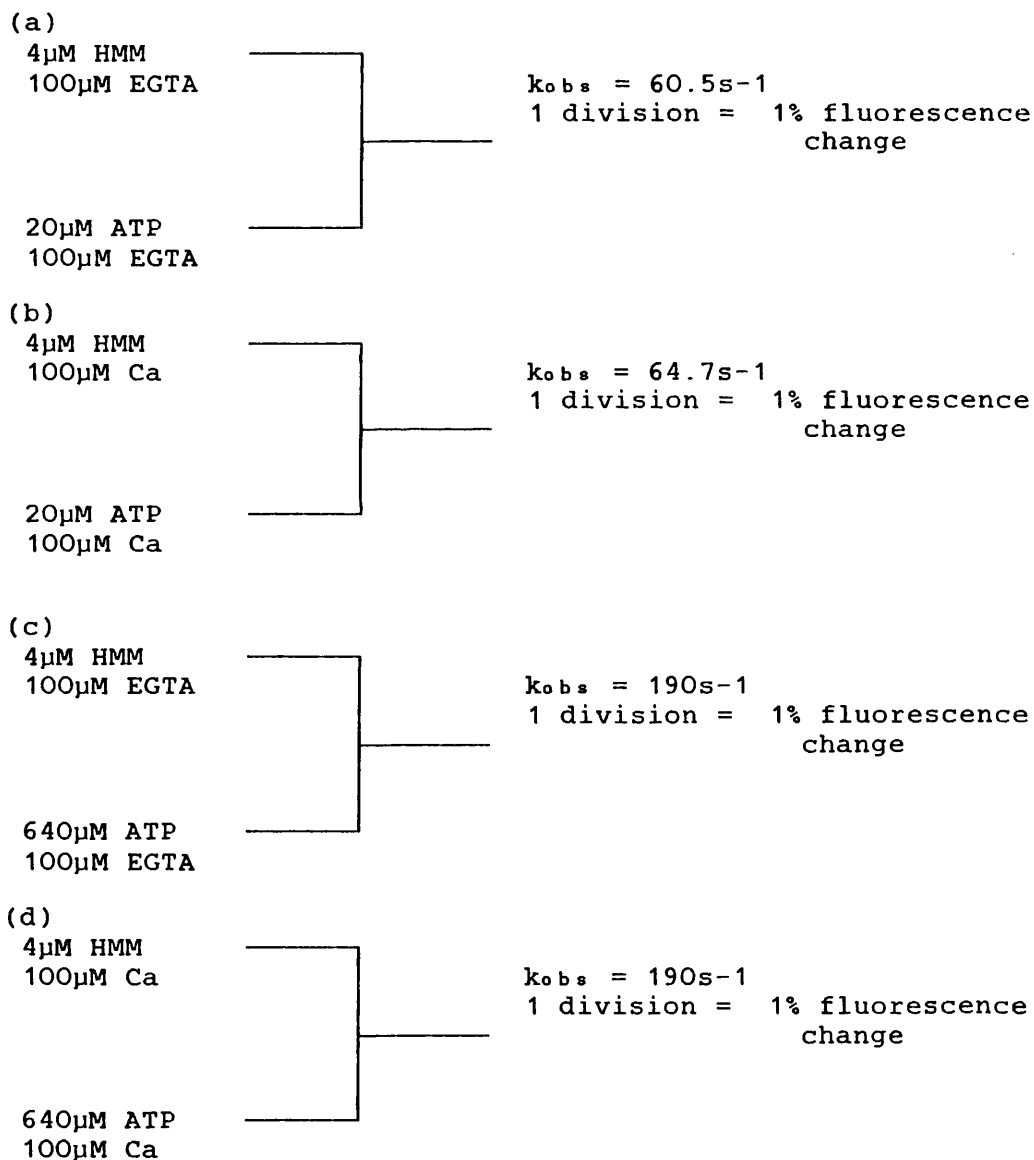


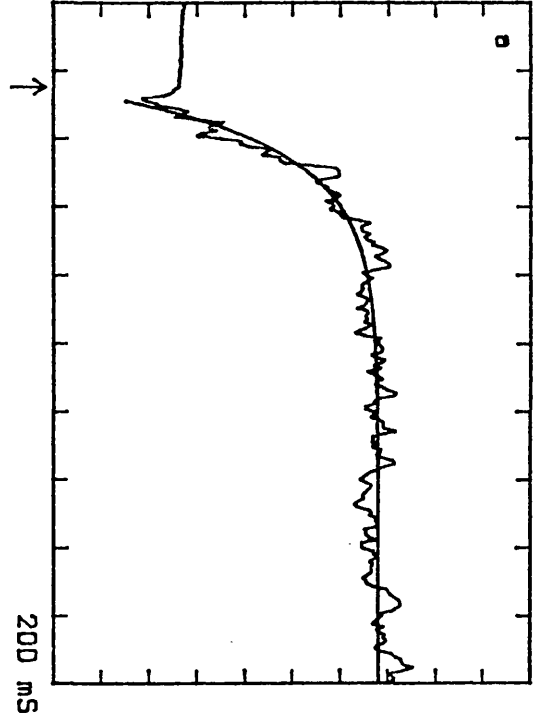
Figure 4-3

ATP binding to HMM in the presence and absence of Ca, as monitored by tryptophan fluorescence.

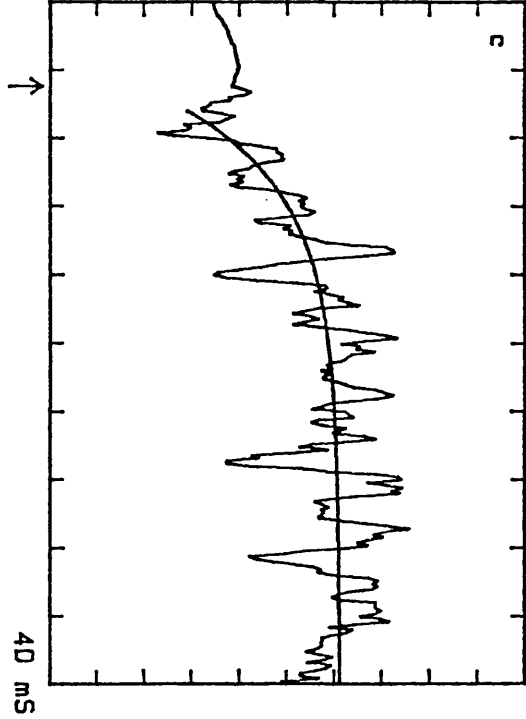
These traces are typical of those from which figure 4-2a and 4-2b were drawn.



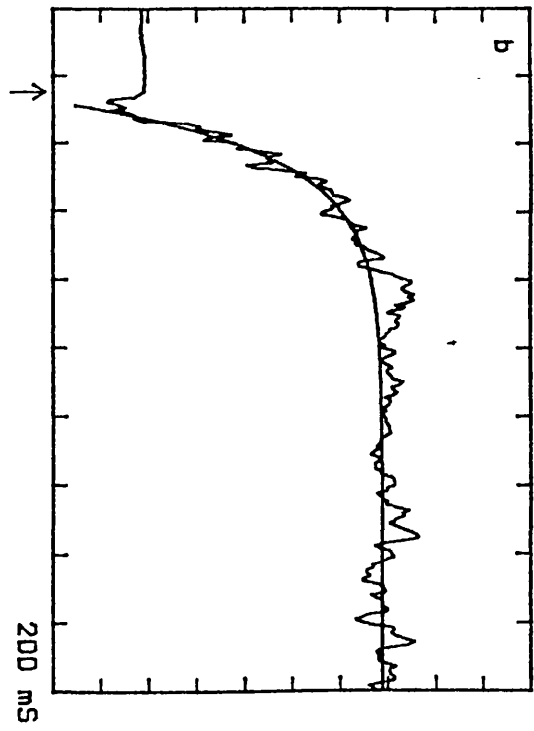
FLUORESCENCE



FLUORESCENCE



FLUORESCENCE



FLUORESCENCE

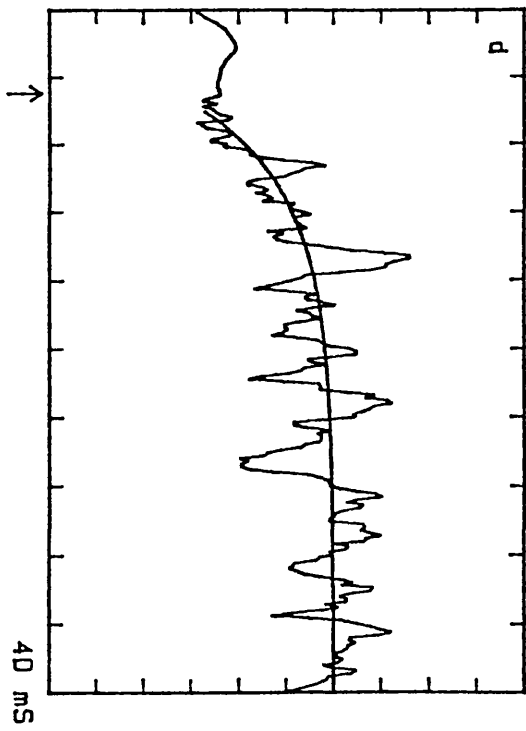


Figure 4-4

Hydrolysis of ATP by HMM in the absence of Ca, followed by perchloric acid quench and FPLC analysis.

Perchloric acid quench of 40 $\mu$ M HMM, 30 $\mu$ M ATP after (a) 2 seconds and (b) 20 seconds. 10 $\mu$ M Ap5A was added to inhibit any potential myokinase activity. Samples were run on a mono Q column in 20 mM Bis-Tris pH 6.5 and eluted on a 0-1.0M NaCl gradient at 2ml/minute and monitored at 254nm (full scale = 0.1 Abs). Relative quantities of AMP, ADP and ATP were determined using the integrator program on the Apple II+ microcomputer.

(c) Plot of the relative amounts of ATP left after incubating with HMM -Ca at various times. ATP disappeared with a rate constant of 0.5s<sup>-1</sup> and there was 6% of the ATP left after 20 seconds.

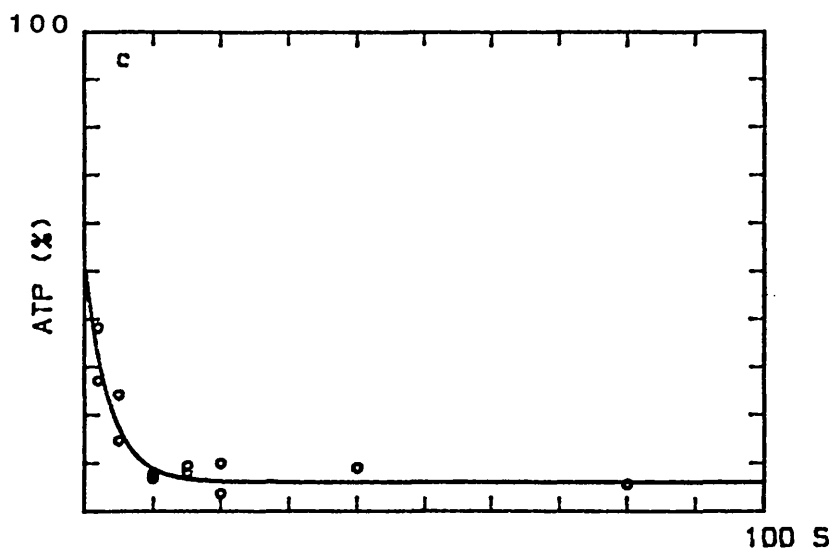
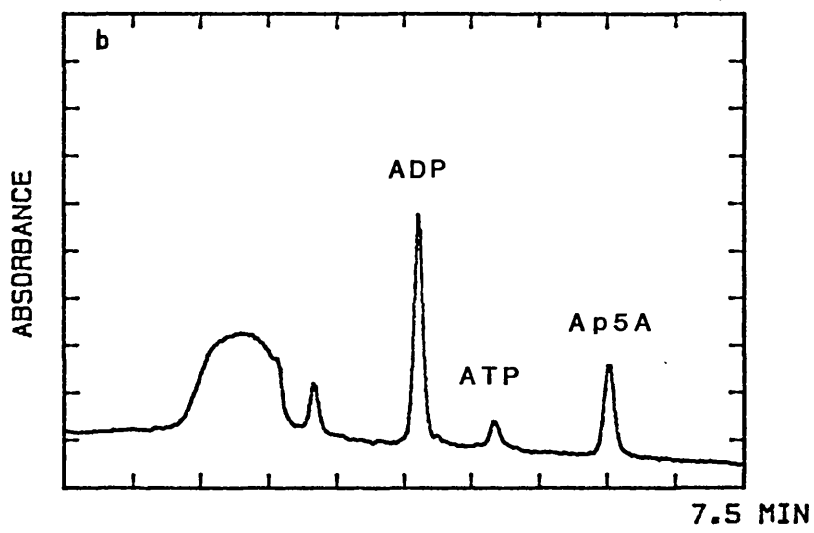
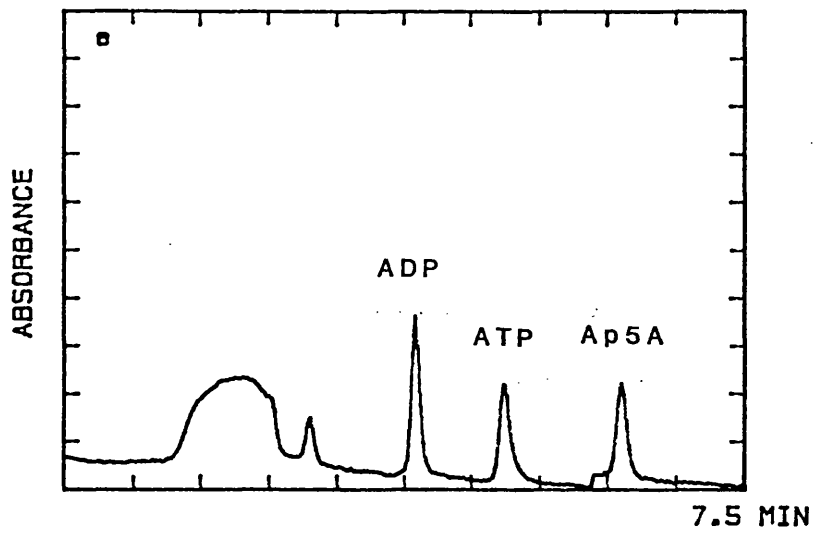
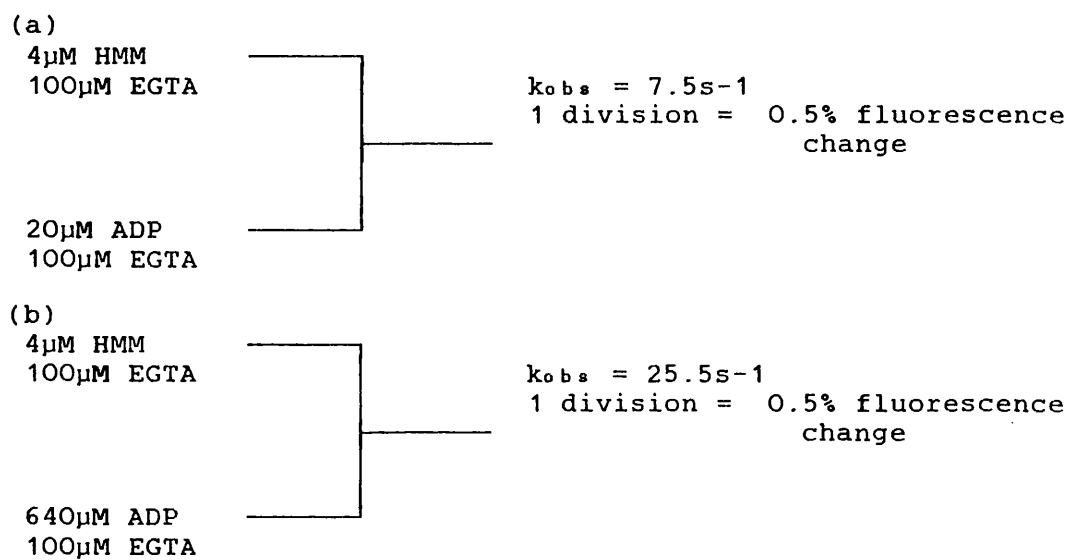


Figure 4-5

Stopped-flow records of ADP binding to HMM in the absence of Ca.



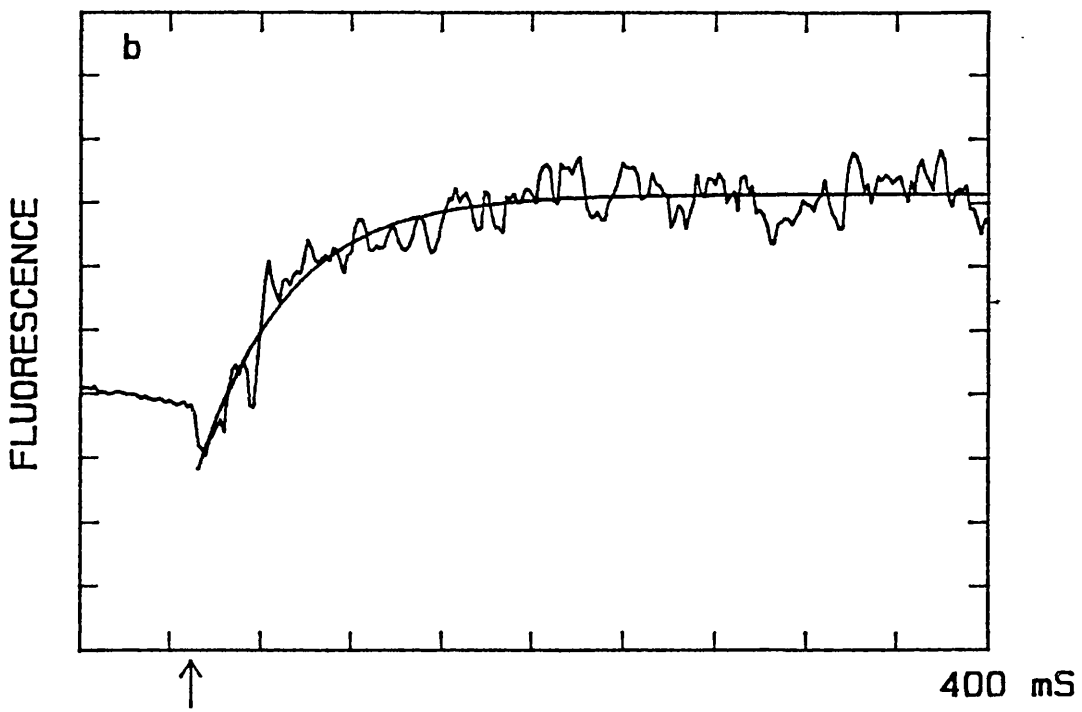
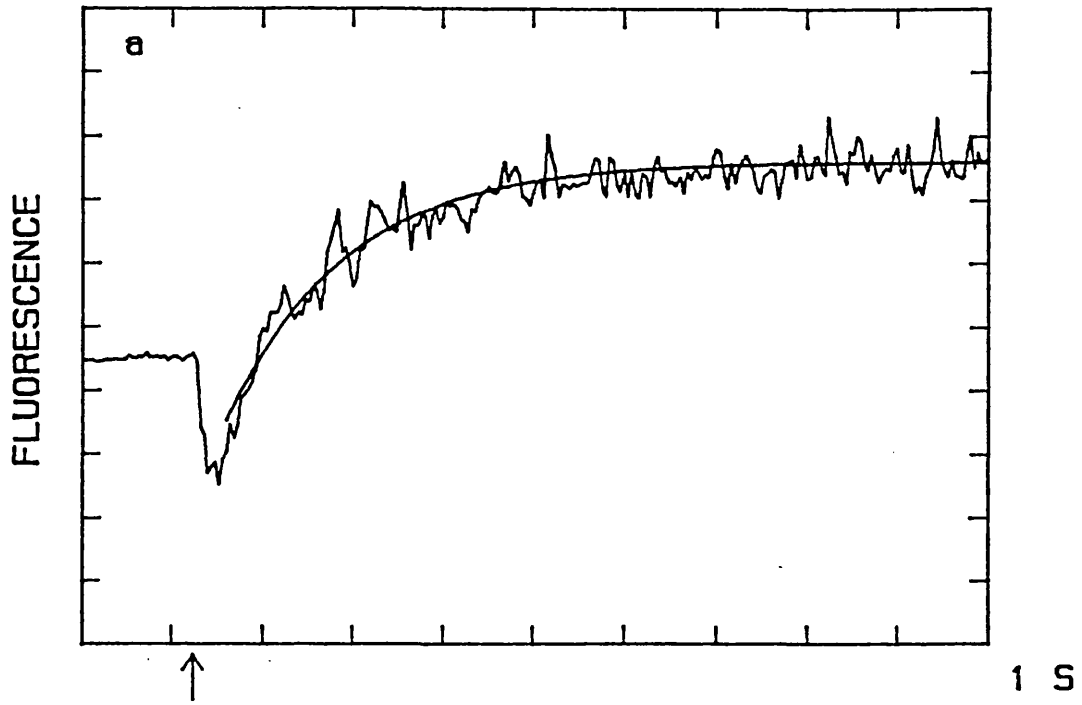
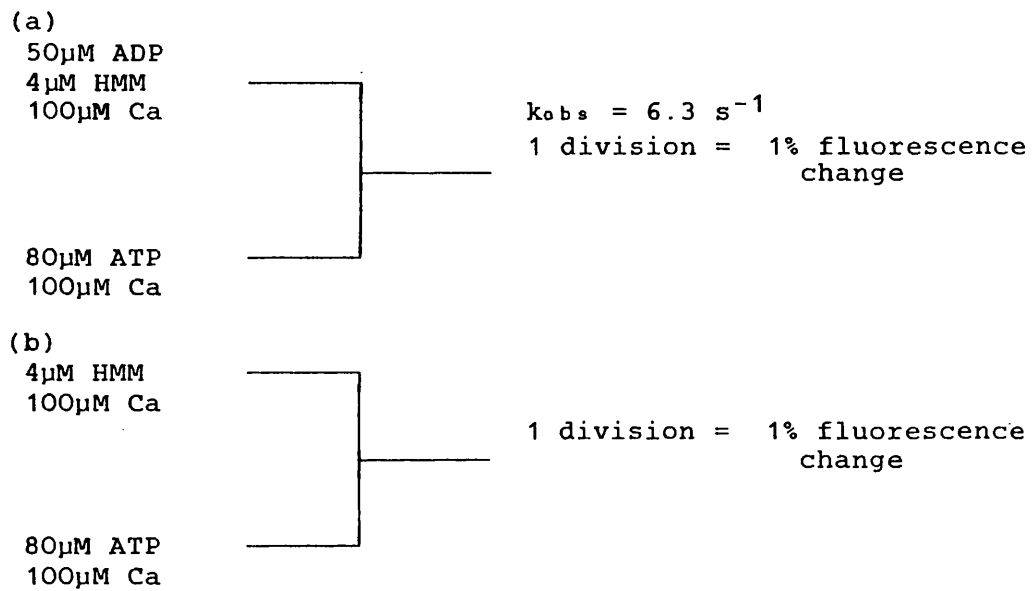


Figure 4-6

ADP dissociation from HMM in the presence of Ca measured by displacement with excess ATP.



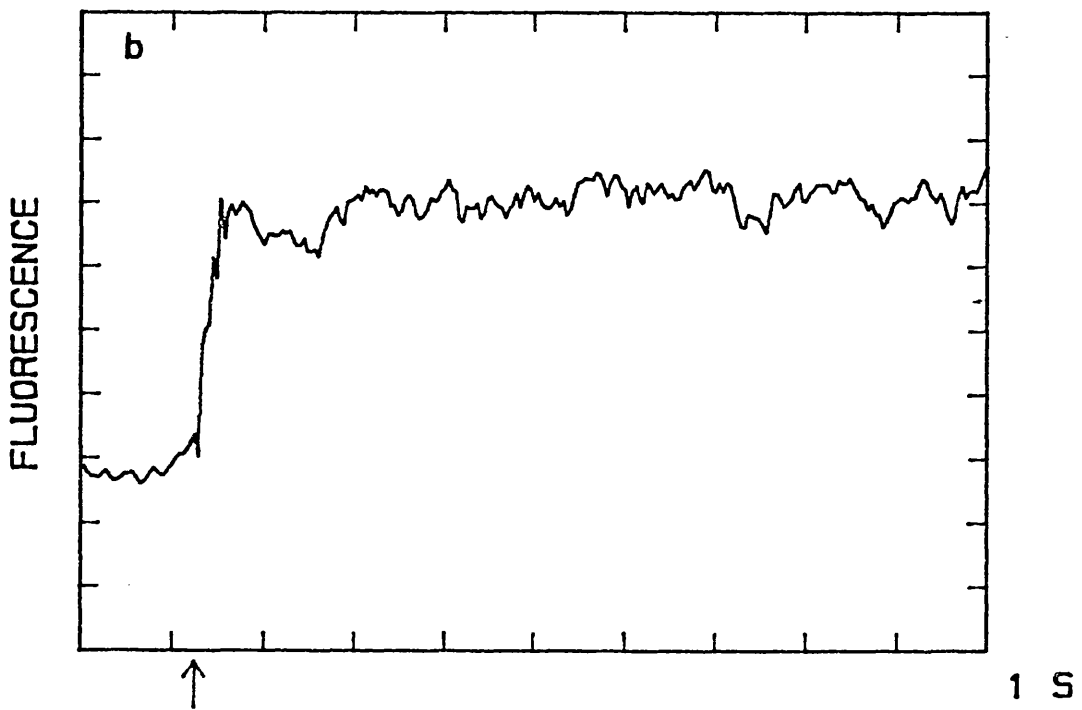
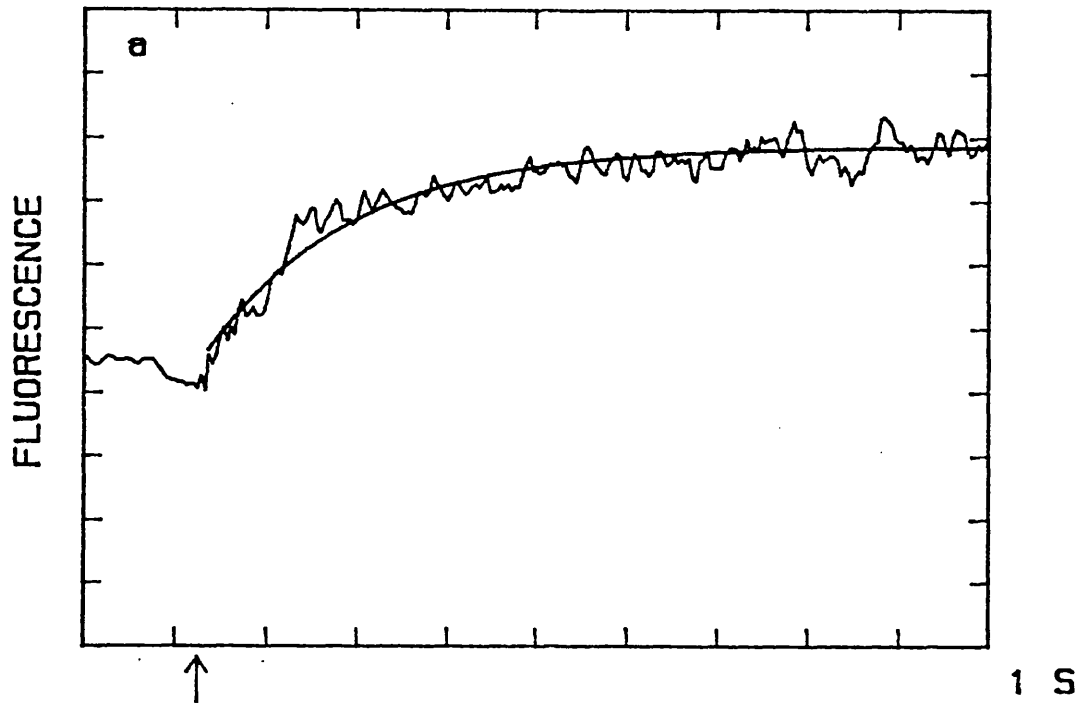
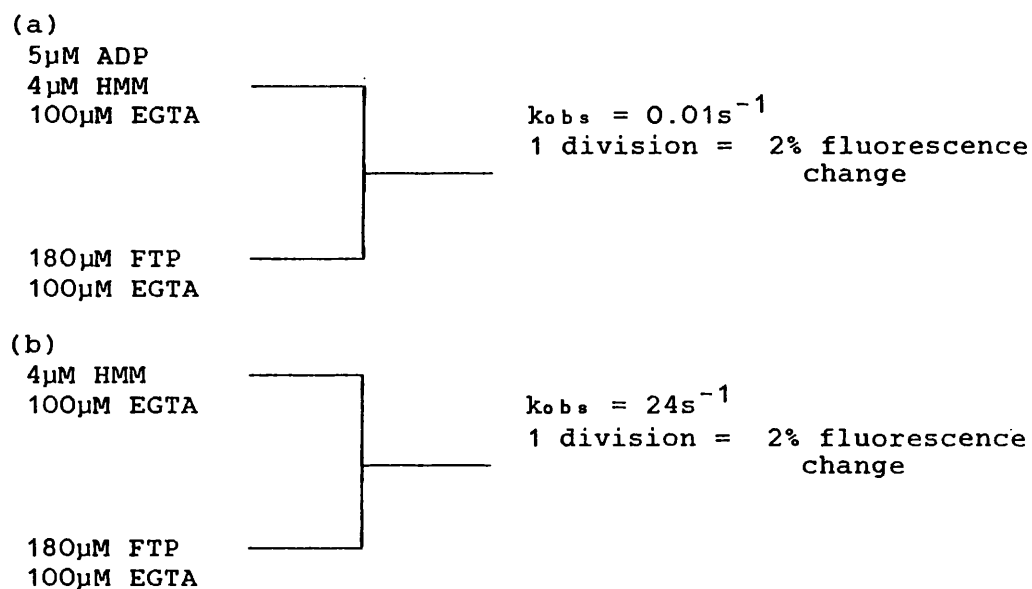


Figure 4-7

ADP dissociation from HMM in the absence of Ca measured by displacement with excess FTP.



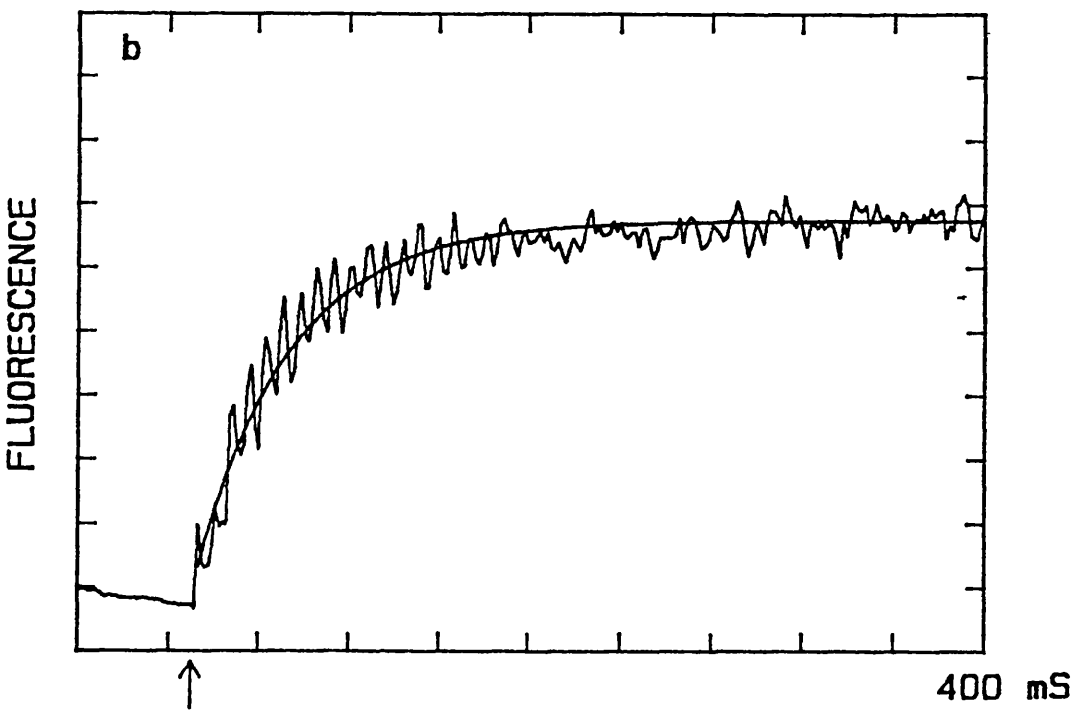
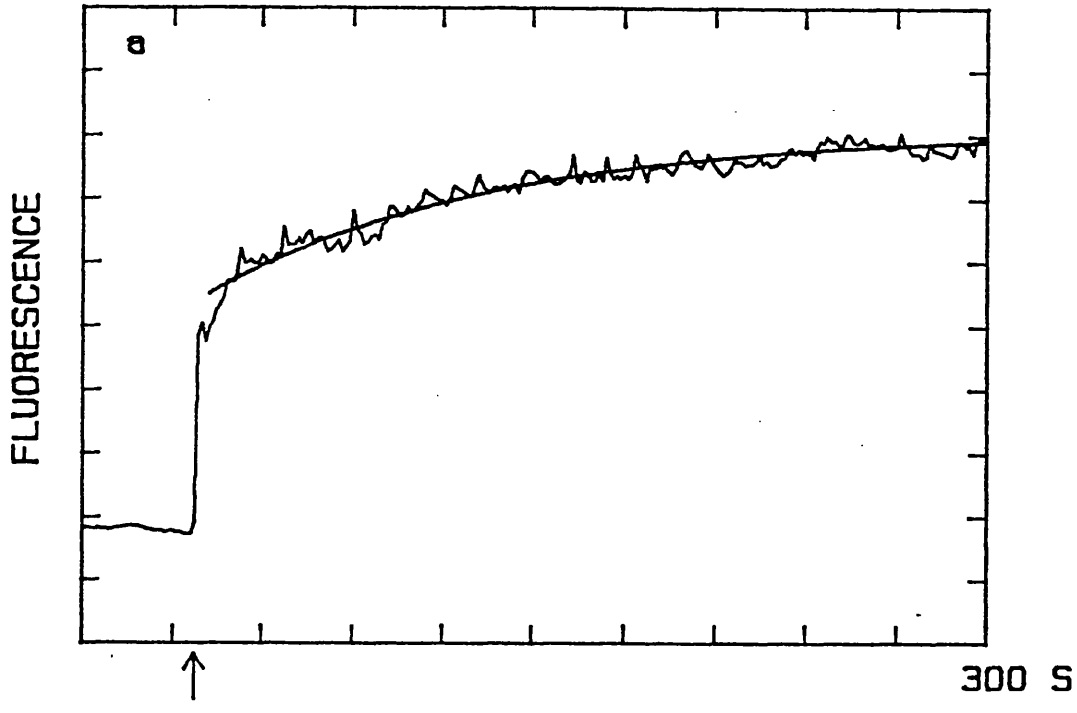
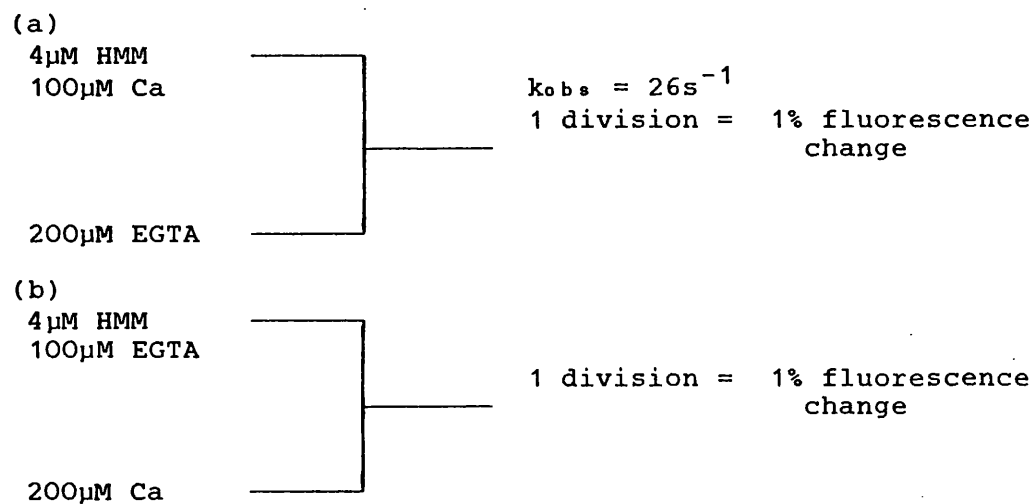


Figure 4-8

Ca binding and dissociation from HMM monitored by tryptophan fluorescence.



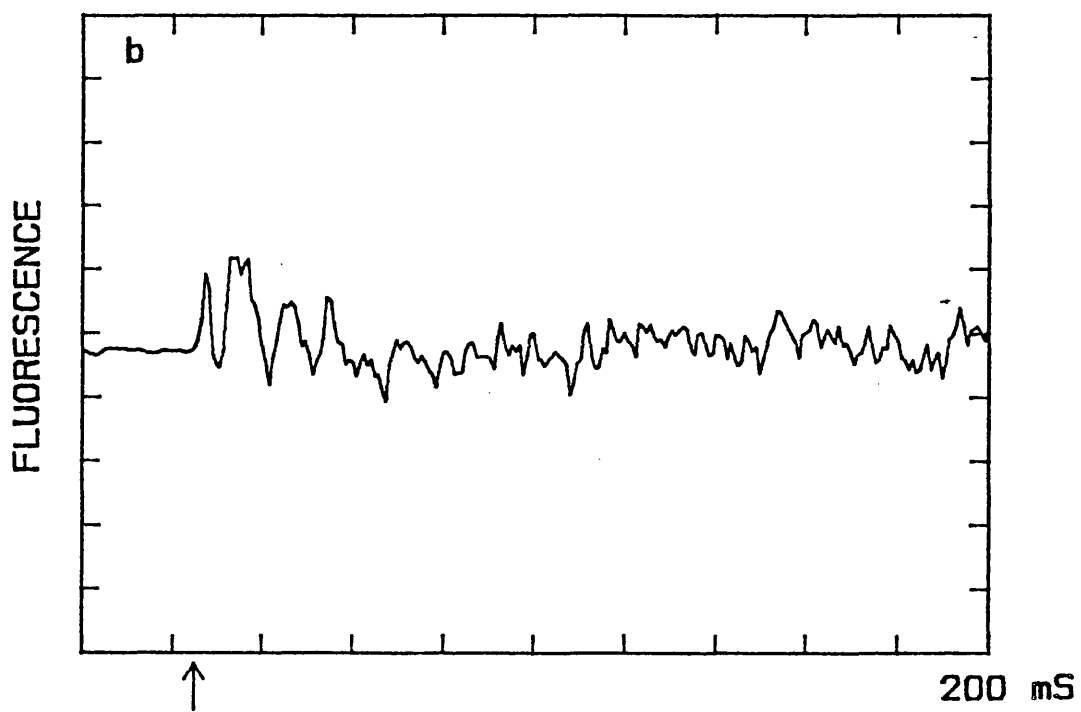
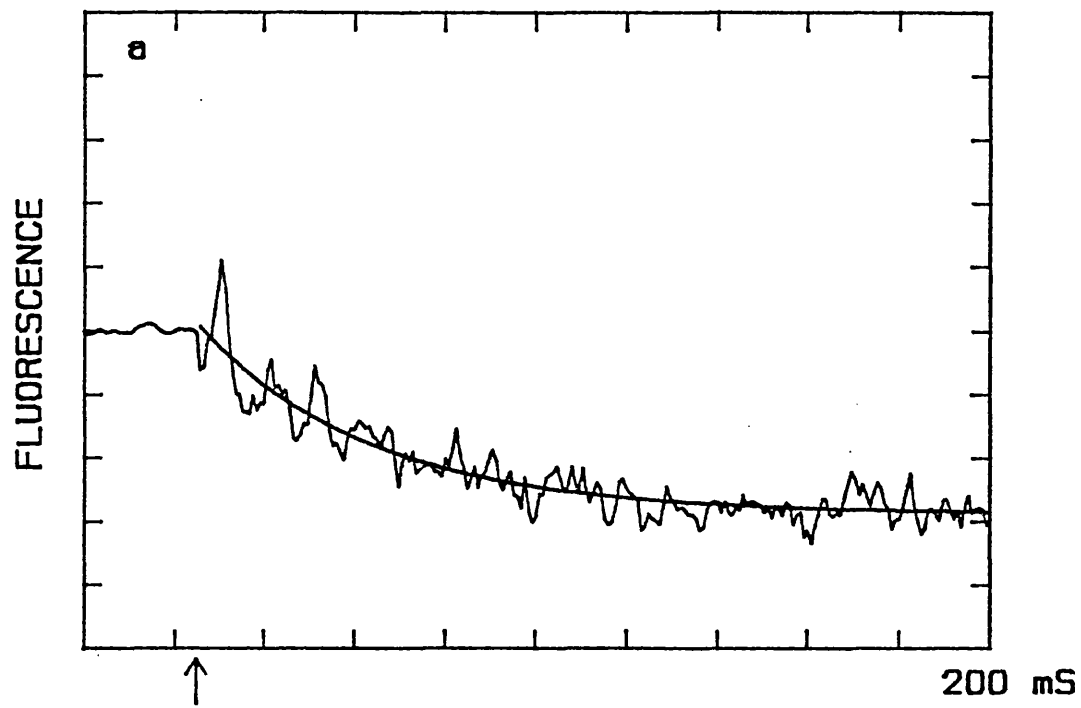


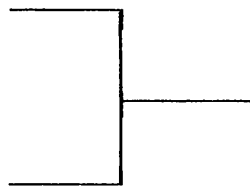
Figure 4-9

The conformational transitions within the HMM.ADP complex induced by the binding and removal of Ca, monitored by tryptophan fluorescence.

(a)

5  $\mu$ M ADP  
4  $\mu$ M HMM  
100  $\mu$ M EGTA

200  $\mu$ M Ca

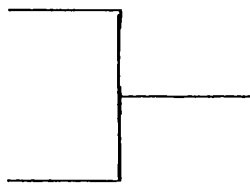


$k_{obs} = 12s^{-1}$   
1 division = 1% fluorescence change

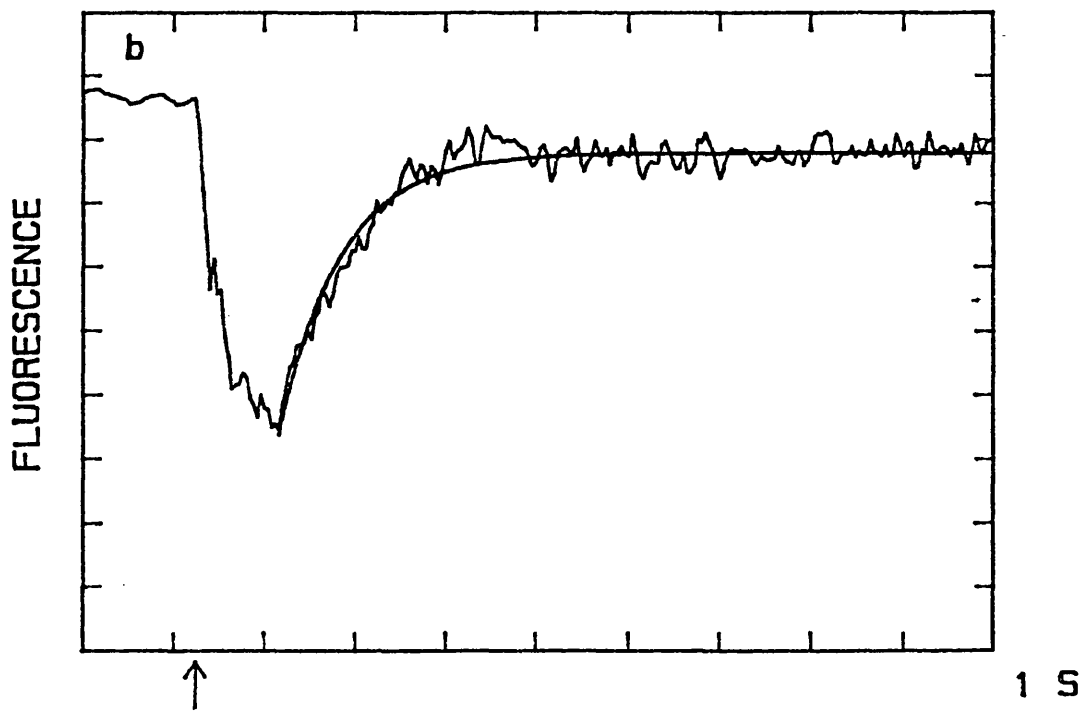
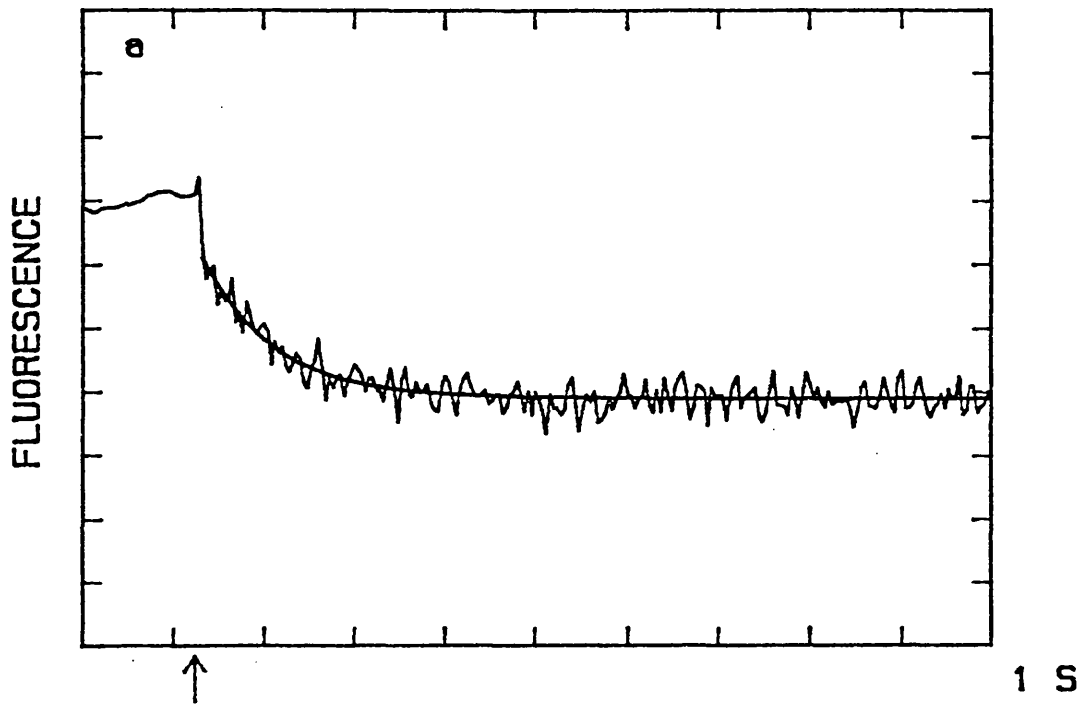
(b)

4  $\mu$ M ADP  
4  $\mu$ M HMM  
100  $\mu$ M Ca

200  $\mu$ M EGTA



$k_{obs} = 14s^{-1}$   
1 division = 1% fluorescence change



CHAPTER 5

FORMYCIN TRIPHOSPHATASE REACTION

## Introduction

The binding of adenosine nucleotides to scallop myosin subfragments induces only small changes in the tryptophan fluorescence, i.e. ADP binding to HMM -Ca has a 6% enhancement and to HMM +Ca a <1% enhancement, placing a limit on the analysis of the ATPase mechanism which is possible by this method. An alternative approach is to use ATP analogues which are themselves fluorescent, and whose fluorescence is changed upon binding to protein. A series of ATP analogues, based on formycin, were synthesised and used to study the ATPase and F<sub>1</sub>F<sub>0</sub> ATPase mechanism.

Formycin can substitute for adenosine in a wide range of biochemical systems. It can be incorporated into DNA and RNA where it acts as a mutagen, due to poor base pairing, and was originally used to study the structure of these compounds (Ward et al., 1969a). Formycin triphosphate (FTP) can act as a substrate for many ATP requiring enzymes such as adenylate kinase (Ward et al., 1969b), a property that has been exploited in the synthesis of FTP from FMP and in the synthesis of FMPPNP from FTP.

Formycin contains a carbon-carbon glycosyl bond rather than the carbon-nitrogen bond which is found in adenosine (figure 5-1a and 5-1b) making the ring structure fluorescent. It also has implications in the stereochemistry of the base in solution. Adenosine exists as the extended, anti-conformation, which is probably complementary to the

conformation required for ATP binding (c.f. Shoham and Steitz, 1980 who examined the ATP binding site of hexokinase). Formycin, on the other hand, has the syn conformation predominating in solution. Here the ribose ring is folded back over the purine ring system (Ward and Reich, 1968) which effectively reduces the concentration of the FTP which is available for protein binding. This may only affect the initial binding rates, since once bound it will be held in the correct conformation by the protein so the rest of the reaction should proceed as for ATP.

When FTP binds to myosin or its subfragments, its fluorescence is enhanced by 500%. Different intermediates along the FTPase pathway show various levels of fluorescence enhancement. This, plus the potentially large signals available, has allowed the mechanism of the enzymic activity of scallop myosin to be studied in greater detail than was possible using ATP and tryptophan fluorescence.

Non-hydrolysable derivatives of FTP, formycin diphosphate (FDP) and formycin imidotriphosphate (FMPPNP) (figure 5-1c), were synthesised and the mechanism of binding studied. The binding of these nucleotides to HMM is discussed in detail in chapter 6.

FTP turnovers have provided a quick and convenient assay system to measure the proportion of regulated molecules in an HMM preparation. Factors which cause a change in this proportion have been followed by FTPase assays. FTP has also been used as a displacing agent to study the ATPase

mechanism as described in chapter 4.

### FTP turnovers

Before detailed studies on the FTPase mechanism were carried out it had to be confirmed the FTP was a suitable substrate for scallop myosin. Although it was known that rabbit S1 and insect S1 turned over FTP (Bagshaw *et al* 1972, White *et al*, 1986), it was possible that scallop HMM might turnover FTP in a Ca insensitive manner. Steady-state FTPase assays, using the malachite green assay to detect free phosphate, demonstrated no effect of Ca on the turnover of FTP by HMM (figure 6-8). A limited turnover experiment, in which the formycin fluorescence was monitored, showed however approximately a 100-fold activation of the regulated HMM FTPase by Ca. This contradictory result is re-examined in chapter 6.

Figure 5-2 shows the turnover of a 5-fold excess of FTP by S1<sup>-RD</sup> and HMM <sup>±</sup>Ca. The turnover by S1 is Ca insensitive (figure 5-2a and 5-2b). The removal of Ca from HMM results in a 100-fold reduction in the rate of the fluorescence decay (figure 5-2c and 5-2d). On FTP binding to HMM -Ca there is a rapid increase in the fluorescence. A brief steady-state is reached and maintained until all the FTP is exhausted. The fluorescence then drops rapidly, followed by a very slow decay ( $k_{obs} = 0.0018s^{-1}$ ). The similarity to the profile observed by Wells and Bagshaw, (1984), suggests that the initial rapid drop is due to product release from the unregulated fraction, and the slow phase occurred as

products were released from the regulated molecules. In the presence of Ca or with  $S1^{-RD}$  there are no inhibited molecules hence the decay was monophasic. From these FTP turnover experiments, it was clear that the presence of two populations was due to the HMM alone rather than an effect transmitted from the actin.

The biphasic nature of the fluorescence decay allows a simple method of analysing the proportion of regulated molecules in any preparation. As will be seen later, some care has to be taken to ensure that equilibration of all the enzyme/substrate complexes occurs. In practice it means that >2 fold excess of FTP over HMM needs to be used. The ratio of the amplitudes of the slow to the fast phase gives the proportion of regulated HMM molecules and was found to vary both between preparations and within a preparation, i.e. the proportion regulated decreased with age. If a preparation was found to be <60% regulated it was discarded. Of 16 typical preparations used, the average degree of regulation was 72% (SD = 7.1).

Figure 5-3 demonstrates many of the essential features of the FTPase mechanism of scallop HMM. The addition of FTP causes a rapid increase in fluorescence until a steady-state is reached. The length of time that this is maintained depends on the amount of FTP added (c.f 5-3a and 5-3b). A relatively rapid decay in fluorescence is seen when the FTP is finally consumed, which corresponds to Pi release from the unregulated molecules. There then follows a very slow fluorescence decay as Pi is released from the regulated

Table 5-1

RELATIVE AMPLITUDE (1)		RATES (s <sup>-1</sup> )						
FTP ( $\mu$ M)	fast phase	slow phase	end point	turnover time of fast phase(s)	observed(2) steady-state	unregulated(3) steady-state	regulated single turnover	
-Ca	10	0.30	0.50	0.20	132	0.038	0.13	0.0014
-Ca	20	0.32	0.32	0.34	240	0.041	0.13	0.0017
+Ca	10	0.87	-	0	48	0.10	-	-
+Ca	20	0.84	-	0	87	0.11	-	-

(1) Amplitudes measured relative to the total enhancement observed on FTP binding to HMM in EGTA using the enhancement after the addition of Ca as the baseline.

(2) The observed steady-state rate calculated from the turnover time.

(3) The turnover rate of the unregulated was calculated from the total turnover time assuming that turnover was due to the unregulated molecules alone (30%).

molecules. The rate, but not the amplitude, of this process is independent of the amount of FTP originally added. Addition of Ca during this slow phase dramatically speeds up product release, readdition of excess EGTA allows FDP to rebind the HMM. The final addition made in figure 5-3 is of excess ATP which allows FDP dissociation to be measured. This experiment demonstrates many of the processes that make up the FTPase reaction (nucleotide binding and dissociation under various conditions) that are examined in greater detail later. Table 5-1 summarises the information regarding the amplitude of the fluorescence signals and the rate of FTP turnover by both the regulated and unregulated HMM populations.

These data show that FTP behaves in a manner analagous to ATP. Turnover of FTP is Ca sensitive and responds to the presence of the two populations of HMM molecules. Each of the phases seen in figure 5-3 is examined in greater detail either in this chapter or chapter 6.

#### FTP binding

Fluorescence stopped-flow experiments were carried out to determine the rate constant of FTP binding to HMM in the presence and absence of Ca. Figure 5-4a and 5-4b show that there is no effect of Ca on these rate constants. The binding of FTP to HMM was monitored over a range of FTP concentrations and the second order binding constant was calculated as  $2 \times 10^5 \text{ M}^{-1}\text{s}^{-1}$ , which is about 20-fold slower than the equivalent rate constant for ATP binding. No

plateau rate was seen since the FTP concentration could not be taken high enough due to the increase in the background fluorescence dominating the desired signal. At equimolar FTP, a 500% fluorescence enhancement was observed upon binding to HMM. Therefore if a 100-fold excess of FTP is used, the observed change is reduced to 5% due to the contribution to the signal from the unbound nucleotide. The traces shown in figure 5-4 are virtually monophasic but there is the possibility that there is a slow phase accounting for <5% of the total signal which is not seen on these fast traces but can be seen when observed over a slower timebase (figure 5-2d).

#### FTP hydrolysis

It has been shown that ATP hydrolysis is not rate limiting in the ATPase pathway (Lyman and Taylor, 1971). Some ATP analogues show anomalous hydrolysis steps (i.e 5-etheno-ATP) (Rosenfelt and Taylor, 1984). The hydrolysis of FTP by HMM was measured by manual quenching procedures followed by FPLC analysis. FTP binding is 20-fold slower than ATP binding, so the resolution of an FTPase experiment could be limited by the rate of FTP binding.

The rate of binding at the concentrations to be used (30 $\mu$ M FTP, 40 $\mu$ M HMM) was measured using the stopped-flow apparatus. If equal sized syringes are used with the stopped-flow apparatus, then a 2-fold dilution of the protein results, which would require an 80 $\mu$ M HMM stock solution. HMM stored at this concentration has a tendency

to aggregate and precipitate. To reduce the concentration of the stock protein required, syringes of different diameters were used. The protein was placed in a 5ml syringe and the FTP in a 1ml syringe. The ratio of the areas of these syringes was 1 : 7.3. With these syringes, concentrations of  $46\mu\text{M}$  HMM and  $219\mu\text{M}$  FTP were required to achieve reaction chamber concentrations of  $40\mu\text{M}$  and  $30\mu\text{M}$  respectively.

Figure 5-5b shows the rate of FTP binding and turnover at these concentrations in the presence of Ca. Although the rate of binding will not be an exponential, it could be approximated to one in order to obtain an estimate of the rate constants of binding. When fitted to a transient curve, rates constants of  $k_{\text{on}} = 1.9\text{s}^{-1}$  and  $k_{\text{off}} = 0.2\text{s}^{-1}$  were obtained. Thus, within 5 seconds, the FTP would have fully bound under these conditions had product release not occurred. Hydrolysis was followed by the manual quench procedure which was used to look at the rate of ATP hydrolysis (figure 4-4). Figure 5-5a shows the FPLC elution profiles for FTP/FDP mixtures at 2 and 40 seconds incubations. In the absence of Ca, hydrolysis was ~90% complete within 10 seconds of mixing (figure 5-5c). The curve closely resembles the loss of ATP with time (figure 4-4c). Thus hydrolysis is much faster than the overall flux through the pathway.

When the hydrolysis rate in the presence of Ca was measured, it was found to occur at a similar rate to product release (as measured in figure 5-5c) which complicates the analysis

of the results and no distinction between hydrolysis and product release could be made.

Quench-flow experiments are needed to accurately determine the kinetics of hydrolysis.

#### Phosphate release

The slow formycin fluorescence decay which was seen during turnovers of HMM -Ca occurred at approximately the same rate as Pi release by HMM during ATP single turnovers (Wells and Bagshaw, 1985). It seems reasonable to assume that this decay is measuring the same process. As noted previously, hydrolysis occurs relatively rapidly and, as will be seen later, FDP release is also more rapid than this process. The major steady-state intermediate is likely to be an HMM.FDP.Pi complex. If so, it is Pi release which is rate limiting and is activated from  $0.002\text{s}^{-1}$  to  $0.2\text{s}^{-1}$  by the addition of Ca.

#### FDP release

FDP release from HMM -Ca was measured by displacement from HMM using excess ATP. Figure 5-6a shows that FDP dissociates from HMM -Ca, with a rate constant of  $0.008\text{s}^{-1}$ . Although this value is only 4 fold faster than the Pi dissociation rate constant, measured at  $0.0018\text{s}^{-1}$  for the same preparation, the difference in rate constants was considered significant. The difference in rates is also apparent in figure 5-3a and 5-3b.

The situation was not quite so clear when the dissociation from HMM +Ca was measured, since there was no suitable displacing agent. Figure 5-6b demonstrated the fluorescence change observed upon addition of Ca to a HMM.FDP complex. A rate constant of  $5.2\text{s}^{-1}$  was measured for the process. It need not be the dissociation rate constant, since it could be a conformational change preceding dissociation. The dissociation rate constant is likely to be of this order in the light of the dissociation rate constants obtained for ADP.

The binding and dissociation of FDP and other non-hydrolysable nucleotides will be discussed further in chapter 6.

#### ATP chase of FTP turnovers

One potential criticism of all single or limited turnover experiments is that the final turnover may be atypical in some way. In vivo the proteins are constantly bathed in substrate which may itself affect the enzymic activity. FTP turnovers provide an opportunity to test this criticism.

Figure 5-7a shows a turnover of FTP by HMM -Ca. The slow decay phase which occurred during the last turnover had a rate constant of  $0.0013\text{s}^{-1}$ . The fluorescence did not return to the start value since some FDP remained bound at the end of the reaction. At the wavelength used to excite formycin fluorescence, (313nm), ATP does not absorb much of the

light. Excess ATP can therefore be added during the brief steady-state and the drop in fluorescence followed. A sharp initial drop should be seen followed by the slow, regulated release of products. In figure 5-7b,  $500\mu\text{M}$  ATP was added 80 seconds after the FTP. The slow phase, when fitted to an exponential, gave a rate constant of  $0.0012\text{s}^{-1}$ , which is the same as that obtained during the final turnover of FTP. The fluorescence decays back to its initial value because the excess ATP prevents any FDP remaining bound at the end of the reaction. Figure 5-7c demonstrates the effect which Ca has on the system. Initially FTP was added in the absence of Ca and, after 80 seconds, excess ATP and Ca were added. The release of products occurred very much more quickly. This process (when observed over a much shorter time) could be fitted to an exponential which gave a rate constant of  $0.2\text{s}^{-1}$ .

ATP chase experiments provide a good method for measuring the relative amplitudes of the slow and fast phases since the start point of the fluorescence decay is better defined than the typical sigmoidal profile of limited turnovers. A biphasic fit to the fluorescence decay was carried out and the signal extrapolated back using the calculated rate constants and amplitudes. This calculation will be used extensively in chapter 6. In figure 5-7b the HMM sample is calculated as being 70% regulated.

### Pyrophosphate dissociation

P<sub>i</sub> is an inhibitor of the ATPase activity of myosin but produces no change in the tryptophan fluorescence. FTP provides a method by which the effect of Ca on the dissociation rate constant of P<sub>i</sub> could be measured. In the presence of Ca, excess FTP bound to HMM.P<sub>i</sub> within the manual mixing time (<5 seconds). In the absence of Ca, FTP bound with a half time of about 100 seconds. P<sub>i</sub> release provides a further example of a ligand where the dissociation step is Ca sensitive.

### IASL labelling of HMM

Wells and Bagshaw (1984) attached a spin label to the reactive thiol group on the myosin head in an attempt to monitor changes in mobility of the head, relative to the rest of the molecule, in response to the removal of the light chains and Ca. No difference in the mobility of the head in the presence and absence of Ca was noted.

Spin-labelling of the reactive thiol on the head of HMM causes a loss in Ca sensitivity of the acto-HMM ATPase when measured by turbidity assays (Jackson et al, 1986). The effect of labelling HMM with an iodoacetamide based spin label (IASL) upon the HMM FTPase was examined. IASL was used since the extent of labelling could be monitored by following the EPR spectrum of the label. When the IASL was free in solution a large EPR signal was seen which was

reduced upon binding. EPR, therefore, allows the amount of IASL which has reacted to be followed, allowing correlation with the FTP turnover results. As labelling proceeded there was a discrete switch of the molecules from the regulated to the unregulated state (figure 5-8). The loss of amplitude of the slow phase correlated with the loss of the EPR signal from the free IASL. Reacting IASL with HMM renders it insensitive to Ca thus, although no changes in mobility in head movement was detected by Wells and Bagshaw (1984), reductions in head mobility cannot be ruled out as the mechanism of control of ATPase activity.

Increasing the salt concentration also can cause a loss in the Ca sensitivity of HMM. It is a change that is reversible and is not a switch from a regulated to unregulated form. The details of increasing ionic strength will be discussed fully in chapter 6.

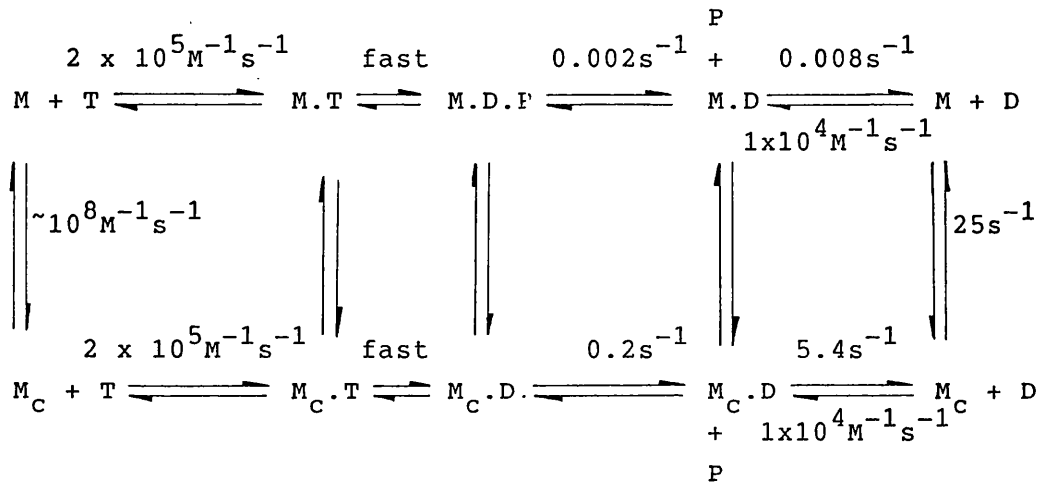
### Discussion

FTP has proved to be a very useful ATP analogue with which to study Ca regulation of scallop myosin ATPase. The product release steps, which are accompanied by small tryptophan fluorescence changes during ATP turnover, produce large changes in the formycin fluorescence.

The simplest scheme for the FTPase mechanism is given below (equation 5-1) and includes those rates which have been measured. It is similar to the minimum scheme for the ATPase mechanism (equation 4-2). The second order FDP

binding constant is measured in chapter 6 (figure 6-1).

Equation 5-1



Generally the kinetic constants obtained for the FTPase are similar to those of the ATPase. The exception being the binding of FTP to HMM which is 20-fold slower than the binding of ATP. This is presumably due to the FTP existing in the syn conformation in solution whereas the active site probably corresponds to the anti conformation (c.f Shoham and Steitz, 1980). The same effect was reported for FTP binding to rabbit S1 (Bagshaw et al, 1972). As was discussed for the ATPase scheme, equation 5-1 is an oversimplification of the mechanism. Evidence for multi-step nucleotide binding and a kinetic trapping of intermediates is presented in chapter 6.

The overriding effect of Ca on the rate of FTP turnover is to increase the rate of product dissociation by at least 100- fold. FTP binding, and probably hydrolysis, remains

unaffected by Ca, leaving Ca to modulate the rate of isomerisation of the nucleotide/protein complexes.

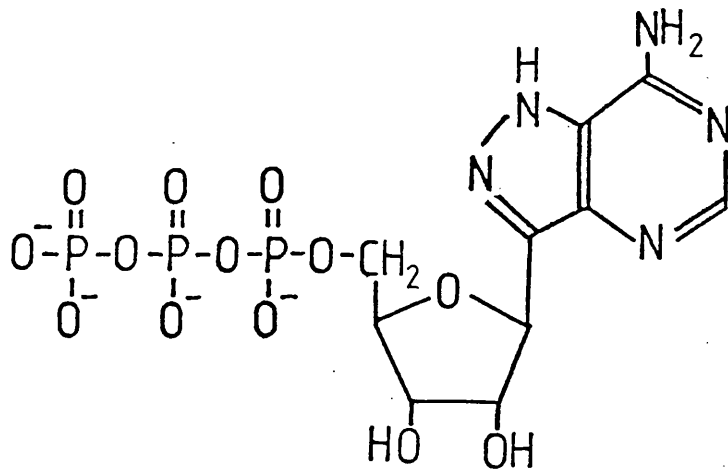
Figure 5-1

a Adenosine 5'-triphosphate - ATP

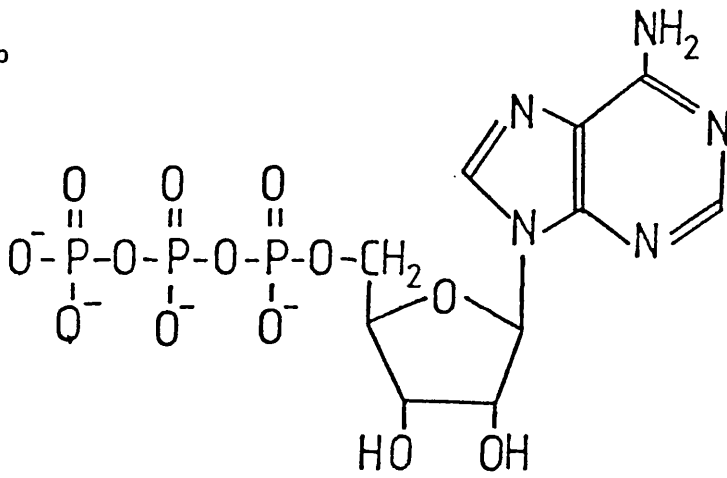
b Formycin A 5'-triphosphate - FTP

c Formycin A 5'-( $\beta$ - $\gamma$ -imidodiphosphate) - FMPPNP

a



b



c

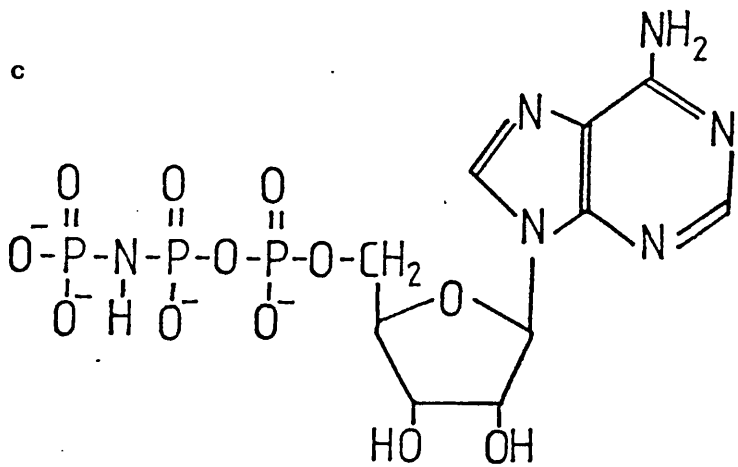


Figure 5-2

The turnover of FTP by  $S1^{-RD}$  and HMM in the presence and absence of Ca.

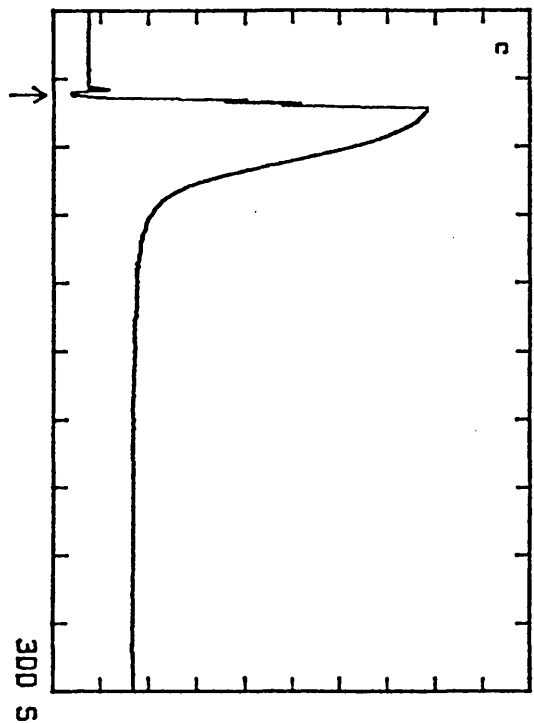
a 10 $\mu$ M FTP was added to 2 $\mu$ M  $S1^{-RD}$ , 100 $\mu$ M Ca at the time indicated. 1 division represents a 15% fluorescence change.

b 10 $\mu$ M FTP was added to 2 $\mu$ M  $S1^{-RD}$ , 100 $\mu$ M EGTA at the time indicated. 1 division represents a 15% fluorescence change.

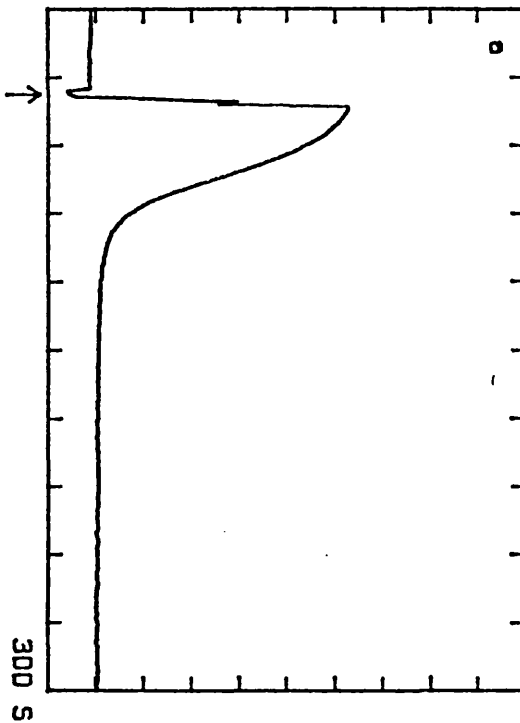
c 10 $\mu$ M FTP was added to 2 $\mu$ M HMM, 100 $\mu$ M Ca at the time indicated. 1 division represents a 15% fluorescence change.

d 10 $\mu$ M FTP was added to 2 $\mu$ M HMM, 100 $\mu$ M EGTA at the time indicated. 1 division represents a 15% fluorescence change.

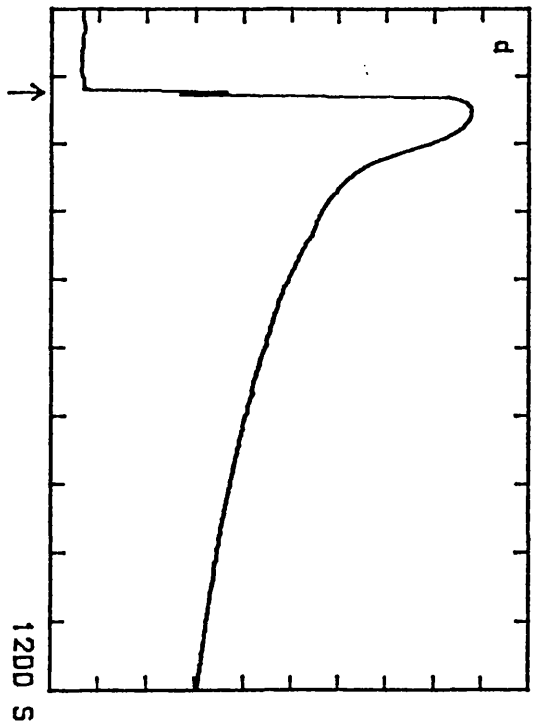
FLUORESCENCE



FLUORESCENCE



FLUORESCENCE



FLUORESCENCE

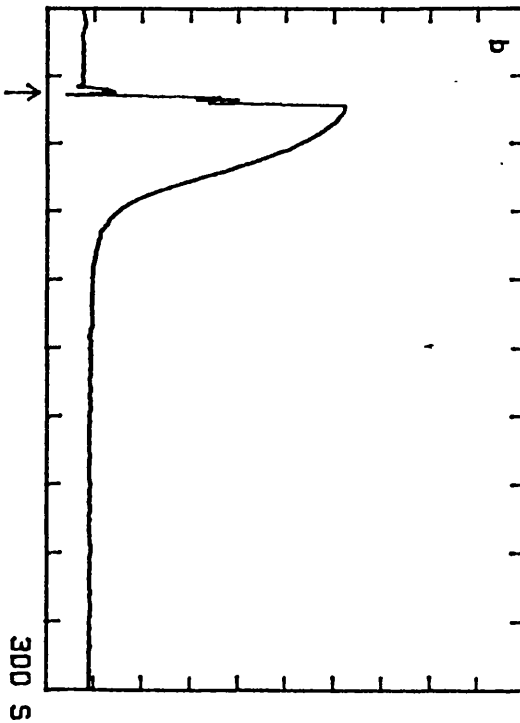


Figure 5-3

Multiple-turnovers of FTP by HMM in the absence of Ca.

To 2 $\mu$ M HMM, 100 $\mu$ M EGTA the following additions were made;

- (i) 10 $\mu$ M FTP in (a) and 20 $\mu$ M in (b)
- (ii) 200 $\mu$ M Ca
- (iii) 200 $\mu$ M EGTA
- (iv) 1mM ATP

1 division represents a 15% fluorescence change in (a) and a 8% change in (b).

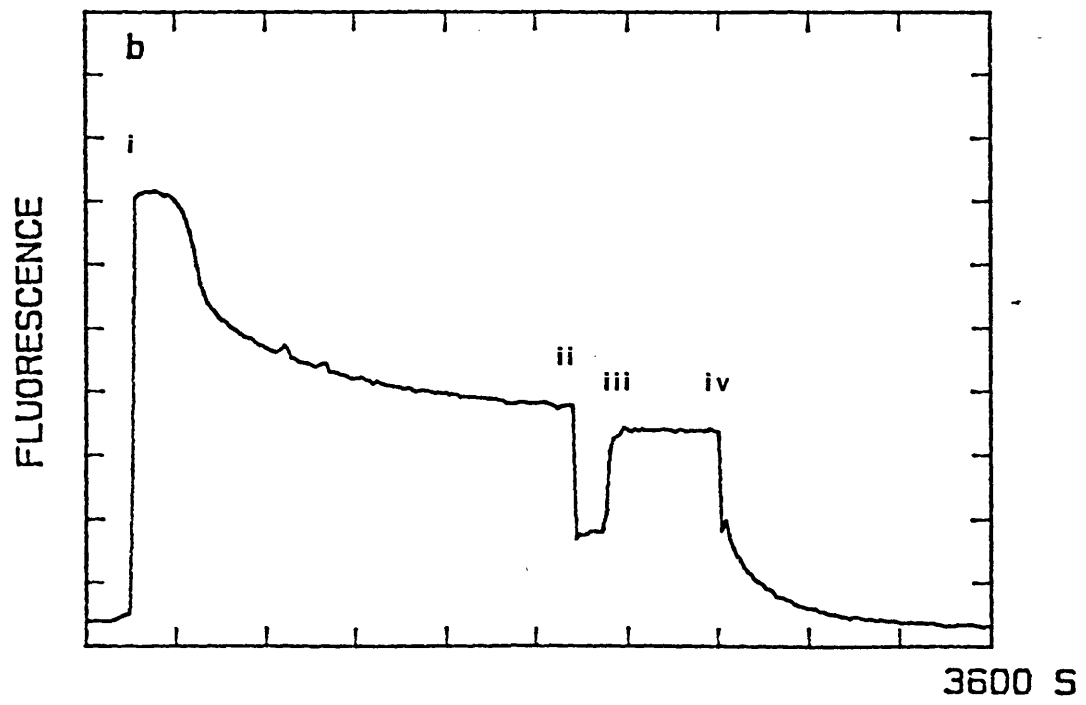
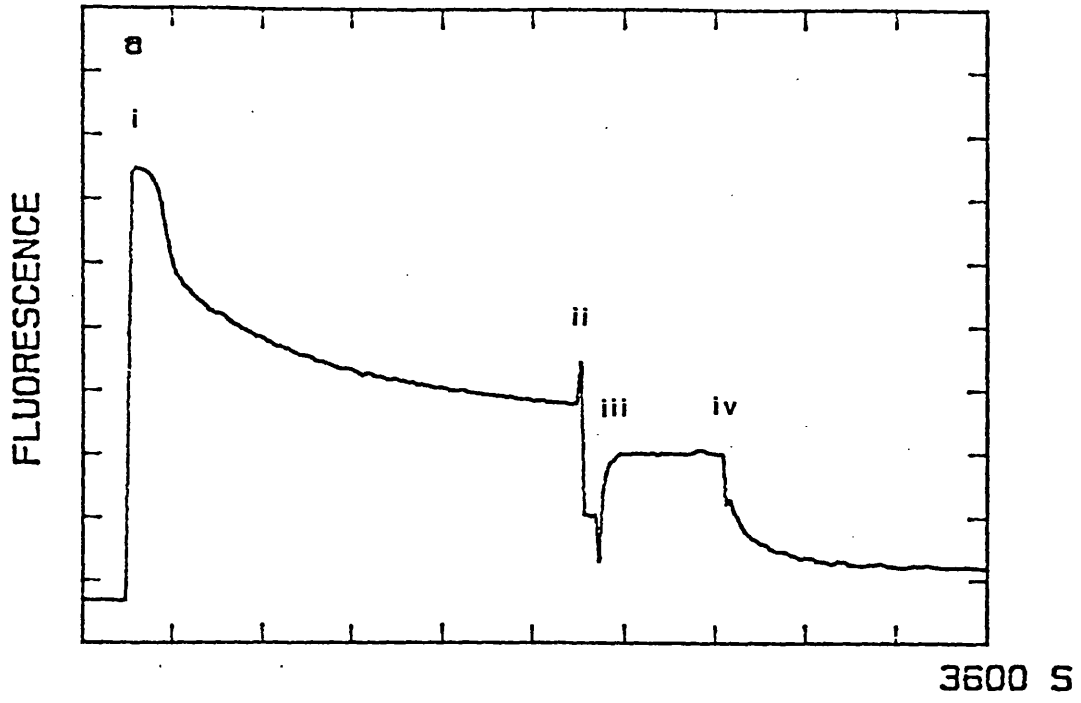
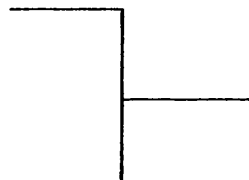


Figure 5-4

FTP binding to HMM in the presence and absence of Ca monitored by the increase in formycin fluorescence.

(a)

4 $\mu$ M HMM  
100 $\mu$ M EGTA

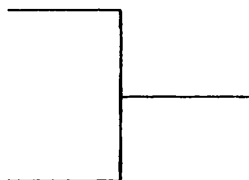


$k_{obs} = 4.3s^{-1}$   
1 division = 5% fluorescence change

40 $\mu$ M FTP  
100 $\mu$ M EGTA

(b)

4 $\mu$ M HMM  
100 $\mu$ M Ca



$k_{obs} = 4.8s^{-1}$   
1 division = 5% fluorescence change

40 $\mu$ M FTP  
100 $\mu$ M Ca

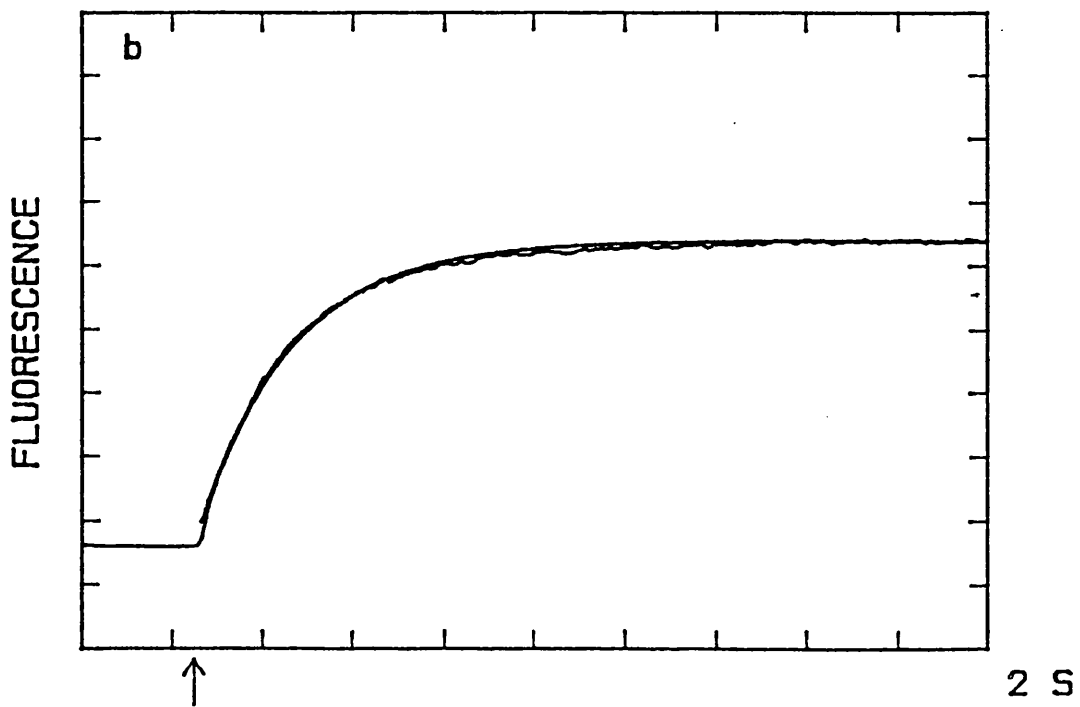
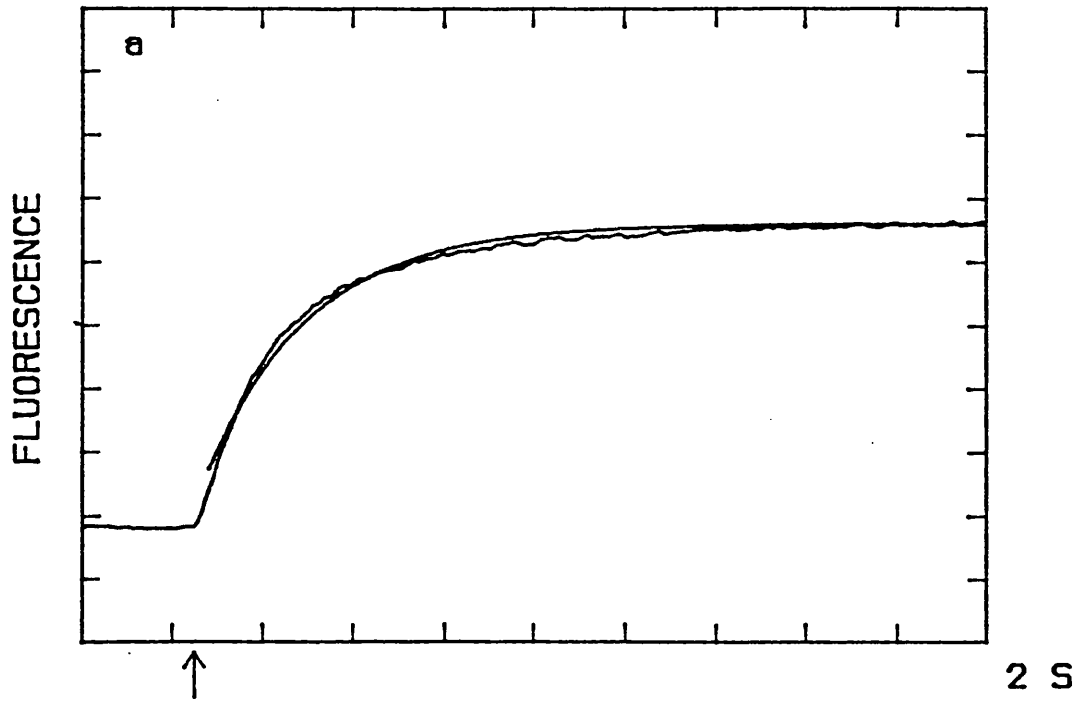


Figure 5-5

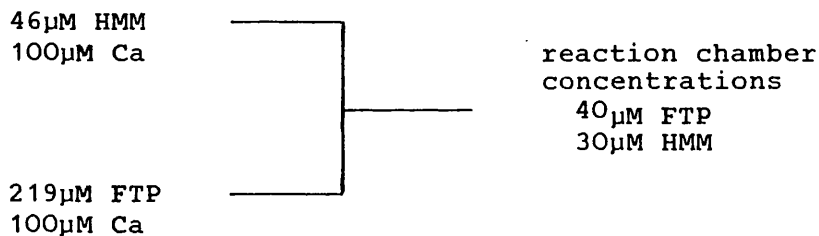
a

Hydrolysis of FTP as measured by perchloric acid quench and FPLC analysis.

FPLC Mono Q separation of a FDP/FTP mixture after (i) 2 seconds and (ii) 40 seconds incubation with HMM in the absence of Ca (40 $\mu$ M FTP, 30 $\mu$ M HMM).

(b)

Binding of FTP to HMM at high protein concentration using unequal volume syringes (ratio of the volumes of the protein syringe to nucleotide syringe = 7.1:1).



(c)

Plot of the relative amount of FTP left (as determined by FPLC) after incubating with HMM -Ca for various times. An exponential fit to FTP disappearance gave a rate constant of 0.5s<sup>-1</sup> with ~6% FTP left after 20 seconds.

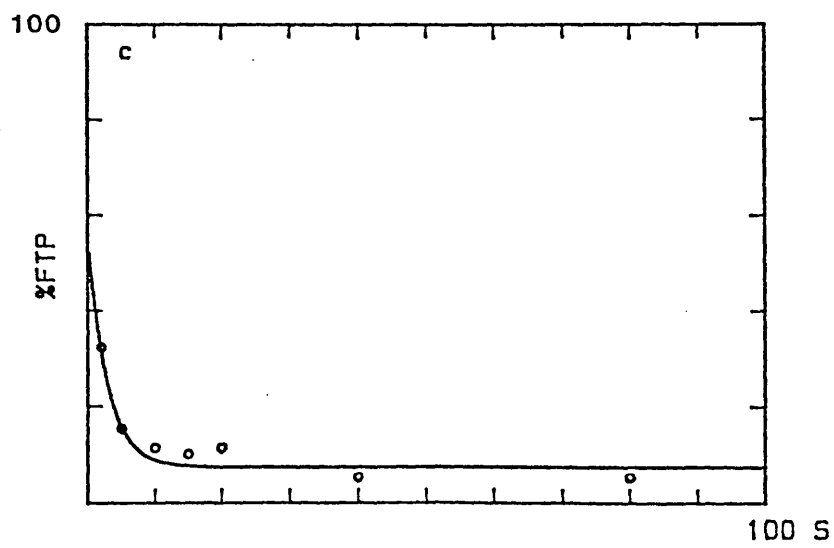
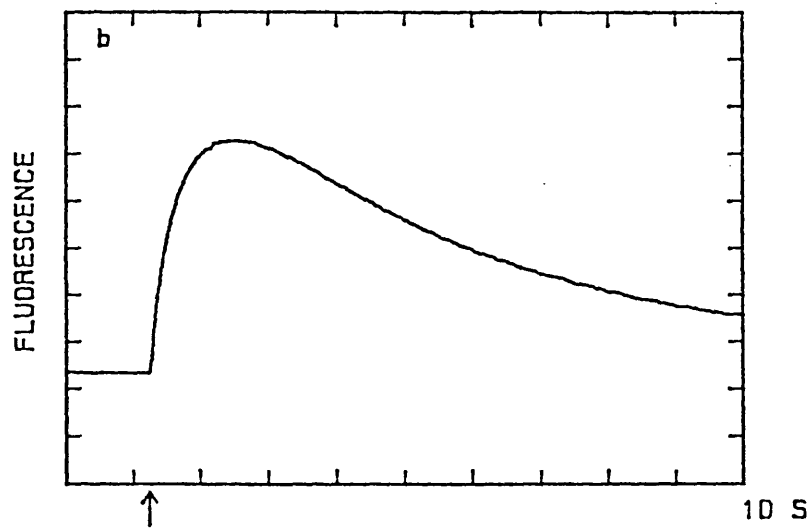
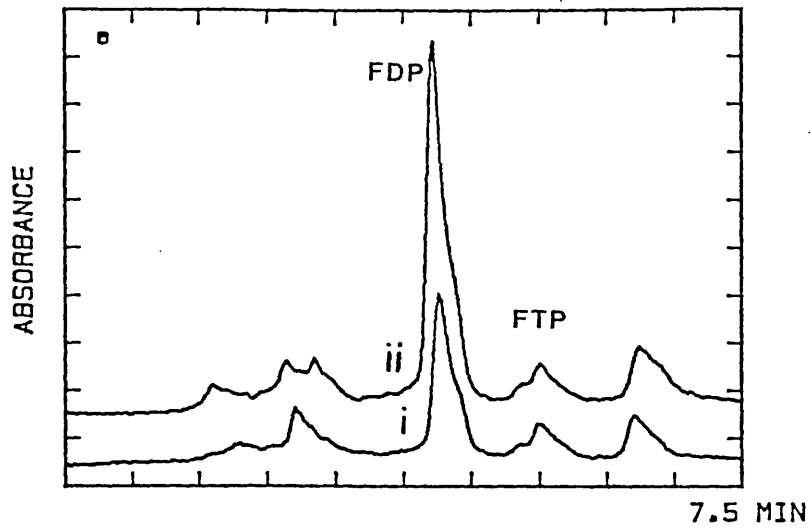
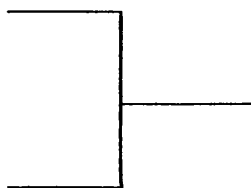


Figure 5-6

Dissociation of FDP from HMM in the presence and absence of Ca monitored by formycin fluorescence.

(a)

6 $\mu$ M FDP  
4 $\mu$ M HMM  
100 $\mu$ M EGTA

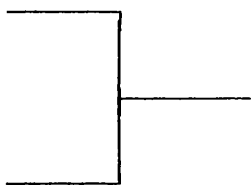


$k_{obs} = 0.008s^{-1}$   
1 division = 2% fluorescence change

500 $\mu$ M ATP  
100 $\mu$ M EGTA

(b)

6 $\mu$ M FDP  
4 $\mu$ M HMM  
100 $\mu$ M Ca



$k_{obs} = 5.2s^{-1}$   
1 division = 2% fluorescence change

200 $\mu$ M Ca

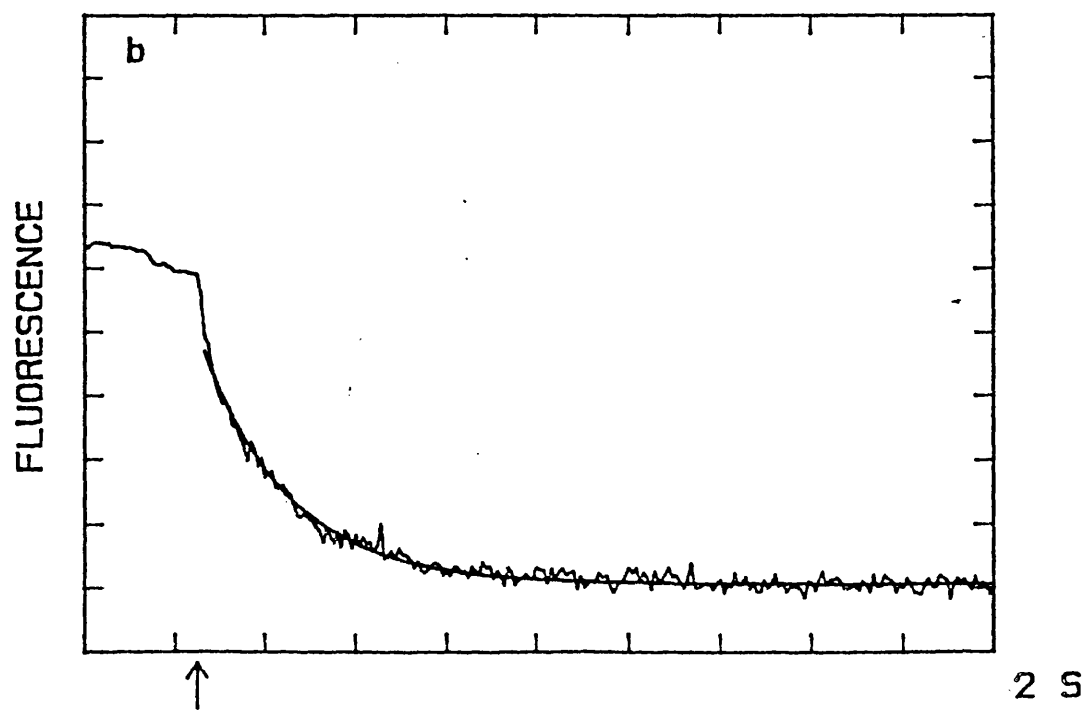
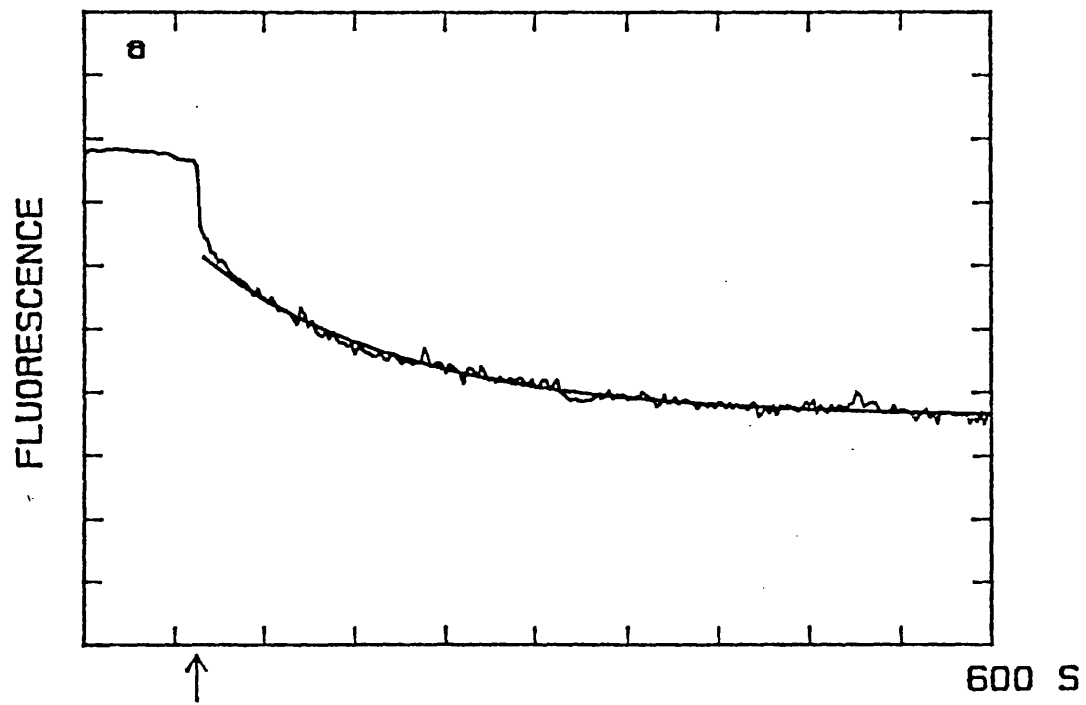


Figure 5-7

The turnover of FTP by HMM in the presence and absence of an ATP chase.

a 10 $\mu$ M FTP was added to 2 $\mu$ M HMM, 100 $\mu$ M EGTA at the time indicated. 1 division represents a 15% fluorescence change.

$$k_{\text{obs}} = 0.0013 \text{ s}^{-1}$$

b 10 $\mu$ M FTP was added to 2 $\mu$ M HMM, 100 $\mu$ M EGTA at the time indicated and 1mM ATP added after 80 seconds.

1 division represents a 15% fluorescence change.  $k_{\text{obs}} = 0.0012 \text{ s}^{-1}$

c 10 $\mu$ M FTP was added to 2 $\mu$ M HMM, 100 $\mu$ M EGTA at the time indicated and 1mM ATP, 200 $\mu$ M Ca added after 80 seconds.

1 division represents a 15% fluorescence change.

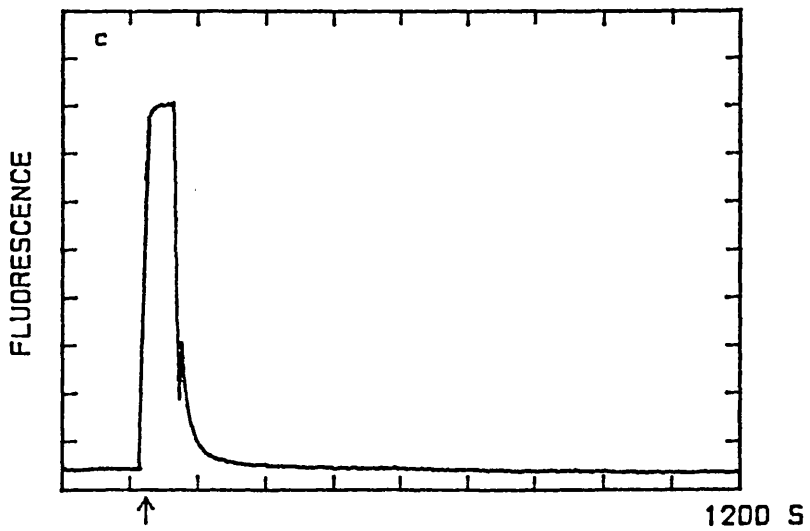
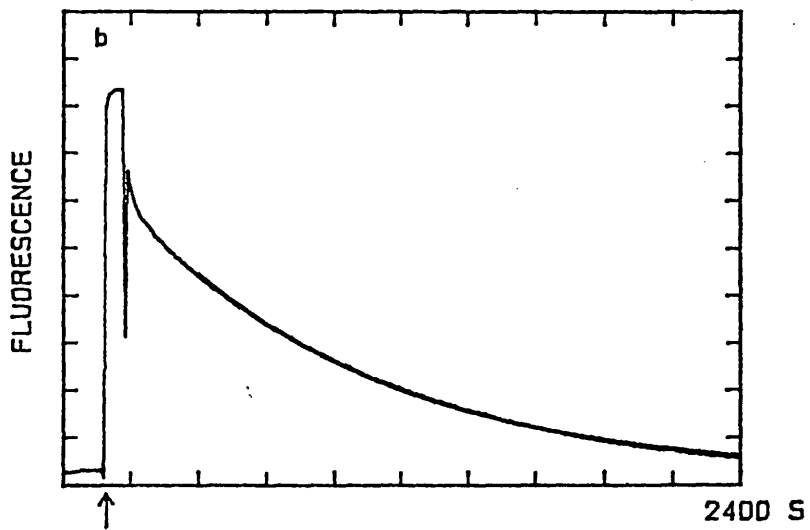
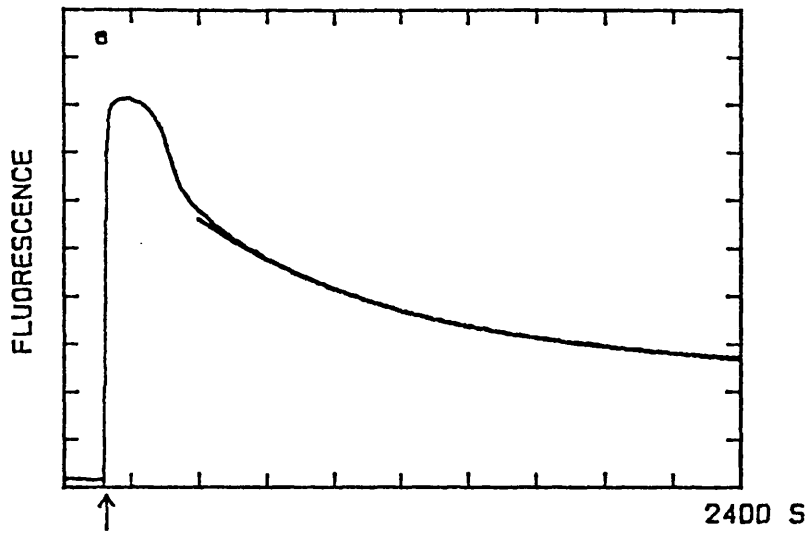


Figure 5-8

The effect of spin labeling with IASL on the Ca sensitivity of HMM. This was monitored by FTP turnovers followed by an ATP chase

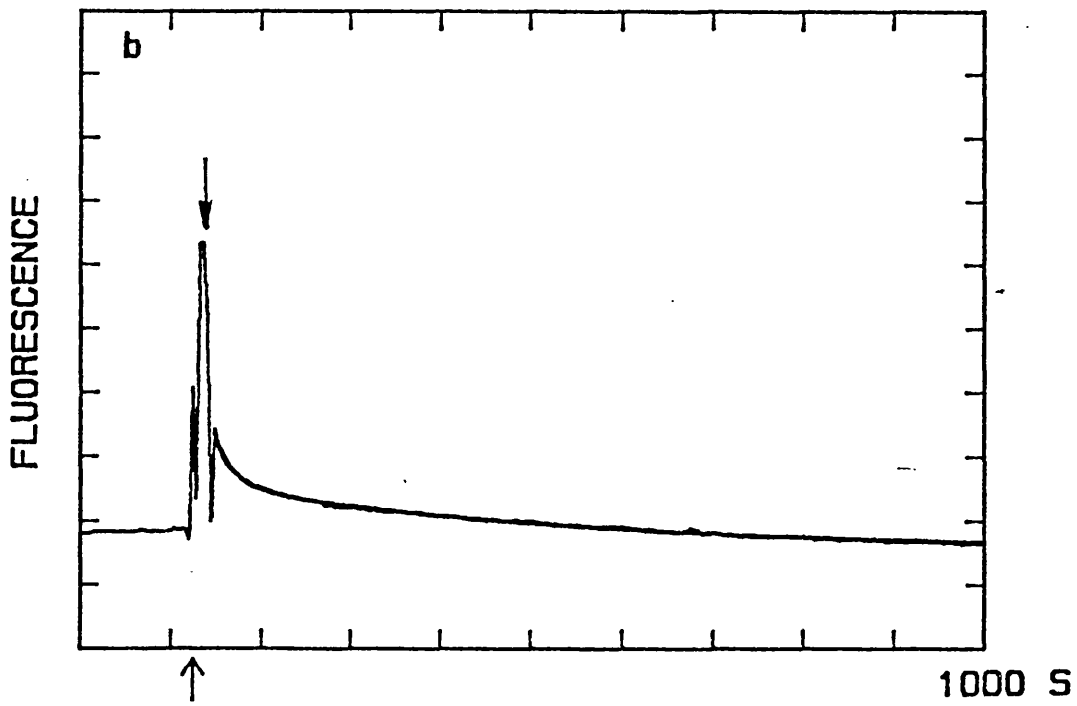
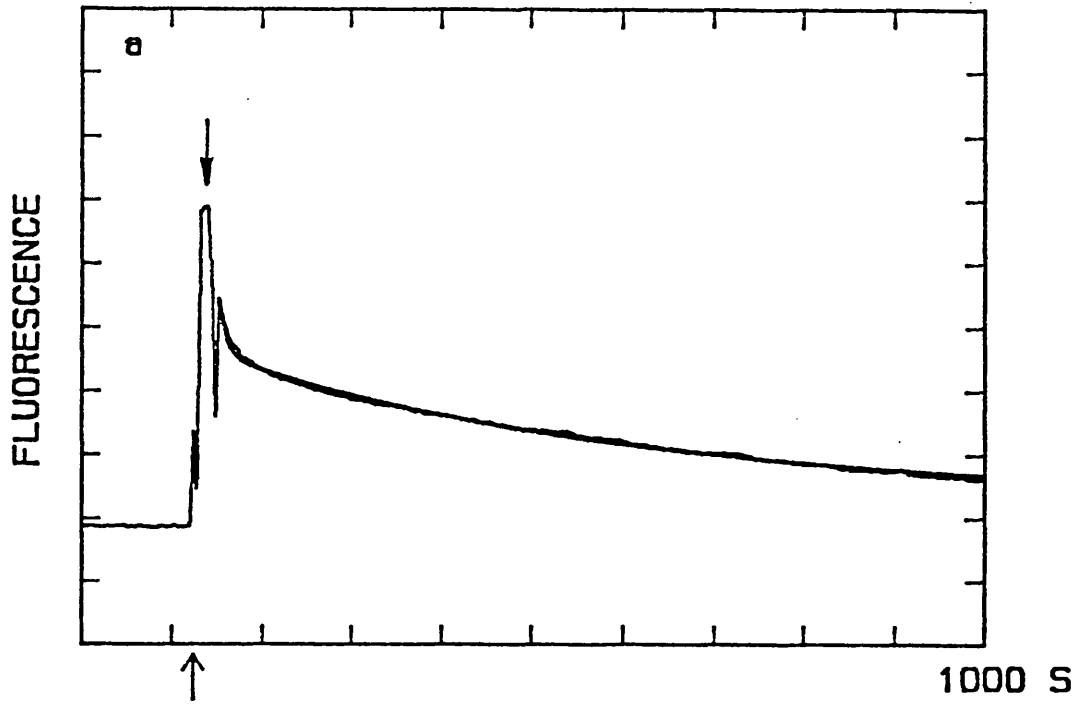
a

At the time indicated (↑) 20μM FTP was added to a solution containing 2μM HMM, 100μM EGTA which had been incubated with a 1.5 molar excess of IASL at 0°C for (a) 5 minutes and (b) 60 minutes. 1mM ATP was added at ↓.

(a)  $k_{\text{obs}} = 0.002\text{s}^{-1}$  49% regulated.

(b)  $k_{\text{obs}} = 0.002\text{s}^{-1}$  21% regulated.

1 division represents a 7% fluorescence change.



CHAPTER 6

TRAPPING OF REACTION INTERMEDIATES

## Introduction

It was concluded in chapter 4 that nucleotide binding was at least a 3 step process. The scheme for binding was deduced despite the very small changes in tryptophan fluorescence which occur. A combination of experimental observations and deductions were necessary to arrive at the 3 step binding scheme. Direct observations and measurements of the slow conformational changes which were proposed were not possible. Formycin nucleotides, with their large fluorescence changes, provide a potential method for observing these transitions.

In chapter 5, the mechanism of the FTPase was shown to be similar to the ATPase mechanism. In this chapter formycin nucleotides are used to probe the enzyme mechanism further leading to a novel mechanism for the FTPase being proposed. The binding of FTP is complicated by the hydrolysis step which occurs soon after binding. Non-hydrolysable nucleotides (FDP and FMPPNP) have therefore been used to study binding. FTP has been useful in probing the product release step under a variety of conditions.

## FDP binding

Binding of FTP and FMPPNP to HMM -Ca cause a 500% enhancement in the fluorescence signal. FDP binding to HMM -Ca was examined to determine both the mechanism of binding and the fluorescence level of the bound state.

The rate of FDP binding to HMM -Ca was monitored as a function of FDP concentration over the range 3-75 $\mu$ M (reaction chamber concentration). Binding was distinctly biphasic with both the fast and slow phases increasing in rate with increasing FDP concentration. At higher FDP concentrations the slow phase decreased in amplitude relative to the fast phase. Two such traces are shown in figure 6-1a and 6-1b.

An analysis of the total amplitude of the observed signal gives information regarding the binding constant and the degree of fluorescence enhancement displayed by the HMM.FDP complex. Only the FDP which binds will contribute to the change in fluorescence, the rest provides background fluorescence. The contribution to the overall signal made by the unbound FDP must be accounted for, to allow the true enhancement to be calculated. Figure 6-1c shows a plot of the fluorescence enhancement against concentration of FDP. A hyperbolic fit through the data gives a binding constant of 37 $\mu$ M and a fluorescence enhancement of the FDP.HMM species of 485% which is very similar to the enhancement seen with FTP binding. Relatively small changes are actually observed due to the high equilibrium dissociation constant.

A binding constant of this order was confirmed by two other stopped-flow experiments. If 50 $\mu$ M FDP was mixed with 6 $\mu$ M FDP, 4 $\mu$ M HMM a fluorescence change corresponding to further FDP binding was seen. However if 100 $\mu$ M FDP was added to

50 $\mu$ M FDP, 4 $\mu$ M HMM no fluorescence change could be detected. In the former experiment, the HMM was initially almost free of FDP but in the second it was practically saturated with FDP.

In the presence of Ca, only a very small enhancement on the addition of FDP to HMM was seen, comparable with the lack of tryptophan fluorescence enhancement seen on ADP binding to HMM +Ca. It seems likely that the lack of signal was due to a combination of a weaker binding constant (c.f FMPPNP) and the HMM:FDP.Ca complex having a lower fluorescence state. No suitable displacing agent was found to determine whether the FDP was bound under these conditions.

#### FMPPNP binding

In the absence of Ca, and at low FMPPNP concentrations, a large fluorescence enhancement was seen on binding to HMM (figure 6-2b). The trace was distinctly biphasic with nearly 50% of the signal having the slower rate. In the presence of Ca the total amplitude was smaller and the slow rate accounted for only 25% of the total signal (figure 6-2a). At higher FMPPNP concentrations (figure 6-2c and 6-2d) the amplitude of the slow phase was greatly reduced, accounting for 7% and 12% of the total signal in the presence and absence of Ca respectively. Ca therefore appears to reduce the appearance of a slowly forming, highly fluorescent species.

In the absence of Ca, as the FMPPNP concentration is

increased the observed fluorescence enhancement remains approximately constant, despite the increase in background fluorescence. This indicates that the amount of FMPPNP bound increases which compensates for the increased background fluorescence. The slow phase was reduced in amplitude but remained at about the same rate (figure 6-2c and 6-2d). The fast phase did increase both in amplitude and rate with concentration. The dependence of initial binding upon concentration, measured from the initial fast phase, gave a second order binding constant of  $2 \times 10^4 \text{ M}^{-1} \text{ s}^{-1}$ . This is approximately 200-fold slower than ATP binding, a reflection of the effect of both the imidotriphosphate and the formycin ring on the binding step.

The amplitude of the fluorescence enhancement seen on FMPPNP binding to HMM over the range  $3\text{-}75\mu\text{M}$  allowed an estimate of the binding constant. In contrast to FDP binding, a signal is seen during binding of FMPPNP to HMM +Ca, allowing the effect of Ca on the binding constant to be seen. In the presence of Ca a binding constant of  $10\mu\text{M}$  was obtained. In the absence of Ca binding was much tighter with a binding constant of  $<2\mu\text{M}$ . Binding is likely to be tighter than this but it cannot be measured accurately at the protein concentrations used.

#### FMPPNP dissociation

FMPPNP dissociation was measured by the addition of excess ATP to HMM.FMPPNP. ATP could only bind to HMM as FMPPNP was released, hence the drop in formycin fluorescence measures

the FMPPNP dissociation rate constant. These rates were quite slow requiring a large excess of ATP to ensure that it was not consumed by the unregulated or free HMM before the end point of the reaction had been reached.

In the presence of Ca, FMPPNP dissociates relatively rapidly, with a rate constant of  $0.07\text{s}^{-1}$  (figure 6-3a). This is similar to the equivalent AMPPNP dissociation rate constant ( $0.03\text{s}^{-1}$ ) that was measured by displacement with FTP.

The problem of trying to measure very slow rate constants was demonstrated when FMPPNP dissociation from HMM -Ca was measured. The release of FMPPNP was biphasic when carried out in EGTA, (figure 6-6ai) with a very slow second phase. The slow phase appears almost horizontal over the time-scale shown here. Fortunately an approximate end point to the reaction can be rapidly achieved by the addition of excess Ca. A biphasic fit to the fluorescence decay in EGTA, using the Ca level to fix the base-line, gives a rate constant of about  $1 \times 10^{-4} \text{ s}^{-1}$ . Attempts to measure this rate more accurately, by fluorescence techniques, fail due to photodecomposition, protein ageing, ATP exhaustion and instrumental instability.

It can be seen from the FMPPNP binding data that it can bind in 2 different states depending upon whether Ca is present. The conformational change accompanying the HMM.FMPPNP to HMM.Ca.FMPPNP transition was followed in figure 6-3b. This was a monophasic change occurring with a rate constant of

$0.12\text{s}^{-1}$ . Both the conformational change and the release step were monitored simultaneously in figure 6-3c by the addition of excess ATP and Ca to HMM.FMPPNP. A biphasic fit gave rate constants of  $0.16\text{s}^{-1}$  and  $0.046\text{s}^{-1}$ .

#### FTP turnovers by HMM at various salt concentrations

The Ca sensitivity of scallop myosin and HMM ATPase is seen best at low ionic strength (20mM NaCl). As the salt concentration is raised, the sensitivity is gradually lost. Steady-state or tryptophan fluorescence assays do not provide much information about how the loss in sensitivity occurs. FTP turnovers provided a method by which the loss in sensitivity could be examined.

Although it proved to be possible to carry out FTPase assays on myosin suspensions, it would be preferable to use myosin solutions. This necessitated working at about 200mM NaCl, a concentration where sensitivity is not seen. It was hoped that by using an alternative anion such as acetate, (Ac), that the range of salt concentrations, over which >70% regulation could be seen, would be extended. A comparison between the effects of NaCl and NaAc on the product release steps was carried out.

At 20mM salt, the turnover in both  $\text{Cl}^-$  and  $\text{Ac}^-$  was indistinguishable. As the salt concentration was increased, a difference between the two anions became apparent. Figure 6-4 shows the rate of product release over a range of NaCl concentrations. At 300mM NaCl, the slow phase had all but

vanished. At intermediate concentrations (100mM and 150mM NaCl) the slow phase had decreased in amplitude but increased in rate (figure 6-4a and 6-4b). NaAc had a similar effect on the product release step, but it occurred over a different range of salt concentrations. A series of these traces are shown in figure 6-5. Even at 600mM NaAc (figure 6-5c) there was a residual slow phase which was Ca sensitive.

Analysis of the data is difficult to carry out unambiguously. A single exponential apparently fits the data reasonably well, but a small, systematic deviation from the calculated fit can be seen. Double exponentials were therefore used to analyse the data although errors in excess of 10% in the calculated parameters occasionally resulted if that phase consisted of only a few data points. Table 6-1 shows the effect of salt on the rate and amplitudes of the slow and fast phases. At the extreme of salt concentrations (20mM and 300mM) the fast and slow phases respectively could not be measured with any great accuracy due to their small amplitude.

Table 6-1

[NaCl] (mM)	Fast phase		Slow phase	
	Amplitude (%)	rate (s <sup>-1</sup> )	amplitude (%)	rate (s <sup>-1</sup> )
20	-	-	78	0.0013
100	16	0.014	58	0.0023
150	32	0.014	36	0.0034
200	59	0.017	16	0.0047
300	≥44	0.053	≤3	0.0044

It had been hoped that an alternative to the Cl<sup>-</sup> anion would provide a greater range of salt concentrations over which the >70% Ca sensitivity could be seen. This would possibly have allowed the use of solubilized myosin in FTPase assays. Although Ac<sup>-</sup> did help to extend the range of salt concentrations over which sensitivity could be seen, the effect was not sufficient to allow routine work at the higher ionic strengths.

Salt appears to affect both the amplitude and the rate of the slow phase but the total amplitude of the decay phase remains approximately constant. This effect is clearly different from the effect of spin labelling HMM (figure 5-8) where the amplitude of the slow phase was altered. Explanations for the salt effect are discussed later.

The effect of increasing salt concentration on myosin FTP turnovers was also examined. Although the amplitude of the slow phase could not be determined, the rate of the slow phase increased in a similar way to HMM. Salt therefore appears to be affecting both proteins in a similar manner.

#### Timed ATP chases during FTP turnovers

It was noticed that the relative amplitude of the fast and slow phases could depend upon either the amount of FTP (or ATP) turned over, or when the ATP was added as the chaser. It seemed unreasonable that the fraction of regulated molecules should change under these conditions as required by equation 4-2. Using the custom-built fluorimeter, excess ATP could be added within a few seconds to a HMM. FTP mixture and the decay in the fluorescence monitored. These traces has a sufficiently well defined start point to allow a reasonably accurate measurement of the amplitude of the fast and slow phases to be made.

Figure 6-6a shows the results from a series of ATP chase experiments. Upon addition of ATP there was a rapid drop in fluorescence (product release from the unregulated HMM molecules) followed by a slow release from the regulated HMM. Excess Ca was added to speed up product release to provide a reaction end point for the exponential curve fitting. The total amplitude for each trace varied, thus the data had to be analysed in terms of relative amplitudes of the two phases. When the relative amplitude of the slow phase was plotted against the time of ATP addition, it was

found to increase, as can be seen in figure 6-6c.

#### Timed ATP chases during FMPPNP binding

The binding of FMPPNP to HMM -Ca is strongly biphasic (figure 6-2a). It should therefore be possible to chase off the FMPPNP before the slow phase has been completed. If the profile of the fluorescence decay changes with the time of the ATP chase, it implies that there is a slow conformational change occurring to the HMM.FMPPNP complex after the initial association.

FMPPNP binds more slowly than FTP, which limits the time at which ATP can be used to chase the FMPPNP off. Figure 6-6b shows the results of a series of ATP chases. Ca was added towards the end of the trace, so that the end point of the reaction was rapidly reached. As for the FTP experiment above, the amplitude of the slow phase decreased as the time of ATP chase decreased (figure 6-6c).

#### Discussion

The results presented here regarding ligand binding and dissociation cannot be neatly explained by any one mechanism. Some of the results conflict with one another and without much further work the precise mechanism of the FTPase and the implications for the ATPase is uncertain.

The mechanism for the FTPase presented in equation 5-1 oversimplifies the reaction scheme. As was discovered for

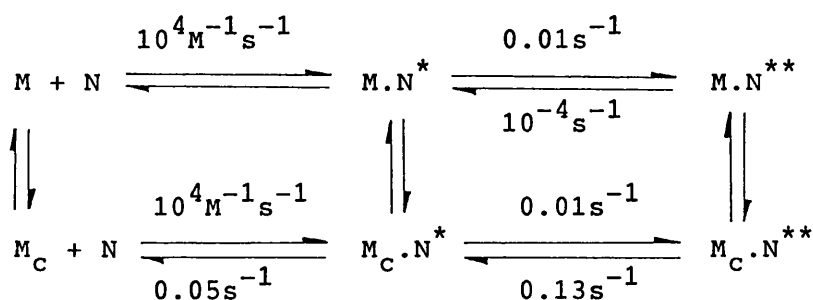
adenosine nucleotide binding, association does not occur in one step. Likewise formycin nucleotide binding is not a single step process. The binding process will again be discussed in terms of non-hydrolysable nucleotide binding (FDP and FMPPNP) anticipating that the conclusions will also apply to FTP binding.

### Non-hydrolysable nucleotide binding

#### FMPPNP binding

FMPPNP binding produces large amplitude fluorescence changes on binding to HMM in the presence and absence of Ca. This has allowed the binding mechanism to be looked at in some detail. A two step binding mechanism can be proposed, initial association forms a low fluorescence species which then slowly isomerises to a more fluorescent state. This is described by equation 6-1.

#### Equation 6-1



Ca alters FMPPNP (N) binding by changing the equilibrium position for the formation of the highly fluorescent bound

species. At low FMPPNP concentrations, and in the presence of Ca,  $M_C.N^*$  rapidly forms, followed by a small amount of  $M_C.N^{**}$  at the slower rate. The final fluorescence enhancement is relatively low due to the equilibrium constant of the second step. At high FMPPNP concentrations more  $M_C.N^*$  forms, forcing more  $M_C.N^{**}$  to be produced giving the full fluorescence enhancement. In the absence of Ca binding is very tight due to the equilibrium constant of the second step which ensures that the full fluorescence enhancement is always seen. At high FMPPNP concentrations less of the slow phase is seen since  $M.N^*$  forms relatively rapidly preventing the  $M.N^*$  to  $M.N^{**}$  change being seen fully.

Equation 6-1 is similar to the two step binding scheme proposed for ADP binding (equation 4-4) and it suffers from the same problems. The second step has a 1000-fold dependence of the equilibrium position on Ca. This must be reflected in the relative affinities of  $M.N^*$  and  $M.N^{**}$  for Ca, implying that  $>1\text{mM}$  Ca would be required to achieve the activated state. The problem can be partially overcome (as seen in equation 4-5) by the introduction of further isomerisation steps. FMPPNP binding therefore involves a minimum of three steps, initial association followed by at least two isomerisations.

FMPPNP binding does produce much larger observed fluorescence enhancements due to the lower binding constant. Although this provides signals with a greater signal to noise ratio, an additional complication is introduced. FDP

binding to unregulated molecules does not contribute to the observed fluorescence change. FMPPNP is likely to lead to a significant fluorescence enhancement when it binds to unregulated HMM thus introducing another phase to an already complex binding curve. This must be born in mind when interpreting the results and prevents complete analysis of the data.

#### FDP binding

When FDP binds to HMM a large fluorescence change is induced, which is far greater than the enhancement induced by ADP binding. Unfortunately the binding constant of FDP for HMM in the absence of Ca is fairly weak ( $\sim 37\mu\text{M}$ ) necessitating high FDP concentrations to achieve  $>90\%$  binding. This introduces a very high background fluorescence making the observed fluorescence changes relatively small. Thus many of the advantages of the large formycin signals are negated when considering FDP binding.

The biphasic FDP binding curves do suggest a two step binding mechanism, with a fast concentration-dependent association ( $\sim 1 \times 10^4 \text{M}^{-1}\text{s}^{-1}$ ) followed by a slower isomerisation. Dissociation, however, occurs relatively slowly with a rate constant of  $0.008\text{s}^{-1}$ . If these two results are combined they suggest a binding constant of about  $0.1\mu\text{M}$ , which is in conflict with the measured value of  $37\mu\text{M}$ .

It has been difficult to produce a satisfactory model to

explain all the FDP binding data. There is a large discrepancy between the binding constant calculated from the amplitudes of the fluorescence signals and the binding constant calculated from the dissociation and association rate constants. Additionally, as the FDP concentration is increased the amplitude of the slow phase should be greatly reduced (as seen with FMPPNP binding). Only a small reduction of the slow phase amplitude was seen at higher FDP concentrations. There is the possibility that rather than just one unique FDP binding site there may be two different sites with differing affinities. This could account for the variation in the calculated binding constants but the evidence for a two site binding scheme is limited.

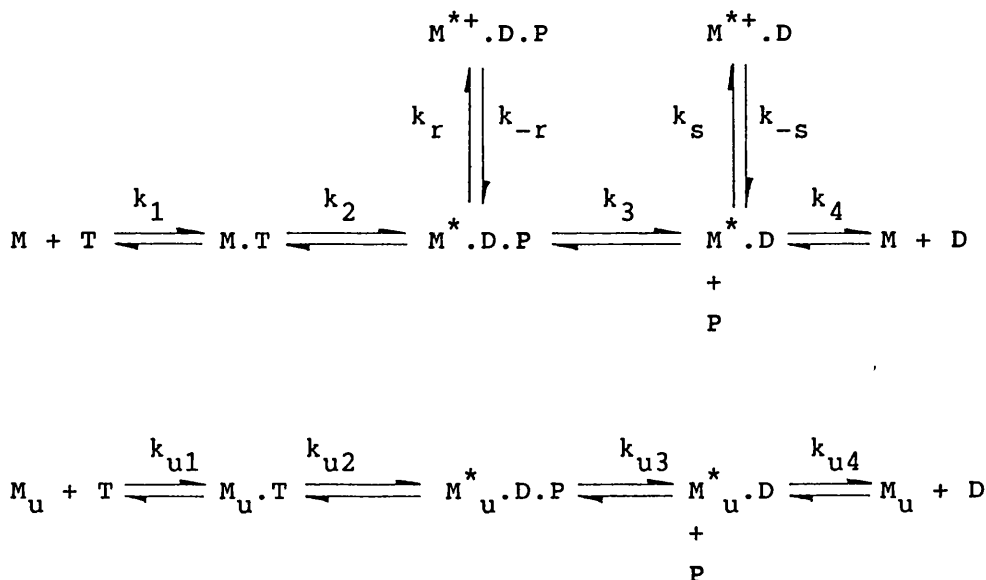
The introduction of a second binding site may help to explain the variation in binding constants but it does not greatly advance the understanding of the entire FDP binding mechanism. The number of phases associated with binding, the number of sites, the fluorescence level of each state and the rate of interconversion between states all become uncertain since only a few of these variables are uniquely measurable. The data acquired so far are really insufficient to fully explain FDP binding.

#### Branched FTPase pathway

The effect that increasing salt concentration has on the product release steps provides some information about the mechanism of Ca regulation. Steady-state assays reveal a gradual loss in Ca sensitivity of the ATPase activity with

increasing salt concentration, but they do not reveal how this loss occurs. If salt simply desensitises the FTPase by turning molecules from the regulated to unregulated states, similar results to the IASL labelling of HMM would be expected (figure 6-8). Alternatively, if salt just increased the rate of the regulated FTP turnover then the slow phase would increase in rate but have a constant amplitude. The observed result was a combination of loss of regulated amplitude coupled to an increase in its rate. A result which is difficult to correlate with the conventional, linear FTPase scheme (equation 5-1). The experimental data can be explained if intermediates can form which are away from the main flux through the pathway, as described by equation 6-2.

Equation 6-2



$M^{*+}.D.P$  represent a species with the same fluorescence as

$M^*.D.P$ , which forms and decays via  $k_r$  and  $k_{-r}$ .

It is only the regulated molecules which are able to form the trapped state. Apart from the inability to trap intermediates, the unregulated molecules are assumed to have the same characteristics as the regulated molecules. This simplifies the assignment of rate constants to various steps in the scheme and places limits on the rates which can be assigned to  $k_r$  and  $k_{-r}$ . The linear portion of the regulated FTPase mechanism has the same kinetic constants as the unregulated scheme (assumed to be equivalent to regulated plus Ca) which predefines these rate constants. If any significant amount of trapping is to occur within a few turnovers of FTP,  $k_r \geq k_3$ . The observed slow fluorescence decay is now a consequence of  $k_{-r}$ . If  $k_r < k_3$  then the slow phase seen during single turnovers would be dramatically reduced.

At low salt concentration, and in the absence of Ca,  $k_r \gg k_{-r}$  and  $k_r \approx k_3$ . If a brief steady-state is established (> 20 seconds) then equilibrium of the  $M^*.ADP.Pi$  to  $M^{*+}ADP.Pi$  step is achieved and most of the HMM molecules trap products. Once the FTP is exhausted product release will be controlled by  $k_{-r}$ . During a single turnover rapid chase experiment, less  $M^{*+}D.P$  would form accounting for an apparent drop in amplitude attributed to the regulated population (figure 6-6c). If ATP was added before the equilibrium with the trapped state was established, then a reduced amplitude slow phase should be the result.

The fluorescence decay associated with single turnovers of FTP does have ~70% of the total amplitude occurring with the regulated rate. Under single turnover conditions the unregulated molecules are never saturated with FTP since the  $K_m$  of the unregulated fraction is about the same as the protein concentration used ( $K_m = k_{\text{off}}/k_{\text{on}} = 1\mu\text{M}$ ). The  $K_m$  of the regulated molecules is much lower ( $0.01\mu\text{M}$ ) thus they achieve saturation with substrate. The effect of the disparity in values of  $K_m$  would be to reduce the observed amplitude of the fast phase relative to the slow phase making the sample appear >75% regulated. The branched scheme predicts a reduced amplitude for the slow phase under single turnover conditions. These two effects appear to almost cancel each other out giving the appearance of 75% regulated and 25% unregulated over a wide range of FTP concentrations.

At first it may appear that the trapped intermediates of equation 6-2 could explain the biphasic nature of the decay in fluorescence seen during a multiple FTP turnover in low salt (figure 5-3) without the need to introduce a second population. The existence of 2 populations was assumed by comparison with the acto-myosin ATPase assays of Wells and Bagshaw, (1985). It could be that both traces could be explained by a one population, branched pathway scheme. It may be possible to choose suitable values of  $k_r$  and  $k_{-r}$  to produce the observed fluorescence decays.

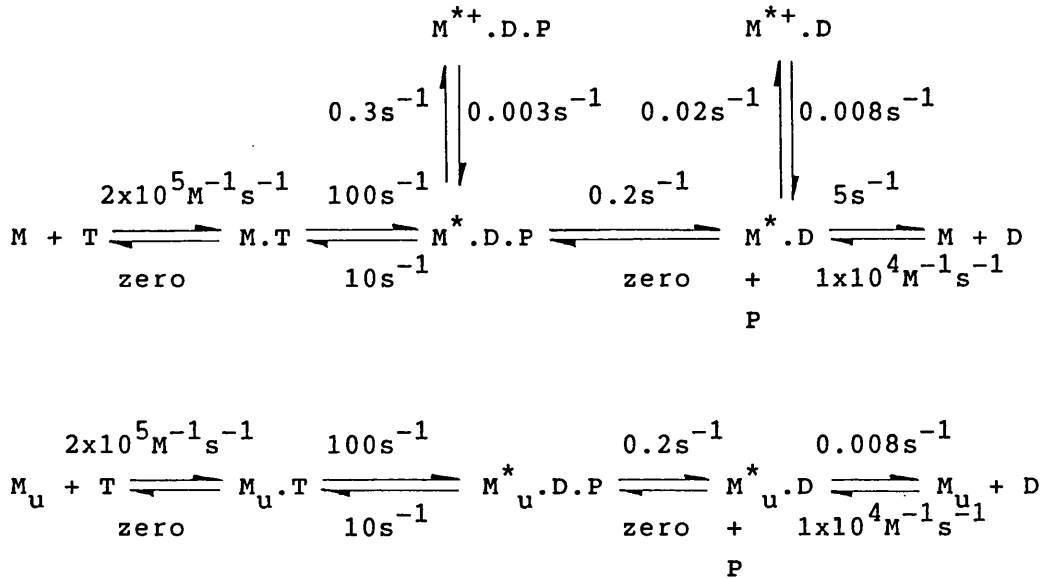
Computer simulations of a proposed kinetic scheme provide a method by which schemes can be shown to be compatible or

incompatible with the experimental results. However, it was not possible to simulate the observed FTP turnovers with just one population of HMM molecules. The requirement for a very slow final turnover was incompatible with the observed steady-state turnover rate.

A series of simulations of FTP turnover by HMM were carried out in which the fluorescence profile were calculated for different values of the rate constants ( $k_r$  and  $k_{-r}$ ). Included in the simulations was the transition  $M^*.D$  to  $M^{*+}.D$  allowing Ca sensitive ADP binding to be introduced. An  $M^{*+}.D$  also makes the scheme symmetrical allowing the linear portion of the scheme to remain insensitive to Ca.

The unregulated molecules are unable to undergo the  $M^*$  to  $M^{*+}$  transition but otherwise behave as the regulated molecules. The rates and equations used in these simulations are described in equation 6-3 (see appendix 1 for a description of the simulation program).

## Equation 6-3



Ca is proposed to exert its effect on the FTPase by increasing the rate of  $k_{-r}$  until  $k_3$  becomes rate limiting. When this occurs the formation of the branched species becomes irrelevant to the overall pathway. Salt has a more gradual effect, decreasing  $k_r$  and increasing  $k_{-r}$ , which causes less trapping but a faster breakdown of the trapped species which do form.

Figure 6-7a simulates the turnover of  $10\mu M$  FTP by  $2\mu M$  HMM in the absence of Ca. ATP chase experiments were simulated by setting the FTP and FDP association rate constants to zero at 50 seconds. The biphasic fluorescence decay is much clearer and no FDP remains bound at the end of the simulation (figure 6-7b). During the brief steady-state in figure 6-7a and 6-7b, 99% of the regulated molecules trap products as a consequence of the values of  $k_r$  and  $k_{-r}$ .

The values placed on  $k_r$  and  $k_{-r}$  are limited by the requirements for a slow final turnover, relatively rapid trapping and a ratio of 75% regulated to 25% unregulated. Figure 6-7c and 6-7d show the effect of reducing  $k_r$  by a factor of 10. If this is done only 90% of the regulated molecules would trap products at steady state. Additionally, the steady-state rate is greatly increased since equilibration with the trapped state takes longer to establish. The simulations do show a slow final turnover but have a much shorter steady-state turnover time plus only about 20% of the total amplitude has the slow rate. The rate constants shown in equation 6-3 provide the best fit to experimental data that could be achieved.

The timed ATP chase experiments (figure 6-6a and 6-6c) demonstrate the loss in regulated amplitude as the time of chase was reduced. The rate of this loss is an indication of the rate at which trapping can occur. From figure 6-6c a value of about  $0.1s^{-1}$  was obtained. The accuracy of this experiment is very dependent on the precise timing of the addition and therefore the rate constant obtained is considered to be a rough estimate. Despite this, the trend is for a loss of the slow phase as the time of ATP chase is decreased.

It was noticed in chapter 5 that slow fluorescence changes accompanied FTP binding to HMM -Ca (figure 5-2). The amplitude of these changes was <5% of the total making them difficult to characterise. This slow phase was not visible

in FTP binding to S1 (figure 5-2), HMM +Ca (figure 5-2), HMM which had been rendered Ca insensitive by high salt (figure 6-4 and 6-5) and to IASL labelled HMM (figure 5-8). This suggests that it is a feature of regulated HMM. Kinetic trapping may therefore occur at all stages of the FTPase scheme but that it is most obvious at the M.FDP.Pi step.

Turbidity assays also provide a method by which kinetic trapping during the ATPase pathway could be detected. Experiments involving single FTP turnovers suffer from the slow binding of FTP, which complicates the analysis of the amplitudes of the fast and slow phases. ATP binding is 10 fold faster thus greatly reducing the problem. If a series of turbidity assays at various ATP concentrations (ranging from sub-stoichiometric to several fold excess) were to be carried out, trapping may be revealed by a reduction in the relative amplitude of the slow phase at low ATP concentrations.

The examination of the hydrolytic step by the manual quench experiments indicated that there were slow transitions accompanying ATP binding and hydrolysis. These effects occurred on the limit of manual addition methods. Quench flow experiments are required to confirm and characterise these processes. These slow changes open up the possibility of a  $M^{*+}.ATP$  complex forming, corresponding to the  $M^{*+}.ADP.Pi$  state allowing inter-conversion between these 2 species.

All of the data regarding the kinetic schemes for the hydrolysis of ATP and FTP has been analysed, ignoring any

effect which cooperativity may have. It has not been necessary to introduce this added complication to explain any of the data presented so far. Ca sensitivity is only seen with myosin and HMM so it could be that communication between the heads is vital for Ca sensitivity. Alternatively it could be that only an intact neck region is needed. The preparation of pure single headed myosin may provide an answer to this.

#### FDP activation of the FTPase

FDP has been observed to alter the rate of FTP turnover by regulated HMM. Figure 6-8 shows steady-state ATP and FTPase assays of HMM. The ATPase can be seen to be Ca sensitive whereas the FTPase is Ca insensitive. This is in contrast with the large degree of Ca sensitivity seen during limited turnovers of FTP. Table 5-1 shows that if small excesses of FTP are turned over then Ca activates the steady-state FTPase by 3-4 fold. A Ca insensitive FTPase appears to result when HMM turns over FTP in the presence of FDP.

When a series of limited turnovers of FTP were carried out, by the addition of successive aliquots of FTP, a gradual activation of the steady-state rate was seen although the slow product release step was unaffected. The steady-state rate was increased from  $0.026\text{s}^{-1}$  to  $0.053\text{s}^{-1}$  by the addition of a second aliquot of  $8\mu\text{M}$  FTP, while the slow phase remained unaltered ( $k_{\text{obs}} = 0.002\text{s}^{-1}$ ). FDP activation was also noted when FDP was preincubated with HMM before the addition of FTP. This effect was only seen when regulated

HMM was used and if the FDP had been pre-incubated with the HMM for more than a few seconds. When unregulated HMM (produced by spin labelling) or S1 was used, no activation was seen, indeed inhibition of the FTPase resulted. Additionally FDP does not activate the HMM ATPase nor does ADP activate the FTPase or ATPase. This activation can best be explained by communication between two different binding sites for FDP, which could either be communication between the sites on both heads or between two sites on the same head. Further work is needed to clarify the situation.

A branched FTPase mechanism can therefore be used to explain most of the data from formycin nucleotide binding and turnovers. Simulations cannot prove a mechanism but they have shown that the scheme can reasonably describe the experimental results.

The complex nature of several aspects of the FTPase mechanism must not be allowed to cloud the basic mechanism of regulation. FTP turnover is highly Ca sensitive providing a large and stable signal with which to monitor turnover. This is model independent, i.e. however HMM turns over FTP, the fact remains that it is a highly Ca sensitive reaction. It is only the exceptionally large and stable fluorescence signals provided by formycin that has allowed the mechanism to be probed in the detail presented in this chapter.

Care must be taken when FTPase assays are used to measure the fraction of regulated molecules in an HMM preparation.

If near stoichiometric FTP is used, an underestimate of the degree of regulation present may be obtained. So long as sufficient FTP is added to allow a steady-state of  $> 20$  seconds to be established, the amplitude of the two phases will accurately report the proportion of regulated molecules.



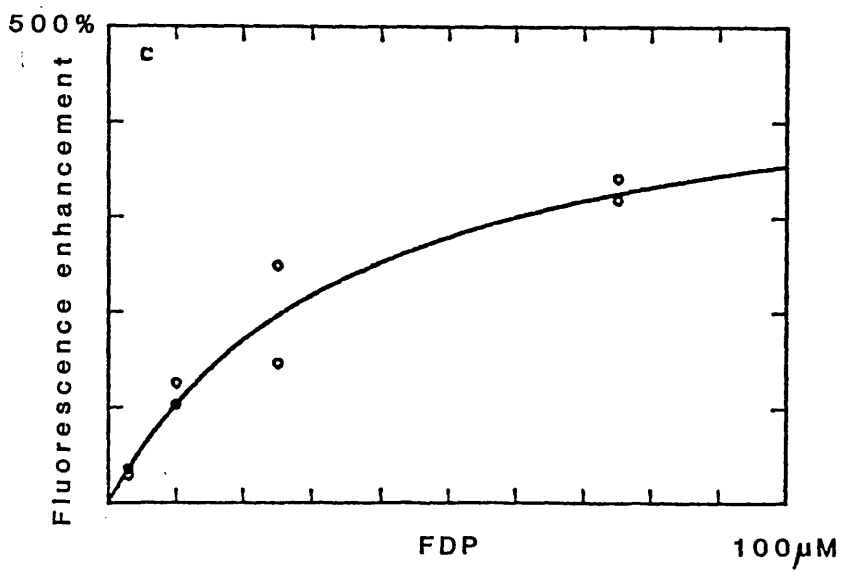
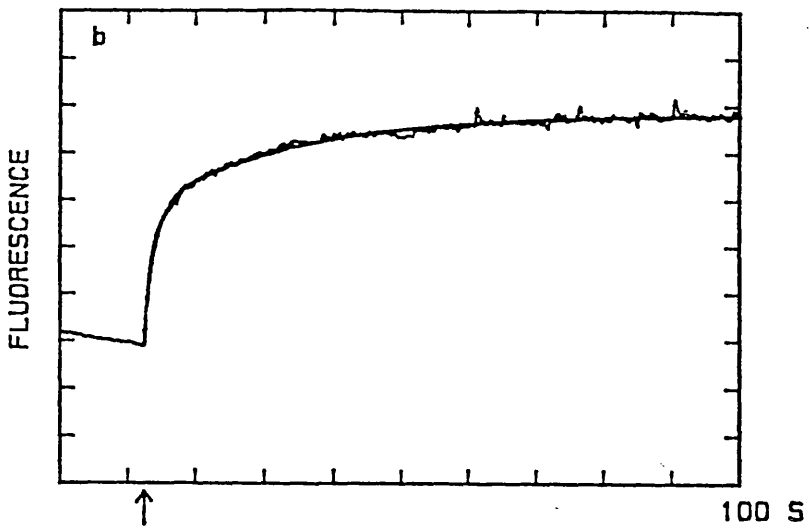
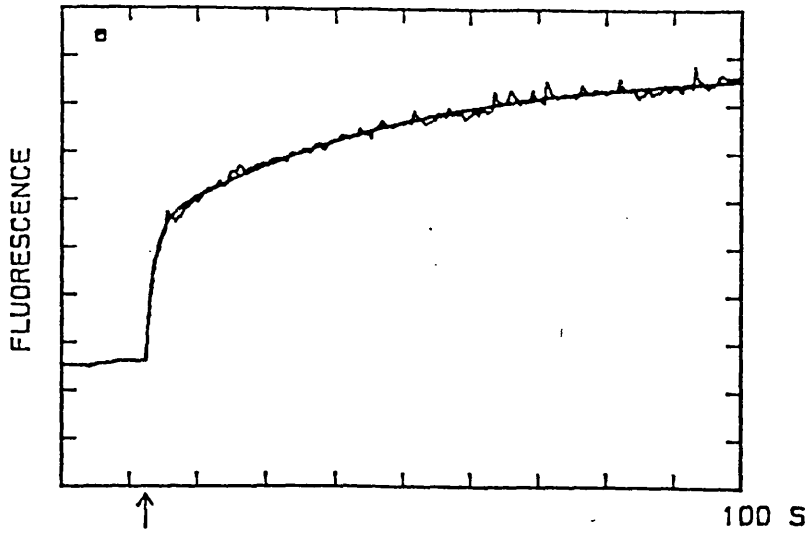
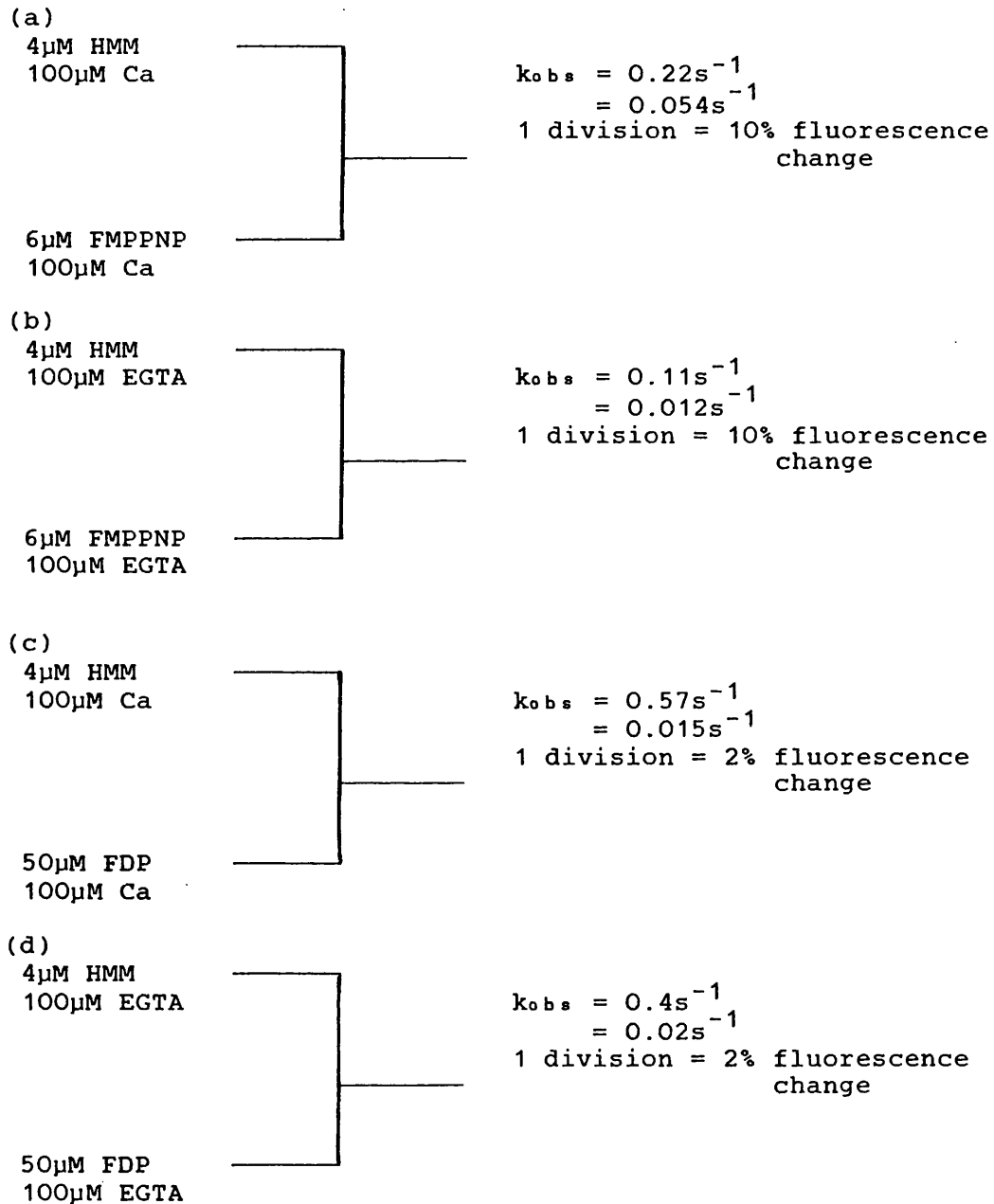
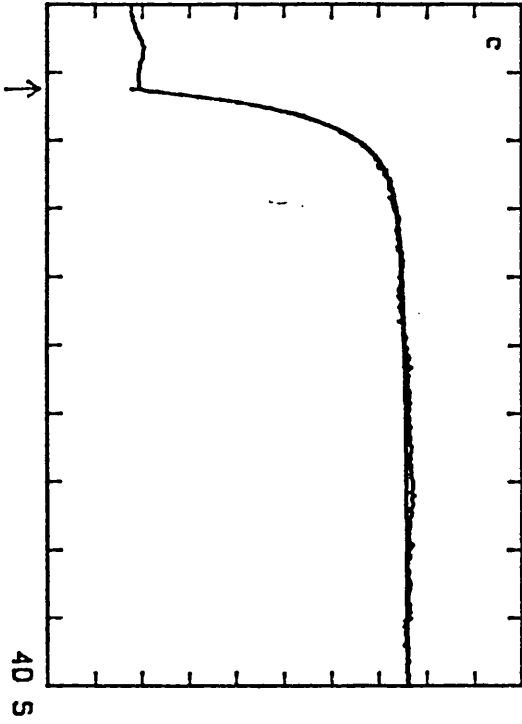


Figure 6-2

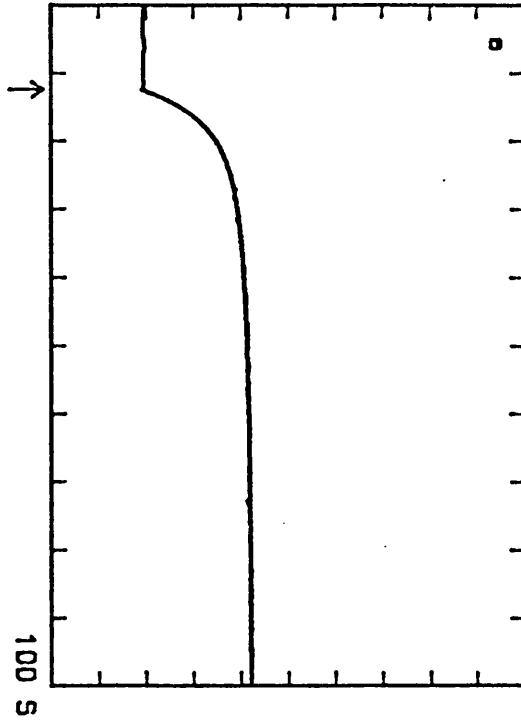
FMPPNP binding to HMM in the presence and absence of Ca, followed by the increase in formycin fluorescence.



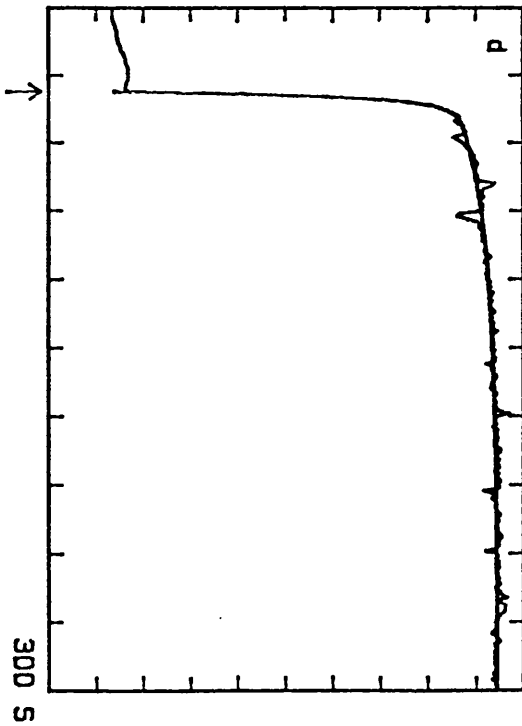
FLUORESCENCE



FLUORESCENCE



FLUORESCENCE



FLUORESCENCE

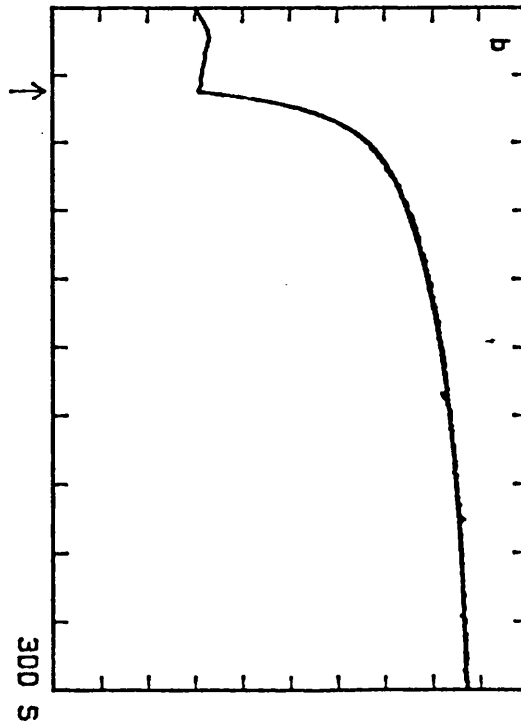
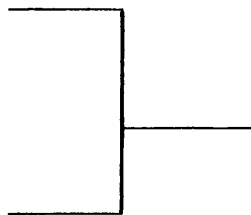


Figure 6-3

FMPPNP dissociation from HMM in the presence and absence of Ca, monitored by the decrease in formycin fluorescence.

(a)

6 $\mu$ M FMPPNP  
4 $\mu$ M HMM  
100 $\mu$ M Ca

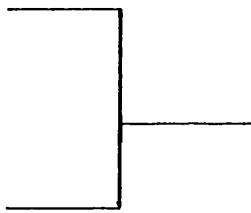


$k_{obs} = 0.074s^{-1}$   
1 division = 6.25%  
fluorescence change

500 $\mu$ M ATP  
100 $\mu$ M Ca

(b)

6 $\mu$ M FMPPNP  
4 $\mu$ M HMM  
100 $\mu$ M EGTA

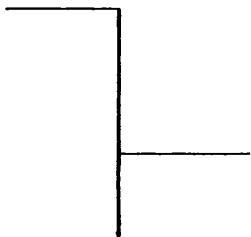


$k_{obs} = 0.12s^{-1}$   
1 division = 6.25%  
fluorescence change

200 $\mu$ M Ca

(c)

6 $\mu$ M FMPPNP  
4 $\mu$ M HMM  
100 $\mu$ M EGTA



$k_{obs} = 0.16s^{-1}$   
 $= 0.046s^{-1}$   
1 division = 6.25%  
fluorescence change

500 $\mu$ M ATP  
200 $\mu$ M Ca

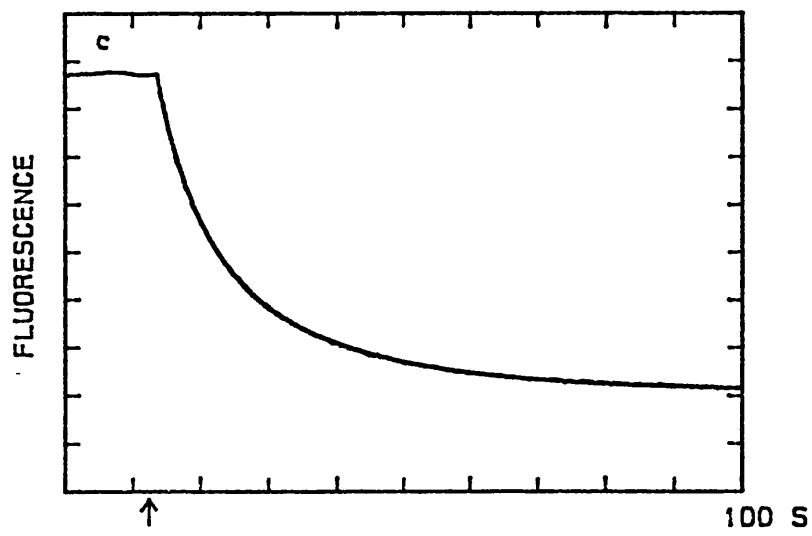
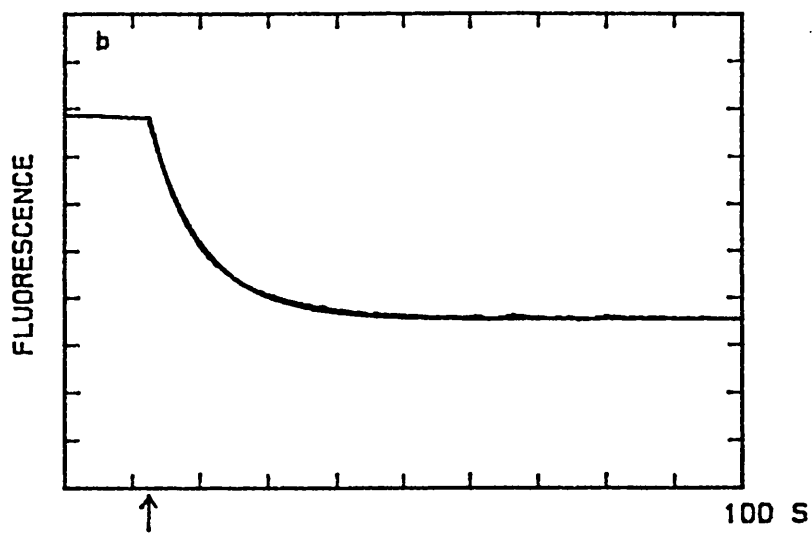
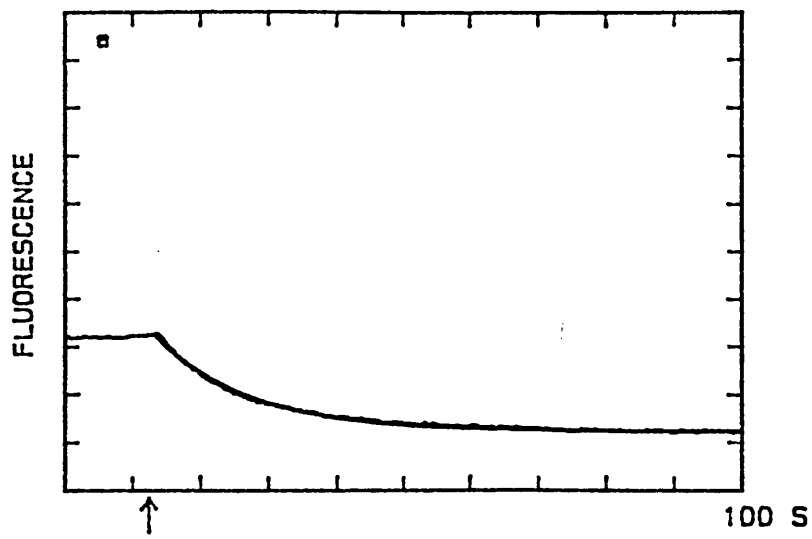


Figure 6-4

The effect of NaCl concentration on the HMM FTP turnover monitored by formycin fluorescence and using ATP chases.

a

10 $\mu$ M FTP was added to a solution containing 2 $\mu$ M HMM, 100mM NaCl, 100 $\mu$ M EGTA at the time indicated. 1mM ATP was added after 60 seconds.

$$\begin{aligned}k_{\text{obs}} &= 0.014 \text{ s}^{-1} \\ &= 0.0023 \text{ s}^{-1}\end{aligned}$$

1 division represents a 15% fluorescence change.

b

10 $\mu$ M FTP was added to a solution containing 2 $\mu$ M HMM, 150mM NaCl, 100 $\mu$ M EGTA at the time indicated. 1mM ATP was added after 50 seconds.

$$\begin{aligned}k_{\text{obs}} &= 0.014 \text{ s}^{-1} \\ &= 0.0034 \text{ s}^{-1}\end{aligned}$$

1 division represents a 15% fluorescence change.

c

10 $\mu$ M FTP was added to a solution containing 2 $\mu$ M HMM, 300mM NaCl, 100 $\mu$ M EGTA at the time indicated. 1mM ATP was added after 20 seconds.

$$\begin{aligned}k_{\text{obs}} &= 0.053 \text{ s}^{-1} \\ &= 0.0044 \text{ s}^{-1}\end{aligned}$$

1 division represents a 15% fluorescence change.

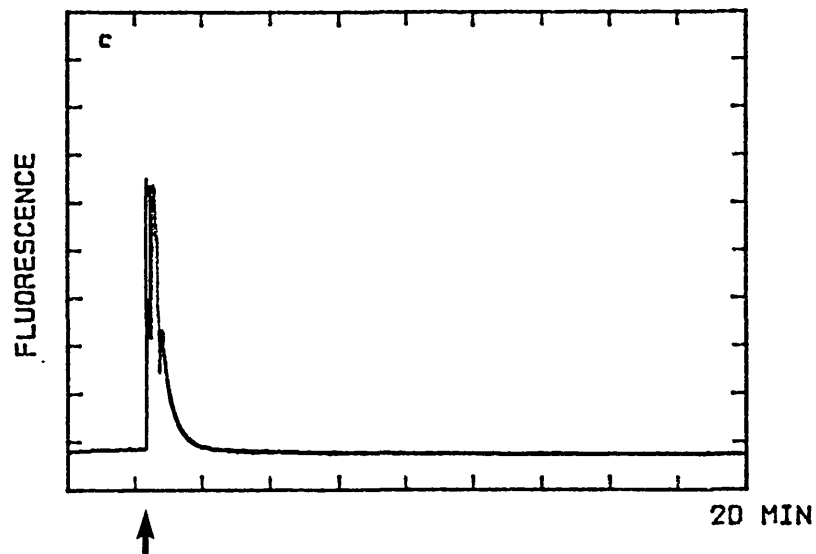
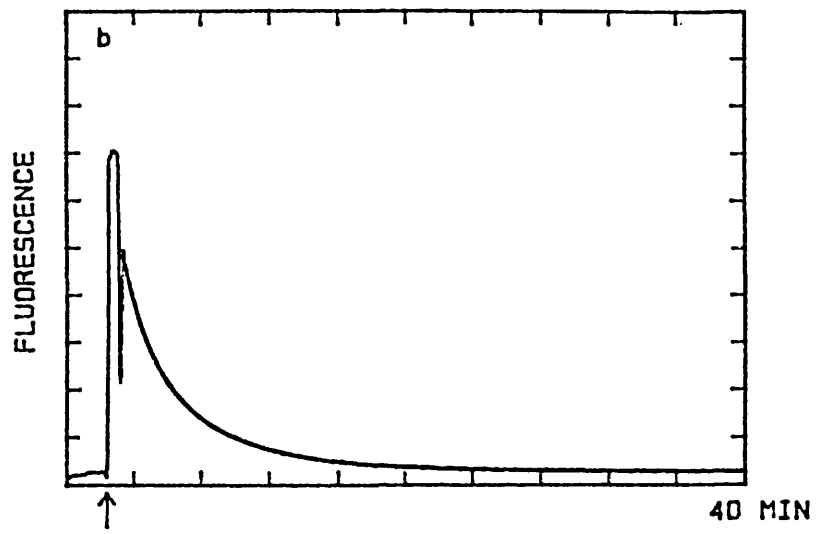
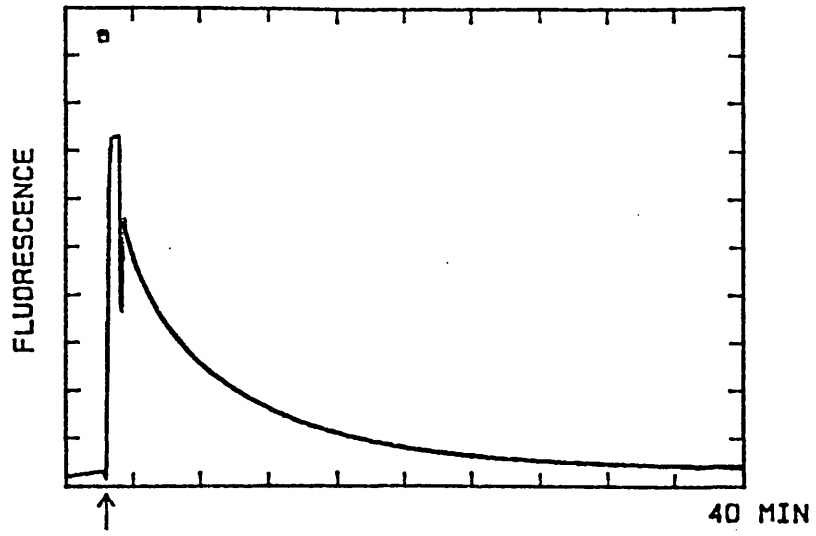


Figure 6-5

The effect of sodium acetate concentration on the HMM FTP turnover monitored by formycin fluorescence and using ATP chases.

a

10 $\mu$ M FTP was added to a solution containing 2 $\mu$ M HMM, 100mM NaAc, 100 $\mu$ M EGTA at the time indicated. 1mM ATP was added after 60 seconds.

$$\begin{aligned}k_{\text{obs}} &= 0.016 \text{ s}^{-1} \\ &= 0.0016 \text{ s}^{-1}\end{aligned}$$

1 division represents a 15% fluorescence change.

b

10 $\mu$ M FTP was added to a solution containing 2 $\mu$ M HMM, 150mM NaAc, 100 $\mu$ M EGTA at the time indicated. 1mM ATP was added after 60 seconds.

$$\begin{aligned}k_{\text{obs}} &= 0.018 \text{ s}^{-1} \\ &= 0.0018 \text{ s}^{-1}\end{aligned}$$

1 division represents a 15% fluorescence change.

c

10 $\mu$ M FTP was added to a solution containing 2 $\mu$ M HMM, 600mM NaAc, 100 $\mu$ M EGTA at the time indicated. 1mM ATP was added after 50 seconds.

$$\begin{aligned}k_{\text{obs}} &= 0.041 \text{ s}^{-1} \\ &= 0.0036 \text{ s}^{-1}\end{aligned}$$

1 division represents a 15% fluorescence change.

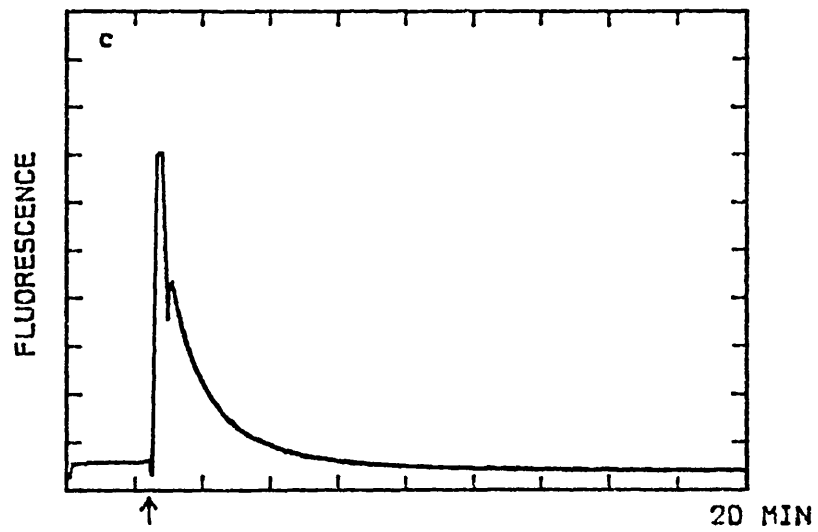
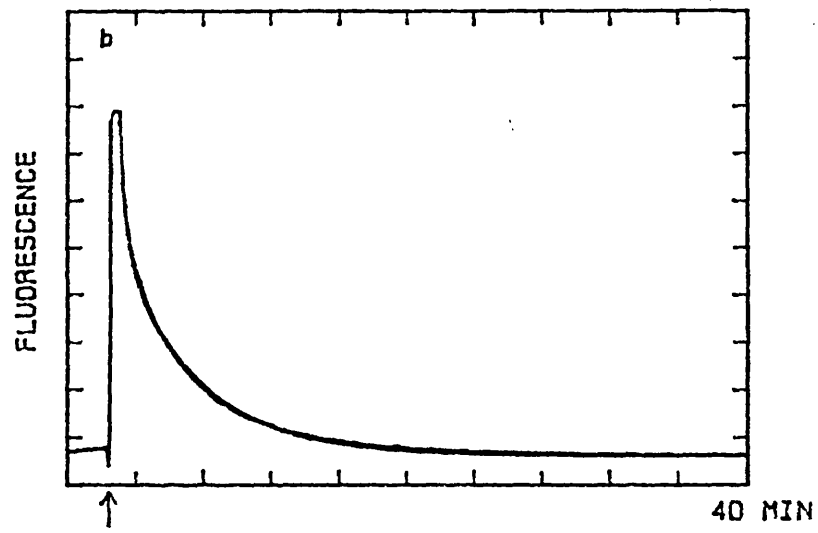
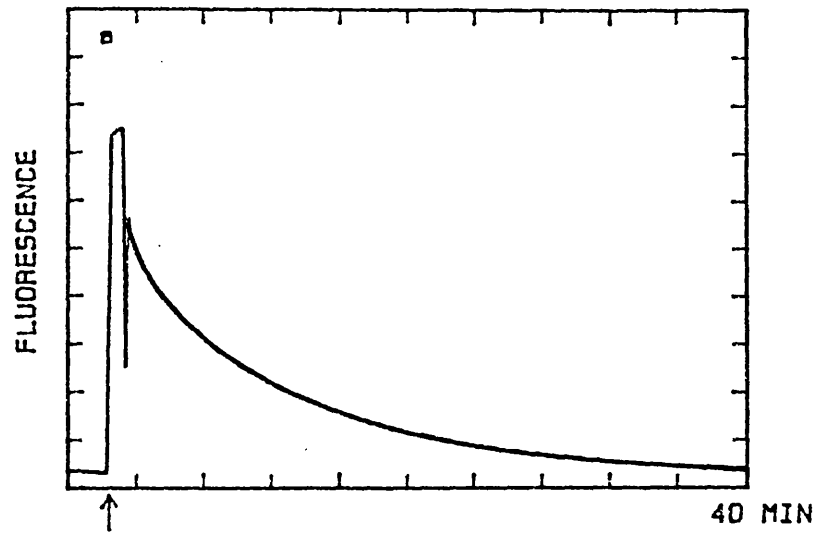


Figure 6-6

(a)

Timed ATP chases during the turnover of FTP by HMM.

10 $\mu$ M FTP was added to 2 $\mu$ M HMM, 100 $\mu$ M EGTA and 1mM ATP added

at:

$$\begin{aligned} \text{(i)} \quad 30\text{s} \quad k_{\text{obs}} &= 0.02 \text{ s}^{-1} \\ &= 0.001 \text{ s}^{-1} \end{aligned}$$

$$\begin{aligned} \text{(ii)} \quad 20\text{s} \quad k_{\text{obs}} &= 0.094 \text{ s}^{-1} \\ &= 0.001 \text{ s}^{-1} \end{aligned}$$

$$\begin{aligned} \text{(iii)} \quad 10\text{s} \quad k_{\text{obs}} &= 0.103 \text{ s}^{-1} \\ &= 0.0012 \text{ s}^{-1} \end{aligned}$$

200 $\mu$ M Ca was added at time indicated ( $\downarrow$ ).

(b)

Timed ATP chases during the binding of FMPPNP to HMM.

10 $\mu$ M FTP was added to 2 $\mu$ M HMM, 100 $\mu$ M EGTA and 1mM ATP added

at:

$$\begin{aligned} \text{(i)} \quad 40\text{s} \quad k_{\text{obs}} &= 0.045 \text{ s}^{-1} \\ &= 0.00016 \text{ s}^{-1} \end{aligned}$$

$$\begin{aligned} \text{(ii)} \quad 20\text{s} \quad k_{\text{obs}} &= 0.081 \text{ s}^{-1} \\ &= 0.00038 \text{ s}^{-1} \end{aligned}$$

$$\begin{aligned} \text{(iii)} \quad 10\text{s} \quad k_{\text{obs}} &= 0.069 \text{ s}^{-1} \\ &= 0.00039 \text{ s}^{-1} \end{aligned}$$

200 $\mu$ M Ca was added at time indicated ( $\downarrow$ ).

(c)

Plot of the relative amplitude of the slow phase against the time of the ATP chase (O - FTP, ● - FMPPNP). Exponential curve shown was fitted through the FTP data points giving a

$$k_{\text{obs}} = 0.1 \text{ s}^{-1}$$

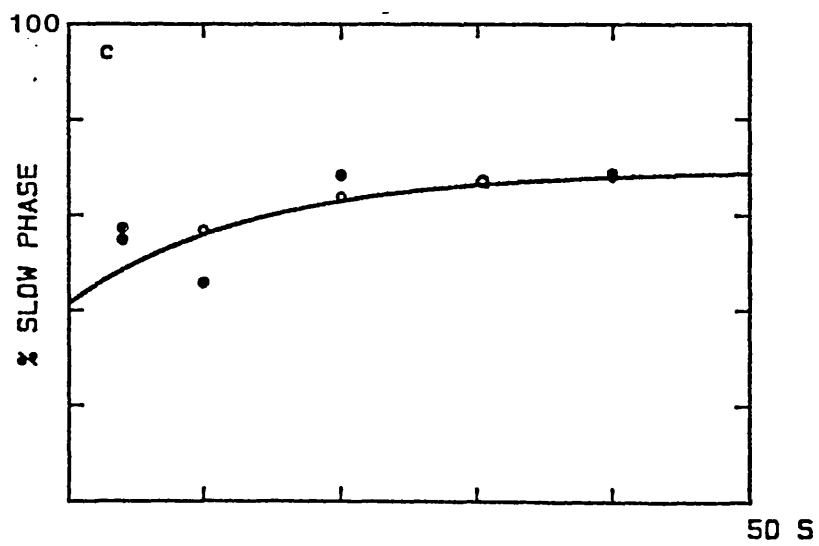
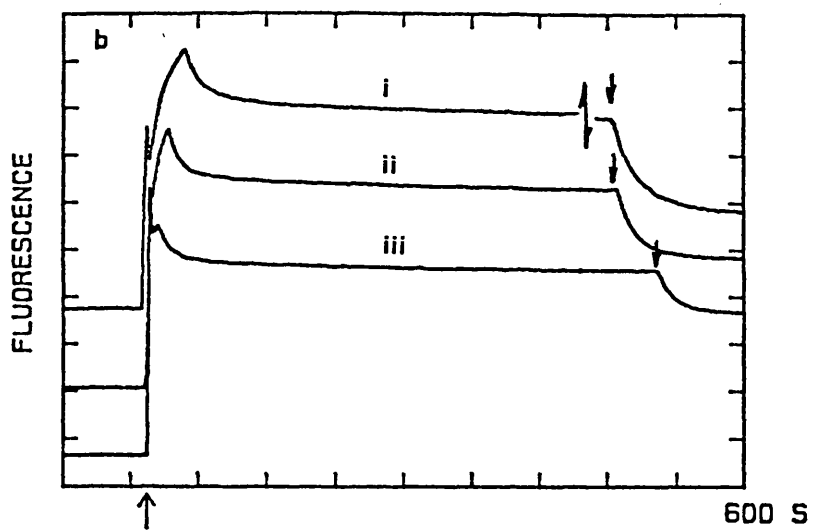
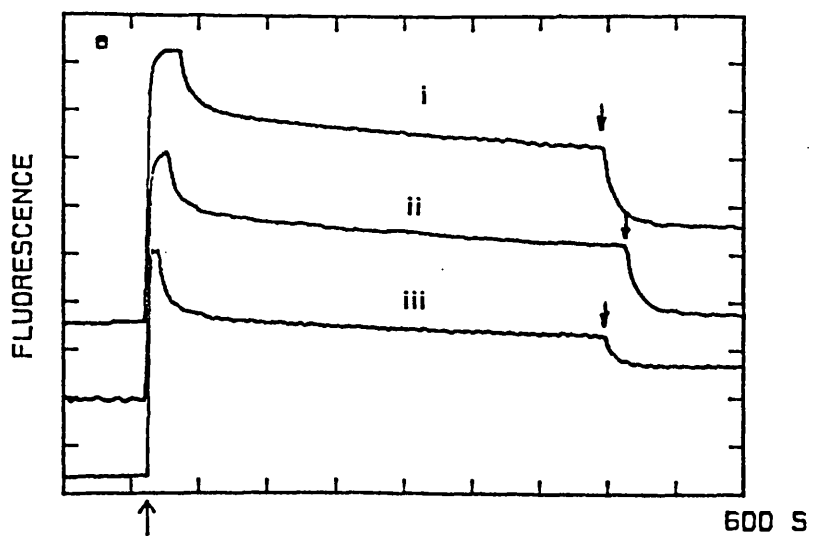


Figure 6-7

Simulations of the turnover of  $10\mu\text{M}$  FTP by  $2\mu\text{M}$  HMM -Ca according to equation 6-2.

Concentrations of  $M$  and  $M_u$  were  $1.5\mu\text{M}$  and  $0.5\mu\text{M}$  respectively and the apparent fluorescence signal plotted in the figures was achieved by summing all the highly fluorescent species ( $M.T$ ,  $M^{*+}.D.P$ ,  $M^*.D.P$ ,  $M^{*+}.D$ ,  $M_u.T$  and  $M_u.D.P$ ).

(a) and (b) show simulations according to the rate constants described in equation 6-3. (c) and (d) are simulated using the same rate constants except for  $k_r$  which is reduced to  $0.03\text{s}^{-1}$ .

(b) and (d) ATP chases have been simulated by setting the FTP and FDP association rate constants to zero after 50 and 20 seconds respectively.

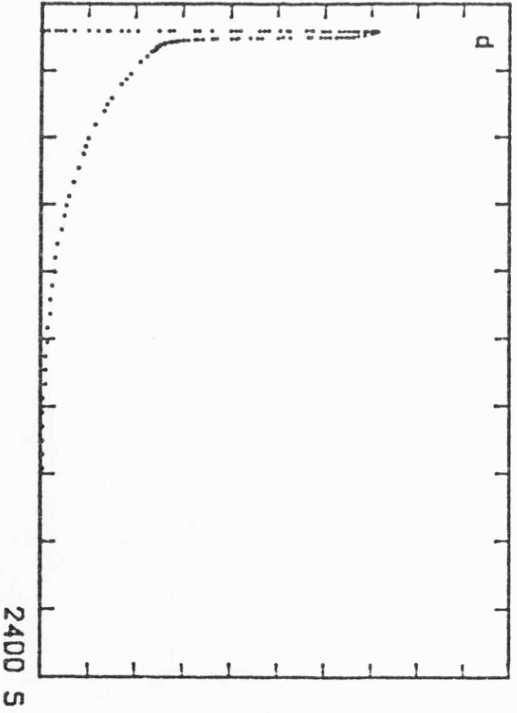
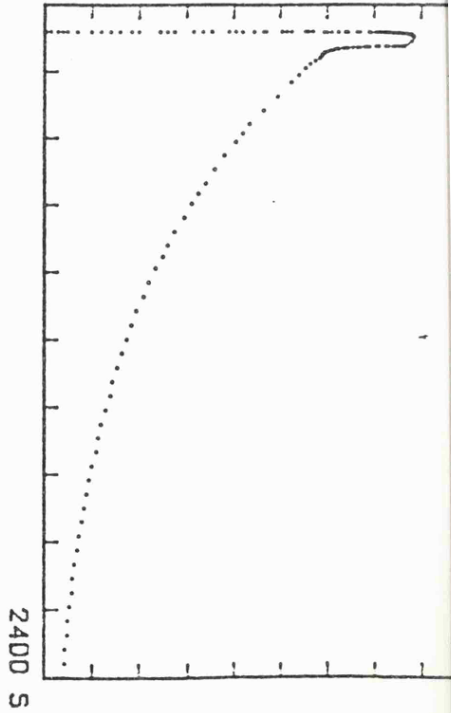
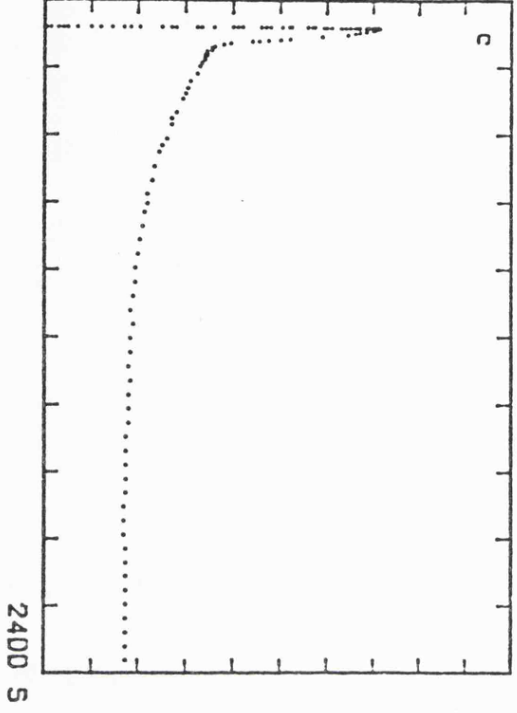
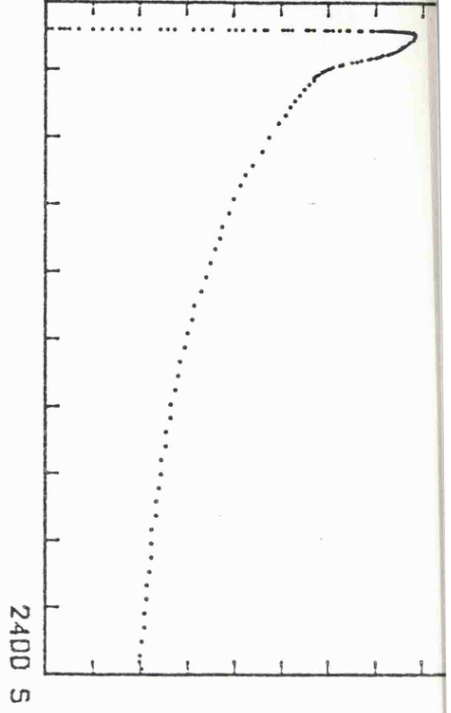
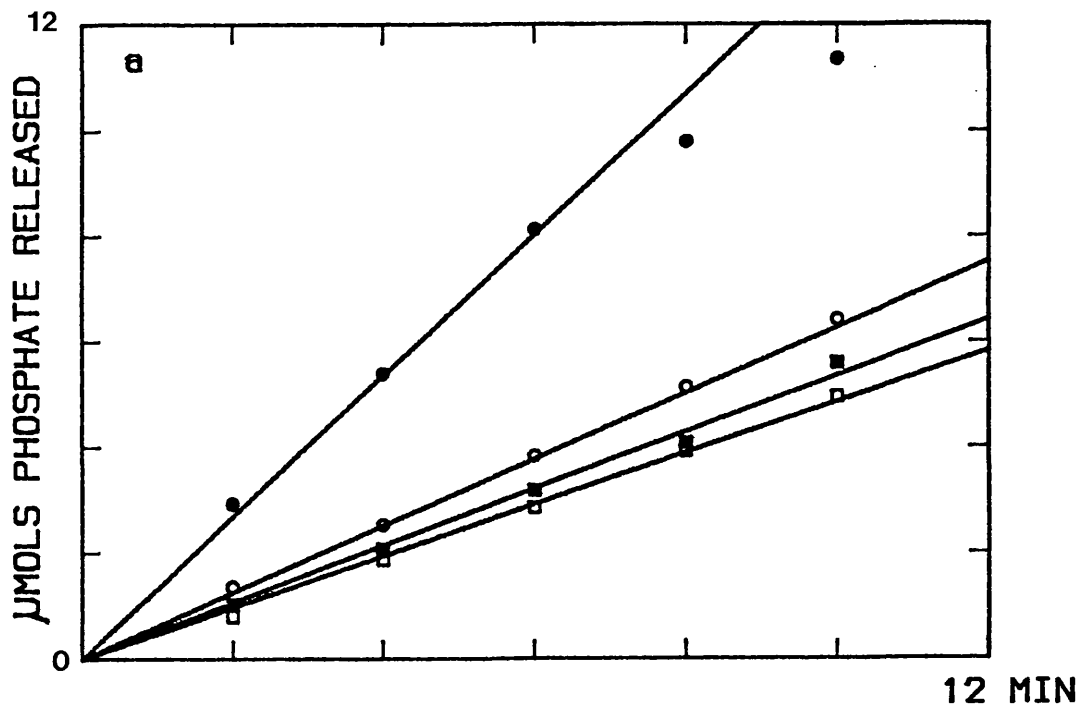


Figure 6-8

Steady-state malachite green assays for the ATPase and FTPase activities of HMM in the presence and absence of Ca.

Both assays contained 2 $\mu$ M HMM, 100 $\mu$ M EGTA and 400 $\mu$ M nucleotide.

- (a) FTPase rate +Ca = 0.09s<sup>-1</sup> (■) Ca sensitivity = 1.12  
-Ca = 0.08s<sup>-1</sup> (□)
- (b) ATPase rate +Ca = 0.22s<sup>-1</sup> (●) Ca sensitivity = 2.2  
-Ca = 0.1s<sup>-1</sup> (○)



CHAPTER 7

MYOSIN FTPase

## Introduction

Scallop HMM exists as a mixture of regulated and unregulated molecules. Is this a property intrinsic to scallop myosin or is it an artefact of HMM preparations? Can the 100-fold activation of the HMM ATPase induced by Ca be seen in myosin? These questions have been answered by performing fluorescence assays on suspensions of myosin filaments.

The Ca sensitivity of scallop HMM is overridden at high ionic strengths (>200mM). Below these concentrations myosin is insoluble making it potentially difficult to carry out optical measurements. HMM is prepared by enzymic digestion of myosin which is an obvious source of potential damage. It is common to produce HMM preparations with over 20% unregulated molecules by over digestion but it has proved impossible to generate preparations with >80% regulated on a large scale. The regulated and unregulated populations have been separated but only on an analytical scale (Jackson et al, 1986). If FTP turnover analysis could be applied to myosin at low ionic strength, both the Ca sensitivity and the existence of unregulated molecules would be detected.

## Fluorescent measurements on suspensions

The fluorescence of a sample depends critically on the intensity of the incident light. Variations may be due to fluctuations in the lamps output or due to changes within the sample. Compensations can be made for small variations

in lamp intensity and samples are usually chosen that absorb only a small amount of the light and whose absorbance does not change during the course of the experiment. If a suspension rather than a solution is used, potential problems exist for ill defined changes in the sample, which may in turn affect the observed fluorescence signal.

Even with the large signals available from formycin fluorescence, optical measurements on suspensions are difficult. Any suspension in which the particles are relatively large, such as myosin filaments, will settle out under gravity ruining any experimental observations especially if measurements have to be made over a long timescale. Continuous agitation of the contents of the cuvette with an over head stirrer overcame this problem. A second problem is then generated. As the particles swirl around the cell, the light scattering properties of the suspension will change, especially if the suspension is not homogeneous, leading to unpredictable and artefactual changes in the fluorescence signal. A gradual change in the assembly state of the filaments would lead to a change in the transmission of the suspension and may well affect the observed fluorescence signal.

The custom-built fluorimeter was used to overcome these problems. Continuous overhead stirring prevented the suspension settling out. The transmission of the sample was followed using the photodiode which monitored any effect of changes in absorbance and light scattering. The performance of the equipment was tested in the following experiments.

FTP was used as the fluorophore, hence compounds which would scatter or absorb light at 313nm were required. Malachite green had the ideal absorption characteristics, an absorption peak near 313nm and an absorption minimum at 350nm. These are the excitation and emission wavelengths used for formycin fluorescence in the custom-built fluorimeter. Initially both the fluorescence signal and transmission signals of a  $10\mu\text{M}$  FTP solution were set to 1 volt. Small aliquots of malachite green were added to absorb the exciting light. As expected from Beer's Law, both the fluorescence and the transmission signals decayed exponentially when plotted against the amount of malachite green added (figure 7-1b). In a second experiment, a glycogen suspension was used to scatter the light since it did not absorb at these wavelengths. As the amount of glycogen added was increased, the transmission signal decayed exponentially as it had done for malachite green, but the fluorescence showed a slight increase (figure 7-1a). This is not due to an increase in the scattered light falling on the photomultiplier, since the filters can cut out >99.9% of all the exciting light.

When light was absorbed by the chromophore, it was lost to the system, causing a decrease in the intensity of the exciting light. In contrast the scattered light was not lost, just redirected, so that the total intensity seen by the fluorophore remained relatively unchanged, leading to little change in the emission intensity.

The exact nature of the effect will depend on the particular scatterer, but the effect of relatively large changes in transmission on the observed fluorescence may well be small. The transmission signal was always monitored during FTP turnovers by myosin and usually showed little change. Efforts were made to prevent any transmission changes in order to simplify the analysis of the results. Providing that a fine suspension of myosin can be prepared, either by careful dilution or dialysis from a high ionic strength solution, formycin fluorescence assays can be carried out successfully.

#### Myosin FTP turnovers

Limited FTP turnover assays using myosin were carried out using the custom-built fluorimeter while continuously stirring the sample. The transmission signal was monitored using the photodiode but no significant changes were noted.

Figure 7-2 shows the turnover in the presence and absence of Ca. In the absence of Ca the fluorescence decay is markedly biphasic with the slow phase having a rate constant of  $0.002\text{s}^{-1}$ . In the presence of Ca the fluorescence decay is very much faster and monophasic. These traces closely resemble the form of FTP turnovers by HMM  $^{\dagger}\text{Ca}$ , especially when the relative amplitudes of the fast and slow phases are considered. An accurate determination of the relative amplitudes of each phase is not possible. The addition of excess ATP during the steady-state phase, which removes the sigmoid approach to the decay phase, caused large

transmission changes as the filaments were dissolved. These transmission changes could possibly have affected the observed fluorescence changes. A crude estimate of the proportion regulated can be made from figure 7-2 as 70% regulated. Myosin therefore exhibits the same two populations in the same ratio as does HMM. Attempts to prepare a more highly regulated myosin sample from fresh scallop adductor muscles were unsuccessful.

The heterogeneity of HMM samples must therefore originate prior to myosin preparation. Damage to myosin (e.g. SH modification or minor proteolytic damage) could possibly occur during isolation from the muscle. SDS gel electrophoresis shows that myosin samples are not contaminated with significant quantities of a HMM size fragment (Wells et al, 1985) hence digestion in the neck region is not the cause of the unregulated molecules. The loss of a small fragment from the N-terminus is not ruled out since the resolution of the gels is insufficient to see the loss of a small (<5Kd fragment from a 110Kd polypeptide). Alternatively, the two populations may be intrinsic to the muscle type. An examination of a more intact system such as myofibrils and muscle fibres is needed to ascertain the origin of the regulated and unregulated molecules.

FTP turnovers by smooth muscle myosin

Contraction in smooth muscle is regulated by Ca dependent phosphorylation of the myosin regulatory light chain. Smooth muscle myosin in vitro exists as an equilibrium mixture between filamentous and monomeric myosin (Mergeman and Lowey, 1981). The addition of ATP to myosin monomers causes a dramatic conformational change to occur. Extended 6S molecules fold up into 10S molecules (Suzuki et al, 1978). Cross et al (1986) showed that 10S myosin traps ADP.Pi at the active site and measured the rate constant of product dissociation in discontinuous single turnover assay at  $10^{-4}\text{s}^{-1}$ . Phosphorylation favours the formation of the polymerisation-competent 6S form. Dephosphorylation can therefore both inhibit the acto-myosin ATPase and inhibit the formation of filaments.

An investigation into the ATPase activity and its control was carried out in collaboration with R.A Cross.

FTP was found to be a good ATP analogue for smooth muscle myosin. Large fluorescence changes were induced by FTP binding, which were reversed upon release of products. FTP was also capable of inducing the 10S state to form from 6S myosin. The ATPase (and FTPase) activity of 6S and 10S myosin was very slow and to ensure that the fluorescence decays had an obvious start point all assays were carried out using ATP chases.

6S monomers turned over FTP with a rate constant of  $0.03\text{s}^{-1}$ . Transition to the 10S state reduced this rate constant 200 fold to  $0.00015\text{s}^{-1}$  (figure 7-3a and 7-3b). How does the trapping occur? 10S myosin is a highly folded molecule with the tail bent back upon itself and attached to the neck region. Is this folding the result of trapping or does it cause trapping? These questions could be answered by determining whether the trapped conformation exists in myosin filaments.

FTP turnover analysis has proved to be a sensitive probe for the state of the smooth muscle myosin active site. The potential exists for further analysis of the control of conformation, filament formation and ATPase activity of smooth muscle myosin using a combination of formycin nucleotides, adenosine nucleotides, light scattering and limited turnover kinetics.

### Discussion

One of the unique features of scallop myosin is the ability to remove the RLC and to replace it with light chains from other species, allowing the function and mechanism of the role of the RLC to be explored. If the effects of foreign light chains on the ATPase activity of HMM or myosin are to be measured by steady-state methods, problems can arise in the interpretation of the results. Unless 100% desensitisation followed by 100% hybrid production can be achieved, then the domination of a slow rate by a relatively small number of highly active molecules may occur, as is

found in conventional scallop HMM preparations. The development of limited turnover assays using FTPase assays should allow the kinetic separation of these populations. The ability to carry out FTP turnover assays on myosin suspensions also enhances the ease with which light chain function can be studied since it is far easier to completely desensitise myosin than HMM (Jackson et al, 1987). Additional impetus has come from the recent cloning of the skeletal muscle RLC (Reinach et al, 1986) opening up the possibility of site directed mutagenesis to probe the role of specific residues in the function of these light chains.

The ability to carry out fluorescence assays on turbid suspensions has opened up a whole new range of experiments previously considered to be technically impractical. FTP turnover experiments on quite opaque suspensions has allowed the behaviour of filamentous myosin to be studied.

Figure 7-1

A comparison between the effects of light scatter and light absorbance on the observed fluorescence signal.

a Both the transmission and fluorescence signal of a solution containing 10 $\mu$ M FTP was set to 1 volt. Small aliquots of a glycogen suspension (<50 $\mu$ l in total) were added and the observed fluorescence and transmission plotted against the volume of glycogen added (fluorescence, ●; transmission, ○).

b Both the transmission and fluorescence signal of a solution containing 10 $\mu$ M FTP was set to 1 volt. Small aliquots of a malachite green solution (<50 $\mu$ l in total) were added and the observed fluorescence and transmission plotted against the volume of malachite green added (fluorescence, ●; transmission, ○).

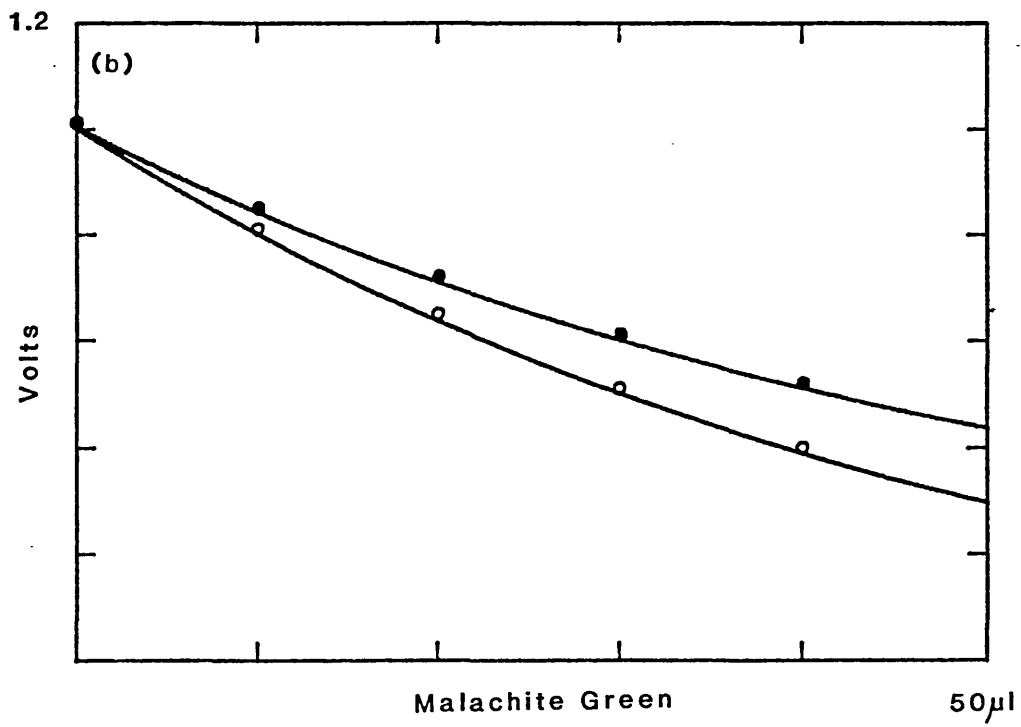
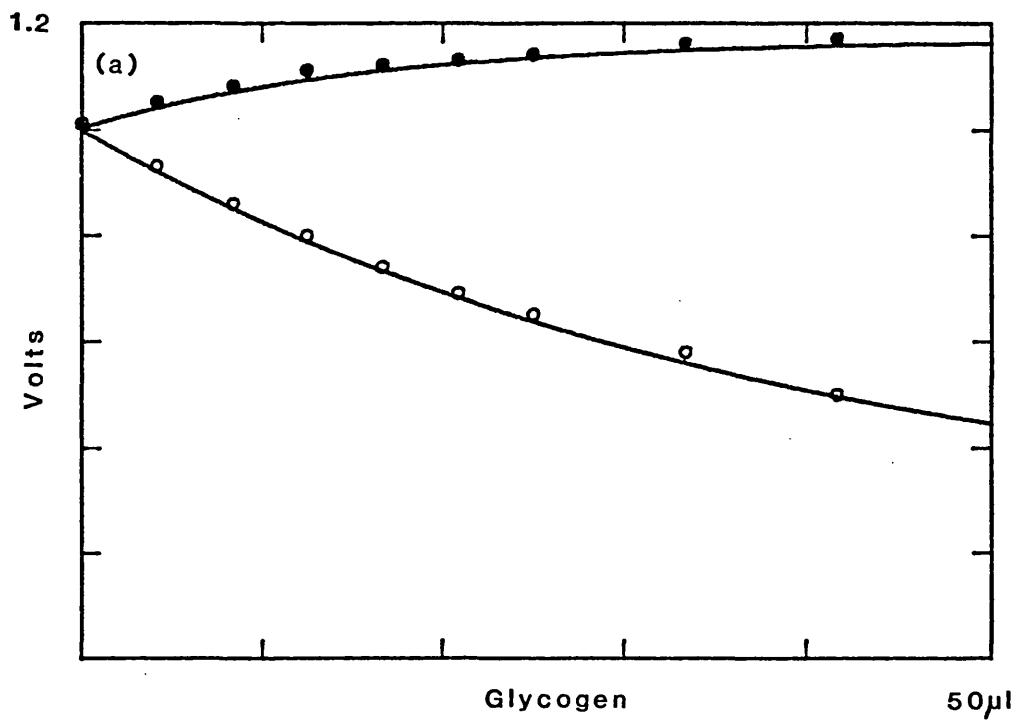


Figure 7-2

The turnover of FTP by myosin in the presence and absence of Ca at low ionic strength (34mM NaCl). These measurements were carried out using the custom-built fluorimeter with an over-head stirrer.

a

At the time indicated 10 $\mu$ M FTP was added to a solution containing 2 $\mu$ M myosin, 100 $\mu$ M EGTA.

b

At the time indicated 10 $\mu$ M FTP was added to a solution containing 2 $\mu$ M myosin, 100 $\mu$ M Ca.

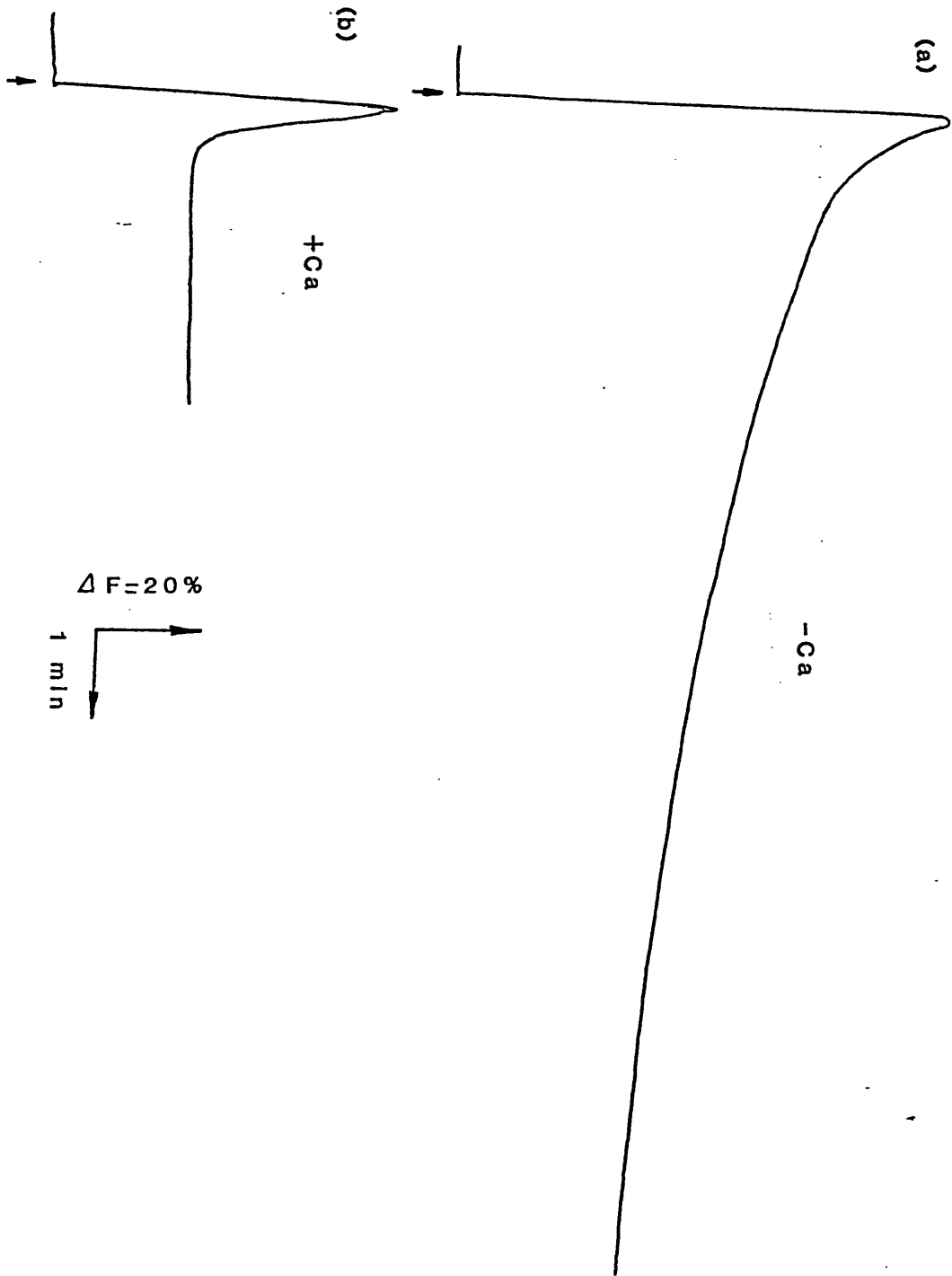
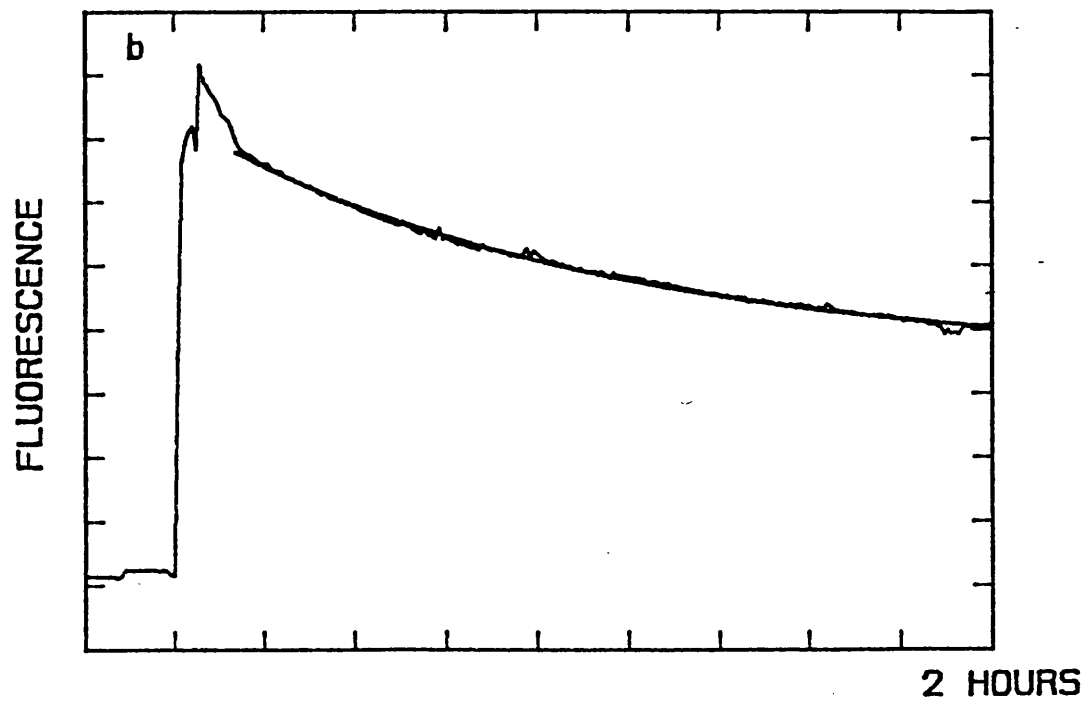
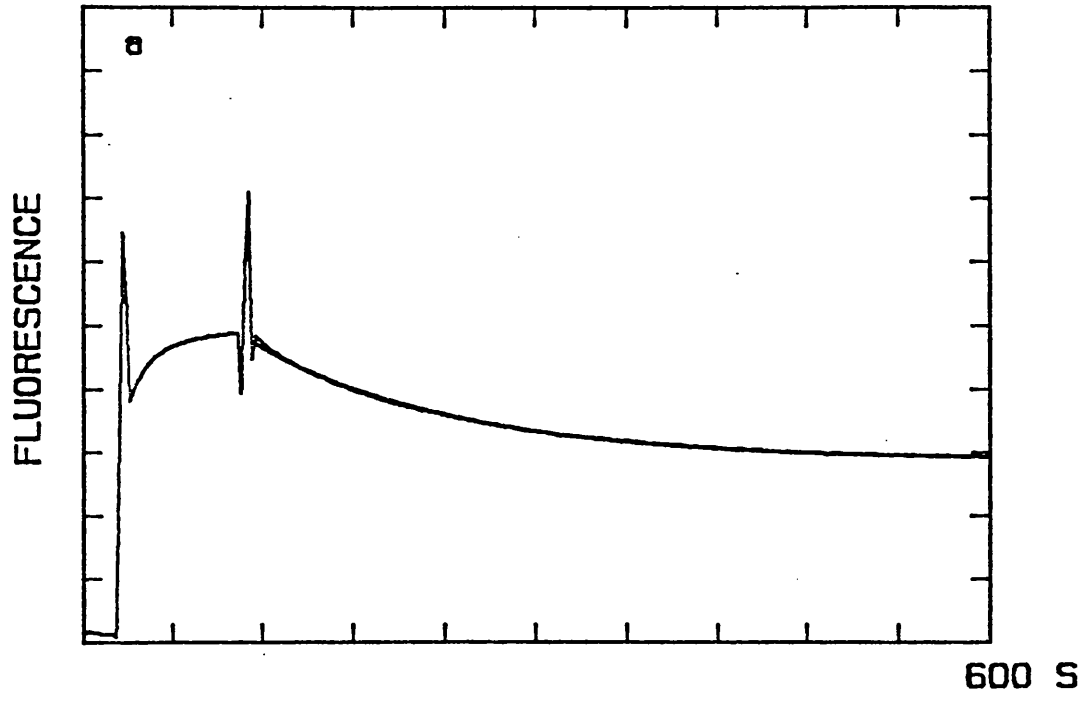


Figure 7-3

FTP turnovers by smooth muscle myosin in (a) the 6S and (b) the 10S conformations.

(a) 4 $\mu$ M FTP was added to 1 $\mu$ M unphosphorylated gizzard myosin, 150mM KCl pH 7.3 at the time indicated. 100 $\mu$ M ATP added after 100 seconds. An exponential fit to the fluorescence decay gave a rate constant of 0.03s<sup>-1</sup>.

(b) 4 $\mu$ M FTP was added to 1 $\mu$ M unphosphorylated gizzard myosin, 325mM KCl pH 7.3 at the time indicated. 100 $\mu$ M ATP added after 100 seconds. An exponential fit to the fluorescence decay gave a rate constant of 0.00015s<sup>-1</sup>.



CHAPTER 8

CONCLUSIONS

In this thesis I have clearly shown that the removal of Ca dramatically inhibits the regulated myosin ATPase and FTPase activity. In the absence of Ca, the ATPase (and FTPase) activity is inhibited approximately 100-fold. A basic four step mechanism was described in equation 4-1, for the ATPase involving ATP binding, hydrolysis, and sequential release of Pi and ADP. Each of these steps consists of several phases, and as each has been explored in greater detail, the more complicated each has become. A simplified view of the mechanism of regulation is seen if the association and dissociation reactions are assumed to be one step processes. Table 8-1 summarises the effect of Ca on a variety of association and dissociation rate constants.

Table 8-1

Nucleotide	Rate (+Ca)	Rate (-Ca)	-Fold change induced by Ca
ATP on	$5 \times 10^6 \text{ M}^{-1} \text{ s}^{-1}$	$5 \times 10^6 \text{ M}^{-1} \text{ s}^{-1}$	1
ADP.Pi off	$0.2 \text{ s}^{-1}$	$0.002 \text{ s}^{-1}$	100
ADP off	$6 \text{ s}^{-1}$	$0.01 \text{ s}^{-1}$	600
AMPPNP on	$\sim 10^5 \text{ M}^{-1} \text{ s}^{-1}$	$\sim 10^5 \text{ M}^{-1} \text{ s}^{-1}$	1
FTP on	$2 \times 10^5 \text{ M}^{-1} \text{ s}^{-1}$	$2 \times 10^5 \text{ M}^{-1} \text{ s}^{-1}$	1
FDP.Pi off	$0.1 \text{ s}^{-1}$	$0.001 \text{ s}^{-1}$	100
FDP off	$\sim 5 \text{ s}^{-1}$	$0.008 \text{ s}^{-1}$	650
FDP on	$10^4 \text{ M}^{-1} \text{ s}^{-1}$	$\sim 10^4 \text{ M}^{-1} \text{ s}^{-1}$	1
FMPPNP on	$2 \times 10^4 \text{ M}^{-1} \text{ s}^{-1}$	$2 \times 10^4 \text{ M}^{-1} \text{ s}^{-1}$	1
FMPPNP off	$0.07 \text{ s}^{-1}$	$10^{-4} \text{ s}^{-1}$	800

In all cases ligand association to form the initial binary complex has been shown to be Ca insensitive, whereas ligand dissociation is highly Ca sensitive. Typically the addition of Ca causes a >100-fold activation of dissociation rates. If only Pi release was activated by Ca, ADP dissociation would then become rate limiting. This is prevented by activation of ADP dissociation. Under relaxing conditions, Pi and ADP dissociation occur at  $0.002 \text{ s}^{-1}$  and  $0.008 \text{ s}^{-1}$  respectively. The addition of Ca causes Pi release to be activated 100 fold to  $0.2 \text{ s}^{-1}$ , and ADP dissociation to be increased 650 fold to  $5 \text{ s}^{-1}$ , preventing it from becoming rate limiting. The Ca sensitivity of P<sub>2</sub> dissociation indicates that it is not the nucleotide ring which is responsible for the Ca effects on ligand dissociation. Other pyrophosphate analogues such as imidodiphosphate also show Ca sensitive dissociation.

Table 8-1 assumes single step binding. A more accurate, and complex, picture has emerged of multistep nucleotide binding in all the cases where binding has been amenable to analysis. Initial association is Ca insensitive but the isomerisations which occur subsequently are Ca sensitive. The removal of Ca allows the formation of trapped enzyme/nucleotide complexes.

#### Origin of the unregulated molecules

It was initially thought that the proteolytic digestion of myosin which is needed to produce HMM caused the damage. It is possible that several small nicks in the regulatory domain

cause a loss of Ca sensitivity but are insufficient to let the resulting HMM fall apart. This is almost certainly the origin of some of the unregulated molecules since slight over-digestion of myosin produces an HMM preparation with >20% unregulated molecules. SDS gel electrophoresis of HMM reveals a ladder of bands, presumably digestion products of HMM. The opposite is not the case, even if the digestion conditions are very mild a preparation with <20% unregulated could not be produced.

FTP turnovers on filamentous myosin, which also showed 20% unregulated fraction, demonstrated that the proportion of unregulated molecules in the HMM sample was not due to the damage caused by tryptic digestion during HMM production, but inherent in the myosin. Possible explanations for the origin of the unregulated molecules are discussed below.

Spontaneous regulatory light chain dissociation, which would lead to the appearance of unregulated molecules, was reported by Bennett and Bagshaw, (1986). This is only a problem if HMM is stored in dilute solution ( $4\mu\text{M}$ ) and in the absence of Ca. Protein was stored in Ca ( $10\mu\text{M}$ ) at high concentration, typically  $>40\mu\text{M}$ . If light chain dissociation was a problem, the addition of excess regulatory light chains should increase the fraction regulated. Also the proportion unregulated should increase over the timescale of about 1 hour. Many assays were carried out in dilute solution and in the absence of Ca where the problem of spontaneous light chain dissociation should manifest itself. Neither of the two effects mentioned above were noticed, indicating that light chain dissociation is not

the cause of the unregulated fraction.

Minor proteolysis may occur during isolation of myosin, but it would have to occur at the N-terminus and result in the loss of only a small peptide. Any proteolysis away from the N-terminus would be seen by SDS gel electrophoresis. Minor losses of material at the C-terminus (at the end of the tail) cannot be the cause otherwise HMM (which has lost most of the tail) would be totally Ca insensitive. An examination of a more intact system, such as muscle fibres, is needed to determine if the unregulated portion of the preparation exists in a less manipulated system.

It is possible that unregulated molecules arise not from irreversible damage but from reversible conformational changes. The proportion of molecules regulated may reflect an equilibrium between regulated and unregulated states. The transition between states would have to be slow otherwise the >95% regulated preparation seen by Jackson et al (1986) could not have existed. Separation of the regulated from unregulated molecules would test this idea. If unregulated molecules were due to slow reversible changes, the 100% unregulated molecules would gradually become Ca regulated as the equilibrium position was re-established. A possible role for these molecules in vivo is discussed below.

#### Role of thin filaments in molluscan regulation

Finding unregulated molecules in myosin preparations suggests that they may well exist in intact muscle. If unregulated

molecules do exist in vivo, what is their role? If they remained uncontrolled they would interact with actin, hydrolyse ATP and undergo cross-bridge cycling. Not only would ATP be hydrolysed unnecessarily but the muscle would be in a constant state of contraction. It is possible that tropomyosin, which is found in molluscan muscle, could control the unregulated myosin heads. Greene and Eisenberg (1980) demonstrated that rabbit S1 exhibited cooperative binding to regulated thin filaments in the presence of Ca, suggesting that even in the presence of Ca, tropomyosin was sterically blocking S1 binding. A similar situation may arise in scallop muscles where, in the absence of Ca, the unregulated myosin heads may well be prevented from binding to actin by tropomyosin. Only when Ca binds to myosin is the concentration of heads that can bind to actin sufficiently high to displace the tropomyosin from the actin binding site. The unregulated molecules may allow the regulatory system to be precariously balanced between the active and relaxed states, hence only a small change in the state of the regulated molecules would be needed to initiate contraction.

These studies using scallop and smooth muscle myosin have revealed the importance of examining a range of myosin fragments. Scallop S1<sup>+RD</sup> binds Ca but does not have a Ca sensitive ATPase. Ca regulation can only be studied using HMM and myosin where the mechanism is intact. Smooth muscle HMM shows little sign of the dramatic trapping of products seen with myosin. The smooth muscle HMM ATPase varies only slightly with salt concentration, whereas the 10S to 6S transition in myosin is clearly illustrated by a 200-fold activation of the

ATPase. Although much useful work can be done using the small subfragments of myosin, some important phenomena involving the regulation of activity can only be seen in the larger fragments or the intact molecule.

#### Regulatory mechanism

Three potential mechanisms for the regulation of the scallop myosin ATPase were presented in the introduction as alternatives.

(i) Steric blocking: proposed as a direct extension of the ideas about thin filament regulation. It involves physical obstruction of acto-myosin interactions by the light chains thus preventing actin from activating the ATPase (figure 8-1a). This is not a viable explanation because it has been clearly shown that regulation proceeds in the absence of actin.

(ii) Restricted mobility: in the absence of Ca the mobility of the myosin heads is restricted to such an extent that they are unable to reach the actin filaments (figure 8-1b). Again actin would play a primary role in this type of regulation, a role which has been shown to be unnecessary.

(iii) Conformational changes: Ca binding to the regulatory domain changes the conformation at the active site, activating the ATPase and modulating actin interactions directly (figure 8-1c). This can function in the absence of actin and, in the light of the results presented in this work, is the most likely.

How will the proposed regulatory mechanism work in practice? In the absence of Ca the ATPase is severely repressed resulting

in the trapping of products at the active site ( $M \cdot ADP \cdot Pi$ ) which can interact only weakly with actin and is therefore unable to undergo cross-bridge cycling. Ca binding to the regulatory domain of myosin or HMM causes the conformation of the active site to be altered in such a way that product release becomes rapid. Removal of Ca reverses this process and induces trapping of products at the active site.

The mechanism of ATPase/contraction coupling described in the introduction suggested two acto-myosin binding states depending upon the state of the active site. Nucleotide favoured the weakly bound state. Scallop acto-myosin interactions appear to function in a similar manner. When nucleotide is trapped at the active site acto-myosin interactions will be weak and contraction cannot occur. Binding Ca to the regulatory domain relieves the trapping, releasing products and allowing actin to interact tightly with myosin to undergo rapid cross-bridge cycling, which continues until Ca is removed from the regulatory domain and the trapped state reforms.

The multidomain structure of myosin heads is suited to this role. Interdomain movements could lead to an 'opening' and 'shutting' of the active site. In the absence of nucleotide, the active site is in the open state, regardless of whether Ca is present and interactions with actin are tight forming the rigor state. In the absence of Ca, nucleotide binding induces a closed state, which traps the nucleotide, preventing rapid dissociation and produces a myosin head which binds only weakly to actin. Ca maintains the open conformation, allowing rapid product dissociation and tight actin binding. The elongated

light chain structure extending from near the regulatory domain to the active site near the middle of the head, provides a potential channel for transmission of information about the Ca site to the ATPase site. Both light chains appear to be involved in regulation, since the ELC has close contacts with the active site (Okamoto et al., 1986), Ca induces movement in the RLC (Hardwicke et al., 1983) and removal of the RLC results in permanent activation of the ATPase (Szent-Gyorgyi et al., 1973).

It is actin which provides amplification of the myosin linked regulatory system to a level required by the organism. Under relaxing conditions all of the myosin heads are inhibited in their activity. Once the muscle has been activated, those heads which can interact with actin undergo cross-bridge cycling, and exhibit the full >2000-fold activation of their ATPase activity. Those myosin heads which cannot interact with actin (away from the region of overlap) do exhibit a 100-fold activation of the ATPase activity consuming more ATP without doing any work. These heads have, however, been brought into a state capable of being actin-activated (Wells and Bagshaw, 1984, 1985). The contribution to the overall ATP consumption by the myosin heads away from the region of filament overlap will be small.

The extreme suppression of the dissociation steps under relaxing conditions leads to the production of a kinetically trapped enzyme/product species. A trapped enzyme/product intermediate has also been found in other myosin systems. Molluscan catch muscle has the ability to maintain tension with

relatively little expenditure of energy. In this case trapping occurs while actin is still attached to myosin in the force generating state, a form of trapping which leads to a slow maximum shortening velocity for the muscle but very low ATP consumption (Ruegg, 1986). Scallops overcome the requirement for both rapid contraction, which is required for swimming, and prolonged contraction, to keep out predators, by using both striated and catch smooth muscles.

In systems where product release has been the rate limiting step, FTP turnovers have provided an excellent method of examining the kinetics of turnover of substrate i.e scallop myosin and smooth muscle myosin. The chief difference between the turnover of FTP and ATP is that the FTP binding rate constants are generally about 10-fold slower than the corresponding ATP binding rate constants. This limits the use of FTP in studying enzymic mechanisms of ATPases with relatively fast turnover rates. If product release is faster than substrate binding in the amenable concentration range, then the observed fluorescence enhancements are very small, and can provide little information. This has been noted for the protein, dynein, which is involved in cilia and flagella motility (Wells, 1987).

Exploitation of the large fluorescence enhancement seen on formycin nucleotide binding has led to to so called 'branched scheme' being proposed. Assuming that the ATPase mechanism follows a similar pathway, what are the consequences of the branched scheme? In vivo there is always nucleotide present, myosin will gradually be hydrolysing ATP at the relaxed rate.

Hence the system is always in a steady-state so that the branched scheme will not affect the ATP turnover rate. It is only during the approach to steady-state that the existence of the branched pathway can be seen. Pre-steady-state conditions can only be seen on the addition of ATP to an ATP free system (non-physiological) or on relaxation, which will occur under physiological conditions. Steady-state considerations do allow the branched scheme to operate in vivo with little effect on the consumption of ATP.

Vibert and Craig, (1985), have provided additional evidence for a correlation between the formation of a trapped enzyme/products complex in vitro and the formation of a similar complex in vivo. They used electron microscopy to follow the structural changes induced in scallop myosin filaments by the addition and removal of ATP. In the absence of ATP an orderly arrangement of myosin heads projecting from the filament could be seen, a pattern that was lost on addition of ATP. Subsequent removal of ATP from the filaments, by washing in a Ca containing wash buffer, resulted in the ordered arrangement being rapidly restored. If, however, an EGTA containing wash buffer was used to remove the ATP, then it took a long time (about 30 minutes) for the ordered structure to reappear. The rates of these processes were not characterised but they do appear to fit in with the time-scale of the in vitro changes seen on product release from scallop HMM.

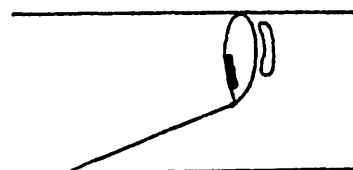
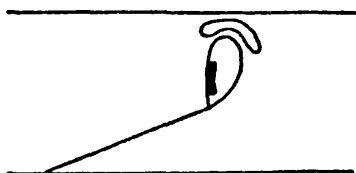
Figure 8-1

Relaxed

Active

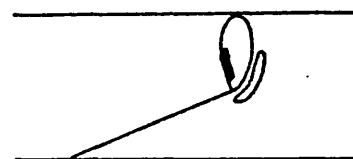
(a)

Steric Blocking



(b)

Restricted Flexibility



(c)

Conformational Changes



APPENDIX 1

SUMMARY OF COMPUTER PROGRAMS

### Summary of computer programs

Data capture and analysis was carried out using an Apple II+ microcomputer. Data from a wide range of apparatus could be entered directly into the computer or data could be fed in through the keyboard or via a graphics tablet. To ensure a flexible system of analysis, data was stored in one of two formats which were interconvertable. A binary file, composed of 500 10-bit numbers, in which the data points were an equal time interval apart, stored the directly entered data and a text file, composed of a variable number of points with unequal time interval usually entered through the keyboard. Text files stored the data as two dimensional arrays which take up more memory space and take longer to manipulate than the binary files, but they do offer greater flexibility in analysis.

Binary files were created using Multirecord, Digitiser, or Chart Recorder and could be manipulated and analysed using Expfit, Datamod and Integrator. Text files were created using Simulation, Digitiser or Datafit and analysed using Datafit. Interconversion of files from one format to another was carried out using Datamod and File Converter.

### Multirecord

The transient recorder saves data as 2048 points with 8-bit resolution. On transfer to the computer the points were summed in groups of four, producing 512 points with 10-bit

resolution. These data were then saved on disc. Often during stopped-flow experiments many identical pushes need to be averaged to increase the signal to noise ratio. Multirecord allows each individual trace to be saved while producing a 'running average' of the traces. At any point the average can be viewed. If required it is then saved.

Multirecord also incorporated a routine to allow external control of the transient recorder's time base. On internal time base control, the transient recorder is limited to a maximum timebase of 100 seconds. A variable time loop allows any time greater than 25 seconds to be used.

#### Chart recorder

Analogue to digital conversions of signals in the -5V to +5V range can be carried out by the computer. If this facility is coupled to a timing circuit, a digital chart recorder is the result. Amplifiers ensure that equipment, whose output signals lie in the range 10mV to 5V, can be linked to the computer.

The Apple II+ computer can act as a digital chart recorder using the above method. Two separate signals can be recorded simultaneously with the minimum time base of 100 seconds and 200 seconds for one and two channels respectively. The data is stored in the same format as used by Multirecord.

### Expfit

Expfit carries out direct least squares fits to mono- or biphasic exponentials on data stored as binary files. It can also be used to average several traces together to improve the signal to noise ratio.

The base line for the exponential fit can either be a horizontal or sloping line. The program alters both the amplitudes and rate constants of the exponential until there is little improvement in the deviation of the experimental data from the calculated curve. It generally takes 3-6 iterations to arrive at the best fit curve, taking 1-2 minutes for single exponential fits and 2-5 minutes for biphasic fits.

### Datamod

Datamod allows the manipulation of binary files by a variety of procedures. The major functions which have been used are:

- (1) Expansion (or reduction) of the X and Y axis for display purposes.
- (2) Digital filtering to improve the signal to noise ratio by removing high frequency vibrations.
- (3) Removing large noise spikes introduced, by electrical interference, during data capture.
- (4) Conversion of binary files to text files to allow equations other than exponentials to be fitted through the

data.

The data in the binary files can also be viewed directly allowing the maximum and minimum values to be seen, which greatly speeds up the manipulations described above. This capacity has also allowed the time of addition during experiments to be accurately determined allowing more precise curve fitting.

#### Integrator

This program was used to analyse the elution profiles of nucleotide separations carried out on the FPLC. Data was entered and saved on disc via the Chart Recorder program.

The base line of the chromatogram was defined by placing a cursor at selected points on the profile. These points were then joined by straight lines. The peaks of interest were defined in a similar manner. The area under each peak was calculated and expressed in absolute terms or as a percentage of the total.

#### Datafit

Used to carry out least square fits, to a variety of pre-defined equations with up to five parameters, on data which has been stored as text files. Data can be entered via the keyboard, graphics tablet or generated by the Simulation program.

### Simulation

Used to simulate kinetic schemes to test whether a proposed mechanism does explain the experimental data. A scheme is defined by a number of species linked via a series of steps. Differential equations linking the species are entered and stored on disc. Once initial concentrations and rates have been entered, the reaction profile is calculated by numerical integration. From the equations, concentrations of all the species are calculated after a time  $\delta t$ . If the change in concentration of the species is small,  $\delta t$  is increased. Conversely, if the concentration change is large  $\delta t$  is reduced. This ensures that most data points are collected during periods of greatest change. Any individual species or several summed together can be saved for future analysis.

### File Converter

Allows the conversion of text files to binary files by extrapolation between the individual data points to ensure the correct number and equal time interval between them.

### Digitiser

This allows the data from the graphics tablet to be entered into the computer either in the form of text or binary files.

APPENDIX 2

PUBLICATIONS

Publications

The actin-activated ATPase of regulated and unregulated scallop heavy meromyosin.

A.P. Jackson, K.E. Warriner, G. Wells and C.R. Bagshaw.

FEBS Lett, 197, 154-158, (1986).

The kinetics of calcium binding to fura-2 and indo-1.

A.P. Jackson, M.P. Timmerman, C.R. Bagshaw and C.C. Ashley.

FEBS Lett, 216, 35-39, (1987).

Measurement of single turnovers of scallop myosin ATPase in the filamentous state.

A.P. Jackson, K.E. Warriner and C.R. Bagshaw.

Biochem Soc Trans, 15, 900-901, (1987).

Transient kinetic studies of the adenosine triphosphatase activity of scallop heavy meromyosin.

A.P. Jackson and C.R. Bagshaw.

Biochem J, 251, 515-526, (1988).

Kinetic trapping of intermediates of the scallop heavy meromyosin adenosine triphosphatase reaction revealed by formycin nucleotides.

A.P. Jackson and C.R. Bagshaw.

Biochem J, 251, 527-540, (1988).

Active site trapping of nucleotides by smooth and nonmuscle myosins.

R.A. Cross, A.P. Jackson, S. Citi, J. Kendrick-Jones and C.R. Bagshaw.

J. Mol. Biol. (1988). In press.

REFERENCES

Albanisi J.P, Fujisaki H, Hammer J.A, Korn E.D, Jones R and Sheetz M.P. (1985). J. Biol. Chem 260, 8649-8652.

Ashiba G, Asada T and Wantanabe S. (1980). J. Biochem 88, 837-846.

Bagshaw C.R, Eccleston J.F, Eckstein F, Goody R.S and Trentham D.R. (1974). Biochem. J, 141, 351-364.

Bagshaw C.R, Eccleston J.F, Trentham D.R, Yates D.W and Goody R.S. (1972). Cold Spring Harbour Symp. Quant. Biol 37, 127-136.

Bagshaw C.R and Trentham D.R. (1973). Biochem. J 133, 323-328.

Bagshaw C.R and Trentham D.R. (1974). Biochem. J 141, 331-349.

Bagshaw C.R and Kendrick-Jones J. (1979). J. Mol. Biol 130, 317-336.

Bagshaw C.R and Reed G.H. (1976). J. Biol. Chem 251, 1975-1983.

Bennett A.J and Bagshaw C.R. (1986). Biochem. J 233, 179-186.

Chalovich J.M and Eisenberg E. (1982). J. Biol. Chem 257, 2432-2437.

Chalovich J.M, Chantler P.D, Szent-Gyorgyi and Eisenberg E. (1984). J. Biol. Chem 259, 2617-2621.

Chantler P.D and Szent-Gyorgyi A.G. (1978). Biochemistry 17, 5440-5448.

Chantler P.D, Sellers J.R, Szent-Gyorgyi A.G. (1981). Biochemistry 20, 210-216.

Chock S.P, Chock P.B and Eisenberg E. (1979). J. Biol. Chem 254, 3236-3243.

Collins J.H, Jakes R, Kendrick-Jones J, Leszyk J, Barouch W, Theibert J.L, Speigel J and Szent-Gyorgyi A.J. (1986). Biochemistry 25, 7651-7656.

Cornish-Bowden A. (1979). Fundamentals of Enzyme Kinetics. Butterworths.

Cross R.A, Cross K.E and Sobieszek A. (1986). EMBO J 5, 2637-2641.

Eisenberg E and Greene L.E. (1980). Ann Rev Physiol 42, 293-309.

Elliott A and Offer G. (1978). J. Mol. Biol 123, 505-519.

Geeves M.A, Goody R.S and Gutfreund H. (1984). J. Musc. Res. Cell Motil 5, 351-361.

Goldman Y.E, Hibberd M.G, McCray J.A and Trentham D.R. (1982). Nature 300, 701-705.

Gordon A.M, Huxley A.F and Julian F.J. (1966). J Physiol 184, 170-192.

Greene L.E and Eisenberg E. (1980). Proc. Natl. Acad. Sci. USA 77, 2616-2620.

Hardwicke P.D.M, Wallimann T and Szent-Gyorgyi A.G. (1983). Nature 307, 478-482.

Harada H, Naguchi A and Yanagida T. (1987). Nature 326, 805-808.

Harrington W.F. (1979). Proc. Natl. Acad. Sci. USA 76, 5066-5070.

- Huxley A.F (1957). Prog. Biophys. Biophys. Chem 7, 255-318.
- Huxley A.F and Niedergengerke R.M. (1954). Nature 173, 971-973.
- Huxley H.E. (1969). Science 164, 1356-1366.
- Huxley H.E. (1973). Cold Spring Harbour Symp. Quant. Biol 37, 361-376.
- Huxley H.E and Brown W. (1967). J. Mol. Biol 30, 383-434.
- Huxley H.E and Hanson J. (1954). Nature 173, 973-976.
- Hynes T.R, Block S.M, White B.T and Spudich J.A. (1987). Cell 48, 953-963.
- Itaya K and Ui M. (1966). Clin Chim Acta 14, 361-366.
- Jackson A.P, Timmerman M.P, Bagshaw C.R and Ashley C.C. (1987). FEBS Lett 216, 35-39.
- Jackson A.P, Warriner K.E, Wells C and Bagshaw C.R. (1986). FEBS Lett 197, 154-158.
- Jackson A.P, Warriner K.E and Bagshaw C.R. (1987). Biochem Soc Trans, 15, 900-901.
- Johnson K.A and Taylor E.W. (1978). Biochemistry 17, 3432-3442.
- Kendrick-Jones J, Lehman W and Szent-Gyorgyi A.G. (1970). J. Mol. Biol 54, 313-326.
- Kodama T, Fukui K and Komentani K. (1986). J. Biochem 99, 1465-1472.
- Kron S.J and Spudich J.A. (1986). Proc. Natl. Acad. Sci. USA 83, 6272-6276.

Kushmerick M.J and Davis R.E (1969). Proc Royal Soc 174, 313-353.

Kushmerick M.J and Paul R (1976). J Physiol 254, 693-703.

Lehman W. (1981). Biochem. Biophys. Acta 668, 349-356.

Lehman W and Szent-Gyorgyi A.S. (1975). J Gen Physiol 66, 1-30.

Lymn R.W and Taylor E.W. (1970). Biochemistry 9, 2975-2983.

Lymn R.W and Taylor E.W. (1971). Biochemistry 10, 4617-4624.

Margossian S.S and Lowey S. (1973). J. Mol. Biol 74, 313-330.

Margossian S.S and Lowey S. (1982). Methods in Enzymology 85, 55-72.

Margossian S.S, Lowey S and Barshop B. (1975). Nature 258, 163-166.

Maw M.C and Rowe A.J. (1980). Nature 286, 412-414.

McLachlan A.D and Karn J. (1982). Nature 299, 226-231.

Mergeman J and Lowey S. (1981). Biochemistry 20, 2099-2110.

Millar N.C. (1984). PhD Thesis, University of Bristol.

Millar N.C and Geeves M.A. (1983). FEBS Lett 160, 141-148.

Millman B.M and Bennett P.M. (1976). J. Mol. Biol 103, 439-467.

Mornet D, Bertrand R, Pantel P, Audemard E and Kassab R. (1981). Nature 292, 301-306.

Munson K.B, Smerdon M.J and Yount R.G. (1986). *Biochemistry* 25, 7640-7650.

Nirenberg M.W. (1963). *Methods in Enzymology* 6, 17-23.

Okamoto Y, Sekine T, Gramme J and Yount R.G. (1986). *Nature*, 324 78-80.

Rall J.A. (1981). *J Physiol* 321, 287-295.

Rayment I and Winkelmann D.A. (1984). *Proc. Natl. Acad. Sci. USA* 81, 4378-4380.

Reinach F.C, Nagai K, and Kendrick-Jones J. (1986). *Nature* 322, 80-83.

Rodbell M, Birnbaumer L, Pohl S.L and Krans M.J.K. (1971). *J. Biol. Chem* 246, 1877-1882.

Rosenfeld S.S and Taylor E.W. (1984). *J. Biol. Chem*, 259, 11920-11929.

Rossomando E.G, Jahngen J.H and Eccleston J.F. (1981). *Anal, Biochem* 116, 80-88.

Rouayrenc J.F, Bertrand R and Kassab R. (1985). *Eur. J. Biochem* 146, 391-407.

Ruegg J. (1986). *Calcium in Muscle Activation*. Springer-Verlag.

Sheetz M.P and Spudich J.A. (1983). *Nature* 303, 31-35.

Shibata-Sekiya K. (1982). *J. Biochem* 92, 1151-1162.

Shoham M and Steitz T.A. (1980). *J. Mol. Biol* 140, 1-14.

Spudich J.A and Watt S. (1971). *J. Biol. Chem* 246, 4866-4871.

- Squire J.M. (1974). *J. Mol. Biol* 90, 153-160.
- Stafford W.F, Szentkiralyi E.M and Szent-Gyorgyi A.G. (1979). *Biochemistry* 18, 5272-5280.
- Stein L.A, Chock P.B and Eisenberg E. (1981). *Proc. Natl. Acad. Sci. USA* 78, 1346-1350.
- Such D, Kabsch W and Mannherz H.G. (1981). *Proc. Natl. Acad. Sci. USA* 78, 4319-4323.
- Sutoh K. (1983). *Biochemistry* 22, 1579-1583.
- Suzuki H, Onishi H, Takahashi K and Wantanabe S. (1978). *J. Biochem* 84, 1529-1542.
- Szent-Gyorgyi A.G, Szentkiralyi E.M and Kendrick-Jones J. (1973). *J. Mol. Biol* 74, 179-203.
- Szentkiralyi E.M. (1984). *J. Musc. Res. Cell Motil* 5, 147-164.
- Taylor K.A and Amos L.A. (1981). *J. Mol. Biol* 147, 297-324.
- Trentham D.R, Bardsley R.G, Eccleston J.F, and Weeds A.G. (1972). *Biochem. J* 126, 635-644.
- Trentham D.R, Eccleston J.F and Bagshaw C.R. (1976). *Quart Rev Biophys*, 9, 217-281.
- Trybus K.M and Taylor E.W. (1982). *Biochemistry* 21, 1284-1294.
- Toyoshima Y.Y, Kron S.J, McNally E.M, Niebling K.R, Toyoshima C and Spudich J.R. (1987). *Nature* 328, 536-539.
- Vale R.D, Szent-Gyorgyi A.G and Scheetz M.P. (1984). *Proc. Natl. Acad. Sci. USA* 81, 6775-6778.
- Vibert P and Craig R. (1983). *J. Mol. Biol* 165, 303-320.

- Vibert P and Craig R. (1985). *J. Cell Biol* 101, 830-837.
- Vibert P, Szentkiralyi E.M, Hardwicke P, Szent-Gyorgyi A.G and Cohen C. (1986). *Biophys J* 49, 131-133.
- Ward D.C and Reich E. (1968). *Proc. Natl. Acad. Sci. USA* 61, 1494-1501.
- Ward D.C, Reich E and Stryer L. (1969a). *J. Biol. Chem* 244, 1228-1237.
- Ward D.C, Cerami A, Reich E, Acs G and Altwerger L. (1969b). *J. Biol. Chem* 244, 3243-3250.
- Wells C. (1987). *Biochem Soc Trans*, 15, 908-909.
- Wells C and Bagshaw C.R. (1983). *J. Mol. Biol* 164, 137-157.
- Wells C and Bagshaw C.R. (1984a). *FEBS Lett* 168, 260-264.
- Wells C and Bagshaw C.R. (1984b). *J. Musc. Res. Cell Motil* 5, 97-112.
- Wells C and Bagshaw C.R. (1985). *Nature* 313, 696-697.
- Wells C, Warriner K.E and Bagshaw C.R. (1985). *Biochem. J* 231, 31-38.
- Werber M.M, Szent-Gyorgyi A.G and Fasman G.D. (1972). *Biochemistry* 11, 2872-2883.
- White D.C.S, Zimmerman R.W and Trentham D.R. (1986). *J. Musc. Res. Cell Motil* 7, 179-192.
- White H.D. (1982). *Methods in Enzymology* 85, 698-708.
- White H.D. (1985). *J. Biol. Chem* 260, 982-986.

White H.D and Taylor E.W. (1976). Biochemistry 15,  
5818-5826.

Winkelman D.A, Meekel H and Rayment I. (1985). J. Mol. Biol  
181, 487-501.